ADDENDUM REPORT ON ELECTROMAGNETIC ATTITUDE CONTROL SYSTEM STUDY

Prepared under Contract No. NAS-5-1728 *by*
WESTINGHOUSE ELECTRIC CORPORATION
Baltimore, Maryland
for

NATIONAL AERONAUTICS AND SPACE ADMINISTRATION • WASHINGTON, D. C. • MARCH 1964

ADDENDUM REPORT ON ELECTROMAGNETIC ATTITUDE CONTROL SYSTEM STUDY

Prepared under Contract No. NAS-5-1728 by
WESTINGHOUSE ELECTRIC CORPORATION
Baltimore, Maryland

Imprint Washington, NASA, Mar. 1964 159p refs

NATIONAL AERONAUTICS AND SPACE ADMINISTRATION

For sale by the Office of Technical Services, Department of Commerce,
Washington, D.C. 20230 -- Price $3.00

TABLE OF CONTENTS

Paragraph		Page
1.0	Introduction	1-1
2.0	Scope of the Study Program Extension	2-1
3.0	Conclusions	3-1
3.1	New Methods of Attitude Control	3-1
3.2	Further Wheel-And-Coil System Study	3-2
3.3	Solar Array Orientation	3-3
3.4	Recommendations for Further Work	3-3
4.0	The Combination Gravity Gradient and Electromagnetic Actuation System	4-1
4.1	Performance Analysis	4-1
4.1.1	Basic Relationships	4-1
4.1.2	The Six-Hour Orbit	4-7
4.1.3	Detumbling	4-20
4.1.4	The Twelve-Hour Orbit	4-20
4.1.5	The Synchronous Orbit	4-25
4.1.6	Sample System Performance	4-30
4.2	Mechanization Summary	4-44
4.2.1	System Plan	4-44
4.2.2	Reliability and Weight Analysis	4-46
4.2.3	Comparison to Other Systems	4-50
5.0	Earth's Magnetic Field and Solar Sensing	5-1
5.1	Statement of the Problem	5-1
5.2	Magnetic Field Sensing	5-2
5.3	Sun Sensing	5-5
5.4	Alternate Sun Sensors	5-13
5.5	Conclusions	5-15

Paragraph Page

6.0 Ground Control 6-1

6.1 System Plan 6-1

6.1.1 Coil Current Equations 6-1

6.1.2 Computation of Angular Velocities 6-2

6.1.3 Computation of Yaw Angular Error 6-6

6.1.4 The Complete Loop 6-10

6.2 On-Board Equipment Mechanization 6-10

6.2.1 Solar Sensing 6-11

6.2.2 Three Axis Magnetometer 6-11

6.2.3 Telemetry 6-11

6.2.4 Command System 6-15

6.2.5 Magnetic Torque Coils 6-16

6.2.6 Miscellaneous Electronics 6-16

6.2.7 Summary of On-Board Equipment Characteristics . . . 6-17

6.3 Analysis of Ground-Based Computer Requirements 6-17

6.3.1 General Capabilities 6-17

6.3.2 Memory 6-18

6.3.3 Feed-Through Time 6-18

6.3.4 Input/Output Requirements 6-18

6.3.5 Applicable Systems 6-19

6.4 Conclusions 6-21

7.0 Solar Array Control 7-1

7.1 Description of Problem 7-1

7.2 Sunline Angle and Control Motions for Solar Arrays 7-3

7.3 Yaw-Oriented Array Control System 7-11

Paragraph Page

7.4 Yaw and Elevation Array Control System 7-17

7.5 Non-Oriented Array 7-18

7.6 Power Supply Mechanization 7-22

7.7 Comparisons of System 7-26

8.0 Optimization of the Wheel and Coil System 8-1

8.1 Errata to Previously Published Six Hour Orbit Data 8-1

8.2 Twelve Hour Orbit 8-1

8.3 Synchronous Orbit 8-7

9.0 The Constancy of the Earth's Magnetic Field 9-1

9.1 Jensen-Whitaker Geomagnetic Data 9-2

9.2 Upper Altitude Magnetic Fields 9-3

LIST OF ILLUSTRATIONS

Figure		Page
4-1	Gravity Gradient Torque vs. Altitude	4-2
4-2	Analog Computer Simulation	4-5
4-3	Earth's Field Components	4-6
4-4	Angular Errors vs. Position & Rate Gain	4-9
4-5	Angular Errors vs. Position & Rate Gain	4-10
4-6	Angular Errors vs. Position & Rate Gain	4-11
4-7	Angular Errors vs. Position & Rate Gain	4-12
4-8	Peak Position Errors vs. Disturbance	4-14
4-9	Position & Rate Errors as f(t)	4-15
4-10	Position & Rate Errors as f(t)	4-16
4-11	Response to Initial Roll Rate	4-17
4-12	Response to Initial Pitch Rate	4-18
4-13	Response to Initial Yaw Rate	4-19
4-14	Detumbling Time vs. Actuator Weight	4-21
4-15	Vehicle Displacement vs. Position & Rate Gain	4-22
4-16	Vehicle Displacement vs. Position & Rate Gain	4-23
4-17	Vehicle Displacement vs. Position & Rate Gain	4-24
4-18	Peak Position Errors vs. Disturbance	4-26
4-19	Position and Rate Errors as f(t)	4-27
4-20	Position and Rate Errors as f(t)	4-28
4-21	Position and Rate Errors as f(t)	4-29
4-22	Approximate Satellite Disturbance Torques - 24 Hour Orbit.	4-36
4-23	Analog Computer Simulation	4-37
4-24	Simulation Results - 6 Hour Orbit	4-39
4-25	Simulation Results - 12 Hour Orbit	4-40

Figure		Page
4-26	Simulation Results - Synchronous Orbit	4-41
4-27	Gravity Gradient & Coils, On-Board Computation	4-45
5-1	Magnetic Field Position for Determining Magnetometer Threshold	5-3
5-2	Cross Section and Top View of Sensor Unit	5-7
5-3	Geometric Principle of Sensor	5-8
5-4	Overlapping of Solar Cell Fields-of-View	5-10
5-5	Interrogation Circuit	5-11
5-6	Output of Linearized Sun Sensor	5-14
6-1	Sunline and Magnetic Field Vectors in Vehicle Coordinates as Measured by On-Board Sensors	6-3
6-2	Reference and Measured Magnetic Field Vectors	6-7
6-3	Reference and Measured Solar Direction Vectors	6-8
6-4	Block Diagram, Ground Computer Requirements	6-12
6-5	Block Diagram, On-Board Control Equipment	6-14
7-1	Vehicle Configuration	7-2
7-2	Diagram of Control Motions	7-5
7-3	Yaw Angle vs. Orbit Angle	7-6
7-4	Elevation Angle vs. Orbit Angle	7-7
7-5	Yaw Angle vs. Orbit Angle, with 180° Shifts	7-8
7-6	Elevation Angle vs. Orbit Angle, with 180° Shifts	7-9
7-7	Aspect Ratio vs. Orbit Angle	7-10
7-8	Average Aspect Ratio	7-12
7-9	Solar Cell Configuration, Yaw Oriented Vehicle	7-13
7-10	Block Diagram, Yaw Orientation System	7-15
7-11	Solar Cell Configuration, Fully Oriented Array	7-16
7-12	Block Diagram, Yaw & Elevation Oriented Array	7-19
7-13	Array Drive	7-21

Figure		Page
8-1	System Parameters vs. Disturbance Torque Level, 6-Hr. Orbit .	8-2
8-2	Wheel Weight vs. Coil Gain	8-3
8-3	Coil Weight vs. Coil Gain	8-4
8-4	Wheel & Coil Weight vs. Coil Gain	8-5
8-5	Optimum Actuation Data vs. Disturbance Torque	8-6
8-6	Solar Pressure Rate Damping & Momentum Dumping Concept . . .	8-8
8-7	Solar Pressure Actuation, Ψ vs. α	8-10
8-8	Solar Pressure Torque vs. Orbit Position	8-11
8-9	Solar Pressure Momentum Dumping Capability	8-12
9-1	Approximate Geomagnetic Equator Field	9-4
9-2	Estimate of Diurnal Regular Change of Magnetic Angle	9-6

LIST OF TABLES

Table		Page
4-A	Simulation Results	4-43
4-B	Summary of Electronic Parts for the Gravity Gradient and Torque Coils Attitude Control System Without Ground Control	4-47
4-C	Reliability of Subsystems	4-48
4-D	System Weight	4-49
4-E	Comparison of System Parameters	4-50
5-A	Magnetometer Requirements	5-4
5-B	Reliability Computation	5-12
6-A	Control System Data	6-17
7-A	Mission Configurations	7-1
7-B	Power and Weight of Power Supply for 6, 12, 24 Hour Orbits	7-22
7-C	Weight, Power, Volume Comparisons of Yaw Oriented and Yaw-and-Elevation Oriented Arrays	7-27
7-D	Reliability of Yaw Oriented and Yaw-and-Elevation Oriented Arrays	7-28

	Weight Lb.	Avg. Power Watts	Reliability P_s for 1 year
Magnetic Torquers	2	1	0.99
3-Axis Magnetometer	2	2	0.99
Constant-Speed Wheel	8	30	0.997
RF Vertical Sensor (includes redundancy)	15	5	0.983
Electronics	15	10	0.944
4 Yaw Rate Gyros (Standby Redundancy)	12	4	0.96
Vapor Jet (Some Redundant Parts)	17	10	0.95
Solar Sensor*	2	1	0.99*
Pitch & Roll Rate Gyros*	6	7	0.98*
Horizon Scanner*	6	5	0.98*
Cold Gas System*	7	X	0.99*
Hypergolic Engine*	25	X	0.98*
	115 lb.	62 W ‡ 27 W *	0.76**

* Short-term use

‡ Long-term system

** P_s for 3 years = 0.52

1.0 INTRODUCTION

This addendum report details the results of continued study on satellite electromagnetic attitude control and related subjects, an investigation conducted for the National Aeronautics and Space Administration by the Westinghouse Electric Corporation (NASA Contract NAS-5-1728). The study program described in this report is an outgrowth of the findings related in an earlier report dated May 1, 1962, and also entitled "Electromagnetic Attitude Control System Study". The purpose for both initial and extended phases of this effort has been to uncover more reliable and lighter means of orienting satellites.

The earlier report dealt chiefly with the design optimization of electromagnetic satellite torquers, with how these torquers might be applied to satellite attitude control (either as accessories to a reaction wheel system or as primary actuators themselves), and with a sample control system design employing electromagnetic actuation. The sample system was one for a vertically oriented vehicle, as would be the case for a communications satellite, a meteorological satellite, or any other vehicle with an earth-oriented mission. In the sample design, a set of magnetic torquers replaced the more conventional cold-gas system in removing stored momentum from reaction wheels. It would be well to match the improvements thus achieved in actuator reliability and weight with a gain in sensor reliability, and a part of the extended program reported here has been so directed. The approach taken has been to substitute, where feasible, sun sensors and magnetometers for the more complex horizon scanners and gyros, and to replace decision-making equipment in the satellite by a ground-based computer. Where attitude sensing by means of magnetometers is not practical (such as in the synchronous orbit) the same principles embodying ground control of a gravity

gradient and magnetic torquer system can be applied with other means of sensing. These other means might be R-F interferometer sensing in a communications satellite or the use of the topographical observations in a meteorological satellite.

There is an obvious advantage in eliminating the reaction wheels and torquing with the magnetic actuators alone. The initial study phase showed this to be a useful method, but there was an accompanying sacrifice in satellite pointing accuracy. Much of this disparity in accuracy can be avoided by adding the gravity gradient as a control torque source complimentary to the magnetic torquers. An investigation of this technique is also described herein.

Having dealt with the problems of vertically positioning a communications satellite, a question also arises concerning its rotation about the vertical. This yaw attitude might be controlled to point a solar cell array. As an additional step, the array might be gimballed for elevation control. The decrease in power supply size thus accomplished by one or both of these steps must be examined in the light of increasing complexity of the controls, and this has also been a subject for study.

The study program objectives have been met in all of the areas discussed above. Moreover, it is seen that an important gain in satellite control reliability and a reduction in weight can be achieved by combining magnetic actuation with the gravity gradient and a ground-based approach to computation and control.

2.0 SCOPE OF THE STUDY PROGRAM EXTENSION

The second phase of the study program has involved the following areas, which will be more specifically defined in this section:

(1) Gravity gradient and electromagnetic attitude control.

(2) Earth's magnetic field and solar sensing.

(3) Ground-based control and computation.

(4) Solar array control.

(5) Further investigation of the reaction wheel and magnetic actuation combination with application to orbits having periods of 12 and 24 hours.

(6) The constancy of the earth's magnetic field, particularly at synchronous altitude.

The work of item (1) above (described in section 4) covered orbits with 6,12, and 24 hour periods. The first two cases were simulated with an analog computer to define performance; the third case was directly calculable since the earth's field was assumed stationary with respect to the satellite. The control simulations were performed parametrically with respect to gravity gradient torque, disturbance level, and system gains. In addition, the system response to large initial errors was examined. The system performance in a detumbling mode was also studied.

Item (2) (see section 5) has to do with determining the methods by which sun sensors and magnetometers might be substituted for horizon scanners and gyros to improve reliability. The mechanizations derived are applicable to any orbit, within the limitations imposed by the findings of section 9, which covers task (6) above and deals with the degree to which the earth's

magnetic field is time-varying at various altitudes. While such a variation is not at all deleterious for electromagnetic actuation, it obviously affects adversely the sensing of attitude by means of magnetometers.

Item (3) is detailed in section 6. An overall ground control system plan is followed by a mechanization plan for the satellite-borne equipment (including reliability and weight estimates) and a data link and ground equipment feasibility estimate.

The findings of task (4) are given in section 7. Three solar cell array mechanizations were compared on the basis of weight, size, and reliability. The first mechanization was a non-oriented array; the second was partly oriented in that the vehicle was rotated about its vertical axis (yaw axis) for sun pointing; the third was fully oriented by providing one axis relative motion between the array and the vehicle in addition to the yaw control of the second. Hence, three hardware areas were studied: the power supply, the yaw control, and the array control.

In the initial phase of the study program prior to the May 1, 1962 report, the indirect electromagnetic actuation system (reaction wheels dumped by magnetic actuators) was evaluated for the six-hour orbit. Task (5) above (see section 8) extends this work to the 12 and 24 hour orbits. In the latter case, because of the direction of the earth's field, a technique for using solar pressure in removing unwanted pitch momentum is considered.

Conclusions concerning all of the tasks and recommendations for further work are gathered in section 3.

3.0 CONCLUSIONS

The principal conclusions will be summarized in this section.

3.1 New Methods of Attitude Control

When the performance of the system using the combination of torque coils and gravity gradient is compared to the results obtained previously for the coils-only system, a considerable improvement in satellite orientation accuracy and in ability to cope with disturbance torques is seen. With typical gravity gradient vehicle structures and pessimistic constant disturbance torques, the largest vehicle orientation errors are on the order of 1° or 2° for a 6-hour orbit and 2° or 4° for a 12-hour orbit. The system is thus one providing intermediate control accuracy (more accurate than coils only and less accurate than wheels plus coils) and extremely reliable actuation components, while eliminating the vertical sensor (i.e., horizon scanner). However, there must still be a measurement of the satellite momentum, and if all control functions are self-contained in the vehicle, three rate gyros must be included. Moreover, the rates to be measured are quite low, beyond the capability range of piezoelectric gyros, thus apparently making it impossible to take advantage of the reliability improvement these gyros may offer. Therefore, unless some further step is taken to eliminate the gyros, the reliability improvement in the actuation elements (represented by magnetic torquers and gravity gradient) will be masked by a rate-sensing unreliability.

Some sensing techniques which can be much more reliable than the gyros are an R-F interferometer method for communications satellites, a map-matching method for meteorological satellites, or the combined use of a sun sensor and magnetometers for either. However, these techniques either require a ground-based function or imply one because the desired signals are not sensed directly,and the necessary manipulations of the signals

are too complex for satellite operation without defeating the purpose of achieving good reliability. One of these methods, the sun sensor and magnetometer method, has been studied in detail and found to be very satisfactory from a reliability and weight standpoint and probably adequate from an accuracy standpoint for altitudes up to approximately 11,000 miles. For higher altitudes the increasing uncertainty of the earth's magnetic field would probably cause intolerable errors in sensing.

Turning to the ground control aspects of the system, however, and assuming an orbit such that the sun and magnetic field sensing combination is appropriate, two conclusions can be made. First, the satellite-borne control equipment, without any redundancy, has an estimated reliability of 92% probability of success for one-year operation. This equipment, which consists of the magnetic torquers, the sensors, the telemetry and command systems, and other control electronics, would weigh approximately 21.5 pounds. These reliability and weight characteristics represent a very significant advance from conventional control methods. Secondly, it has been concluded that the ground-based computation is feasible with several types of existing equipment.

3.2 Further Wheels-and-Coils System Study

The general conclusions reported previously for six-hour orbit application of the wheels-and-coils system are also applicable for the 12-hour orbit. In this system, momentum is removed from the reaction wheels by magnetic torquers. Because the magnetic field is weaker at the higher altitude, the optimum combined weight of wheels and coils in the 12-hour orbit is approximately 2-½ times that in the 6-hour orbit for a given disturbance level. However, some of the disturbance causes are also lower in magnitude at the higher altitude, which would tend

to compensate for the weaker field.

3.3 Solar Array Orientation

Fully and partly oriented an non-oriented array configurations were considered for a communications satellite, and the partly oriented array method was found to be best. The size and weight for the non-oriented case was found unreasonable, whereas the complexity of the fully oriented case proved questionable. For the partly oriented method, the earth pointing satellite is rotated about the vertical to point the solar array as nearly as possible toward the sun.

3.4 Recommendations For Further Work

The control system combining electromagnetic actuation with gravity gradient and ground control has important advantages in reliability and weight for earth-oriented satellites. Its performance capabilities and feasibility have been determined in general and with regard to several detailed areas, but the development of the system is certainly not complete. The findings to date on this system give hope that a real advancement in reliability can be made, and it is strongly recommended that further work be done. This further work could be done in a series of steps, as follows:

(1) Additional feasibility studies;

(2) Planning for in-space evaluation;

(3) In-space evaluation

These three steps will be divided into sub-tasks and explained in the following paragraphs.

3.4.1 Tasks Related to Feasibility

(1) Further Technical Definition of Ground Control Equipment

As a result of the present studies, the equations which describe the functions to be performed by the ground control equipment have been

defined. A study must then be made to determine the best method of mechanizing these equations. One solution would involve the use of magnetic tape storage for signal ephemeris with the computation being done with analog computing equipment. Another employs a digital computer which computes each data point using the Jensen and Whitaker program and a solar program. The final result might also be that a combination of digital and analog equipment is best from the standpoint of cost, availability, accuracy, and ability to meet overall requirements.

(2) Computer Study of Non-Linearities

An analog computer study must be made to determine the system performance under actual operation conditions. The study should include the effects of delays and availability of ground stations in the selected orbit and the system non-linearities. These include sensor thresholds, blackouts, and on-off control technique of coil torques as well as the delays in transmission and computation.

(3) Determination of Ground Control Station Availability, Manpower, Logistics, and Economics

A survey must be made of existing tracking stations to determine tracking, communication, and computing capabilities which have application to the overall control system. The availability of this equipment for the intended in-space demonstration must be established. The overall manpower and equipment requirements must be specified which will define both the economic and technical feasibility.

(4) Construction and Evaluation of Solar Sensor

All of the equipment required for the operation of the control system is essentially off the shelf with the exception of the solar sensor described in section 5. Assuming that the sensing plan will, in fact, employ a sun sensor

and magnetometers, then the various preliminary designs evolved in the previous study must be further studied to determine comparative size, weight, power, reliability, and performance. Then the design selected for use should be built and tested.

(5) Orbit Position Control Study

The use of a plasma, ionic or other mass dispensing actuator should be investigated to meet the requirement of the intended 6-hour mission, and its characteristics will be documented for use in the satellite design.

(6) Payload Magnetic Characteristics

A survey should be made of the expected payload magnetic leakage flux and its effect on magnetometers; conversely, the possible effect of the magnetic acutator fields on the payload should be examined.

3.4.2 Tasks Related to Demonstration Program Planning

(1) Preparation of Detailed Program Plan

This task would include the complete specification of the program. The manpower, equipment, costs, schedules, facilities to be used, operating procedures, and testing methods should be defined.

(2) Preparation of Component and Systems Specifications

Each item of hardware should be defined electrically and mechanically, and the performance, life and environmental capabilities of the equipment should be specified.

3.4.3 Tasks Related to Demonstration in Orbit

(1) Design and construction of satellite

(2) Qualification test of in-space hardware

(3) Laboratory evaluation of overall system

(4) Preparation and dissemination of detailed operating procedure to tracking stations

(5) Mock satellite control test using global communication network and tracking station ground computational facilities

(6) Launching of test satellite

3.4.4 Principal Satellite-Borne Equipment

The principal on-board attitude and orbit control equipment, with intent to avoid complexity, would be as follows:

Sensors

Solar sensors and magnetometers

IR earth horizon scanner

RF attitude sensing equipment

Actuators

Coils

Orbit control thruster

Communication Link

Transmitter

Receiver

Several independent means of sensing attitude would be provided, as shown above, for the prupose of making comparative checks.

3.4.5 In-Space Evaluation

The following is a very brief listing of the information to be obtained from an orbital test of the control system:

(1) Assess Long Term Accuracy and Rate Control Capability

During the one year life in orbit, the attitude errors of the satellite would be measured with the angular rates, to ascertain the performance of the combination gravity gradient and electromagnetic actuation system.

(2) Determine Motion Predictability and Disturbance Torque Capability

Prior to launching the vehicle, the disturbance torques to which it will be subjected would be measured and defined as precisely as possible. Then when the satellite is injected into orbit and has been despun, subsequent motion of the satellite in the absence of control torques should be predictable. It is intended that this predictability be checked, and in so doing true data on the magnitude of disturbance torques in space will be obtained. This information will be helpful to all attitude control system designers.

It is worthy of note that with a coil actuation system, precise low level torques can be generated thus making the measurement of disturbance torques possible. Usually, with a mass-dispensing actuation system, the effects of disturbance torques are masked in the limit cycle oscillation.

(3) Evaluation of Magnetic Yaw Angle Control

Heretofore, it has been common practice to measure yaw angle errors with a gyro and use a mass-dispensing device to effect corrections of a yaw angle error. In this system, the yaw angle error would be measured with static sensors and the corrective torques will be generated by the electromagnetic actuators.

(4) Evaluate Passive Sensory Techniques

At least three independent techniques of measuring satellite attitude are planned for incorporation into the system. These include:

(a) Solar Sensor and Magnetic Field

(b) R.F. Interferometer Technique

(c) I.R. Scanner

If power, weight, and space considerations prove favorable, a TV camera tube would also be incorporated. The intent of using multiple techniques is to assess the accuracy and reliability of each technique. The R.F. interferometer technique is particularly interesting for possible application to communication satellites. Also, the TV tube technique has application to Aeros. The solar sensor and magnetometer technique may have application to any vehicle at altitudes where the magnetic fields are known or predictable (e.g., Samos and Midas).

(5) Determination of Operational Limits and Most Desirable Operating Procedure.

(6) Reliability and Operating Costs.

4.0 THE COMBINATION GRAVITY GRADIENT AND ELECTROMAGNETIC ACTUATION SYSTEM

The performance of the combination gravity gradient and electromagnetic actuation system was determined in six and twelve hour orbits and its feasibility in the synchronous equatorial orbit was also established. In the synchronous orbits, the steady state position accuracy and angular rate behavior were determined using a number of vehicle configurations, disturbance torque levels, and control loop gains. In addition, the response to large angular errors was obtained together with the transient detumbling characteristics. The procedures employed and the results obtained are given in the following paragraphs.

4.1 Performance Analysis

4.1.1 Basic Relationships

The first step in proceeding with the system simulation was to establish the vehicle configuration which in turn defines the magnitude of the gravity gradient torque. The expression for gravity gradient torque in terms of the mass distribution of the vehicle is given as follows:

$$T_{gg} = 3/2\,\omega^2\,(I_x - I_z)\,\sin 2\alpha \times 13.55 \times 10^6$$

T_{gg} = gravity gradient torque - dyne-cm

ω = orbital rate - radians/sec.

I_x = roll moment of inertia - slug-ft.^{2}

I_z = yaw moment of inertia - slug-ft.^{2}

α = angular displacement from the vertical - degrees

If a body as shown in Figure 4-1 is assumed, then the gravity gradient torque is 21.6 dyne cm/degree in the six hour orbit. The gravity gradient torque on this vehicle as a function of altitude is given also in Figure 4-1.

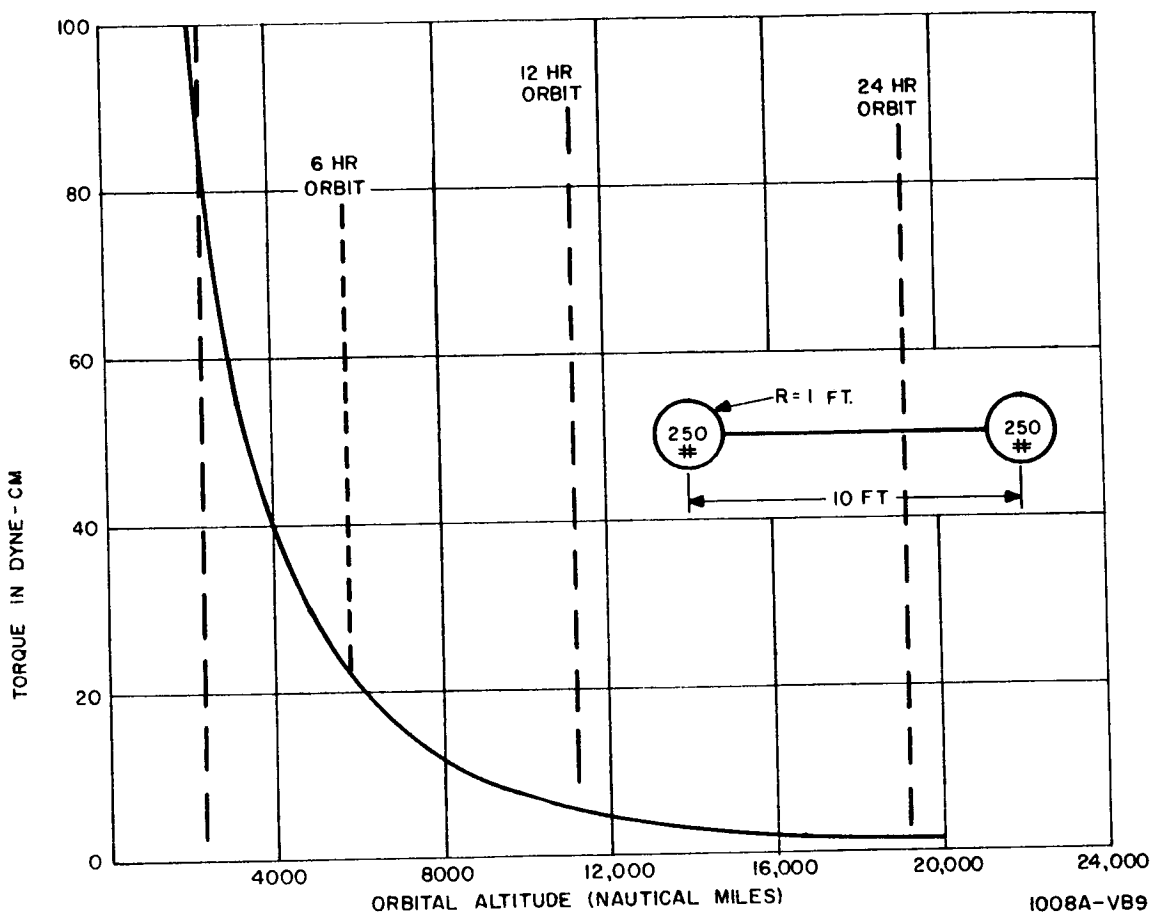

Figure 4-1 Gravity Gradient Torque vs. Altitude

For the nominal vehicle then the moments of inertia were assumed to be:

I_x = 388 slug-ft.^{2} - roll moment of inertia

I_y = 388 slug-ft.^{2} - pitch moment of inertia

I_z = 38.8 slug-ft.^{2} - yaw moment of inertia

which yields approximately the gravity gradient torque as shown in Figure 4-1.

The equations which describe the angular motion of the vehicle were then written with respect to the orbit axes, wherein the roll axis (x) remains in the orbit plane perpendicular to the local vertical, the pitch axis (y) is perpendicular to both the local vertical and the orbit plane, and the yaw axis (z) lies along the local vertical. For purposes of steady state performance, the angular errors between the vehicle axes and the orbit axes were kept small and the equations which describe the angular motions of the vehicles are given as follows:

$$I_x \dot{p} = T_{dx} + T_{mx} + T_{qq} + I_y(q + q_o)r - I_z r\,(q + q_o)$$

$$I_y \dot{q} = T_{dy} + T_{my} + T_{qq} + I_z rp\; I_x pr$$

$$I_z \dot{r} = T_{dz} + T_{mz}$$

p, q, r - vehicle angular rates

T_{dx}, T_{dy}, T_{dz} - disturbance torque components

T_{mx}, T_{my}, T_{mz} - electromagnetic control torques

T_{gg} - gravity gradient torque

The equation which describes the electromagnetic torques is given as follows:

$$\vec{T} = T_{mx} + T_{my} + T_{mz} = \vec{B} \times \vec{I}$$

$\vec{B}$ = Earth's field vector

$\vec{I}$ = Coil current vector

The coil current vector is further defined as follows:

$$I_{cx} = K_1 (M_y B_z - M_z B_y) + K_2 (\Psi)$$

$$I_{cy} = K_3 (M_z B_x - M_x B_z)$$

$$I_{cz} = K_4 (M_x B_y - M_y B_x)$$

I_{cx}, I_{cy}, I_{cz} - Coil Current Components

K_1, K_2, K_3, K_4 - Gain Constants

M_x, M_y, M_z - Components of Vehicle Angular Momentum

B_x, B_y, B_z - Earth's Field Components

Ψ - Yaw Position Error

The analogue computer simulation of these equations is shown in Figure 4-2. The earth's field components as measured with respect to the orbit axes were determined from the Jensen and Whitaker[-2] program and were simulated approximately with an oscillator formed by integrators 1 and 3 and inverter 15 which generates sine and cosine functions together with appropriate D.C. levels. These components are shown in Figure 4-2.

The torques acting on the vehicle were summed in integrators 2, 5, and 6 and the angular rates p, q, and r were generated. The angular rates were integrated in 7, 4, and 19 to generate the angular errors ϕ, θ, and Ψ .

[-2] See Section 9.1 of this report.

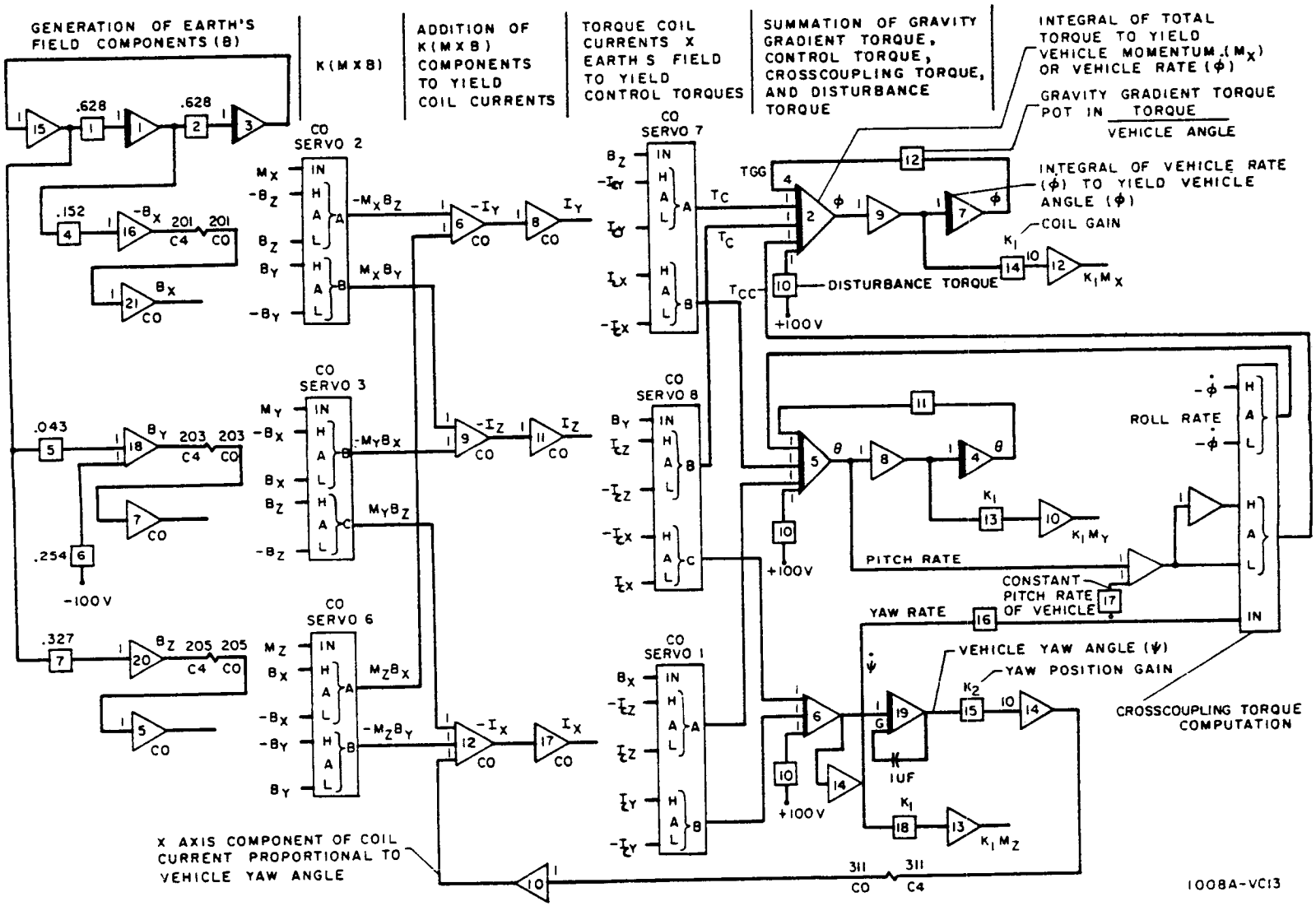

Figure 4-2 Analog Computer Simulation

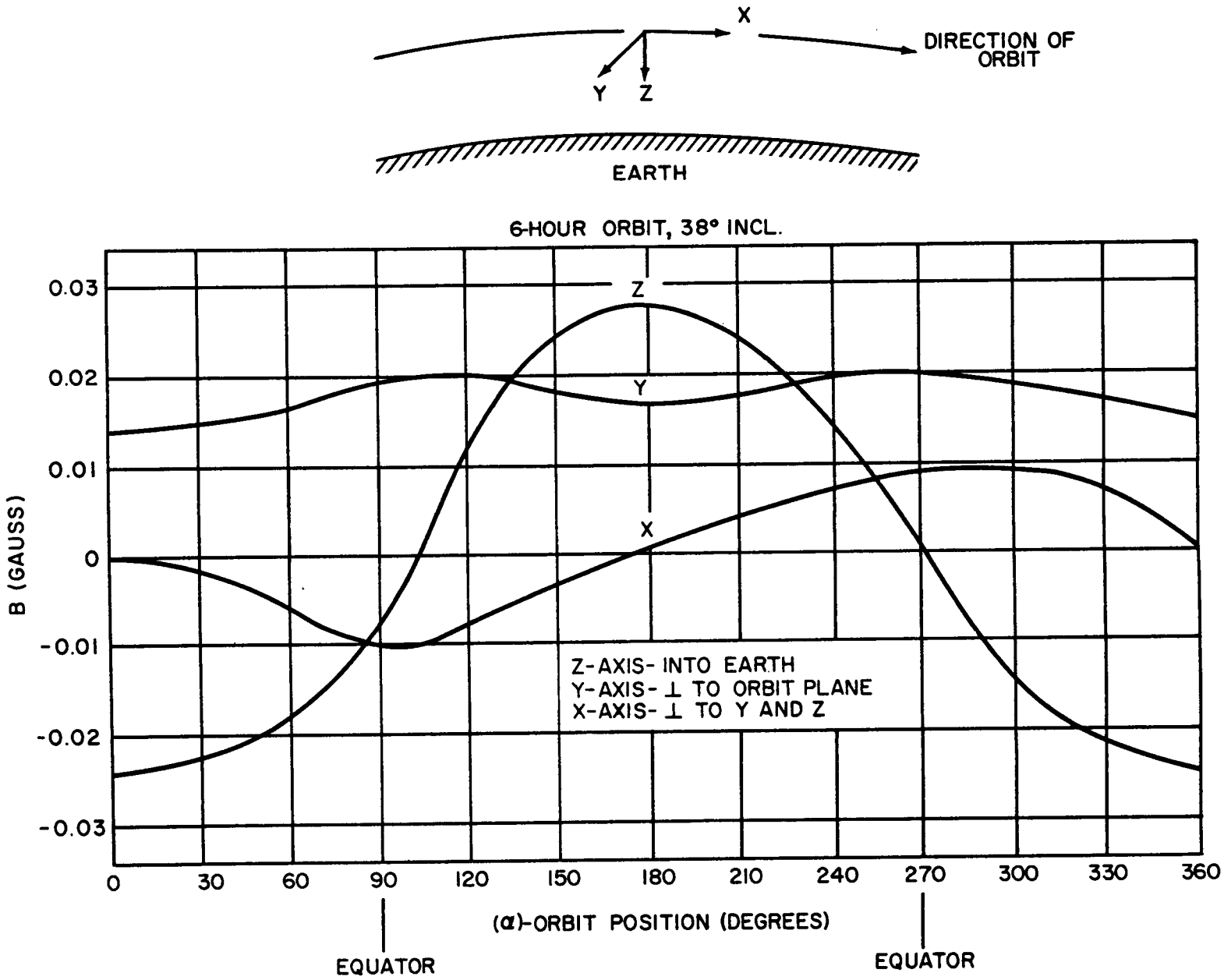

Figure 4-3 Earth's Field Components

The angular rates were multiplied by the appropriate field components in servo multipliers 2, 3, and 6 to generate the coil current components. The components in servos 7, 8, and 1 were used to generate the componenets of torque on the vehicle. A signal proportional to the yaw angle error was also introduced into the inverter 12 to generate an x-axis coil current proportional to yaw angle error. Signals proportional to ϕ and θ were also introduced into the roll and pitch torque integrators respecitvely to simulate the effects of gravity gradient torques. The cross coupling torque between the pitch and roll axes were generated by the cross coupling servo which is driven by yaw rate (r).

4.1.2 The Six-Hour Orbit

In proceeding with the simulation, a vehicle in which $I_x = I_y = 10\ I_z$, yielding a gravity gradient of approximately 25 dyne-cm per degree in a six hour orbit, was assumed. A disturbance torque of 25 dyne-cm was continuously applied about each axis of the vehicle and the rate and position errors were recorded as the rate and position gains were varied in the process of determining the optimum gain combination. The following curves are pessimistic in that they were prepared with the indicated level of disturbance torque applied constantly about each axis of the vehicle (in an actual space application, they are not constant, but sinusoidal) and the resultant errors are larger than a reasonably designed vehicle would experience. The object here was to evaluate the performance of the coils and gravity system under very adverse conditions. Figure 4-4 shows the peak position errors plotted as a function of rate (K_1) and position (K_2) gain. It may be observed that the pointing accuracy improves as the rate or momentum transfer gain is decreased for a given value of yaw position gain. Also, if the yaw position gain is raised to a high level, the system becomes unstable. This latter result is to be expected since in certain portions of

the orbit a strong component of B_z exists which reacts with the x-axis coil current due to position error to produce a destabilizing component of torque. When the yaw position gain is raised to a level such that more unwanted momentum is added to the system in a given orbit than the momentum transfer system can return to the earth, then the vehicle must tumble. The former result is also to be expected since the position and rate loops act independently of one another. As is shown, the consequence of more rapid momentum transfer is larger position errors.

As the gravity gradient torque is increased to 50 dyne-cm per degree, an improvement in position accuracy results for corresponding values of rate and position gains as is shown in Figure 4-5. The effect of increasing the gravity gradient torque is similar to increasing the position loop gain in a linear servo which normally results in a reduction of the position error.

A similar set of curves was obtained for gravity gradient torques of 10 and 5 dyne-cm/degree in the six hour orbit which reflects a vehicle with more equal moments of inertia. Figure 4-6 shows the vehicle displacements which occur for a wide range of position and rate loop gains when the gravity gradient is 10 dyne cm/degree and a continuous disturbance torque of 20 dyne-cm was applied about each axis. Figure 4-7 shows similar characteristics except that the gravity gradient torque has been reduced to 5 dyne-cm and the disturbance torque has been reduced to 10 dyne-cm. These curves in effect reflect the fact that a reduction in position loop gain will increase the position error for a given disturbance torque level. It should be mentioned that the displacements shown in Figures 4-4 through 4-7 are the peak displacement errors and the average angular error is approximately half the peak error.

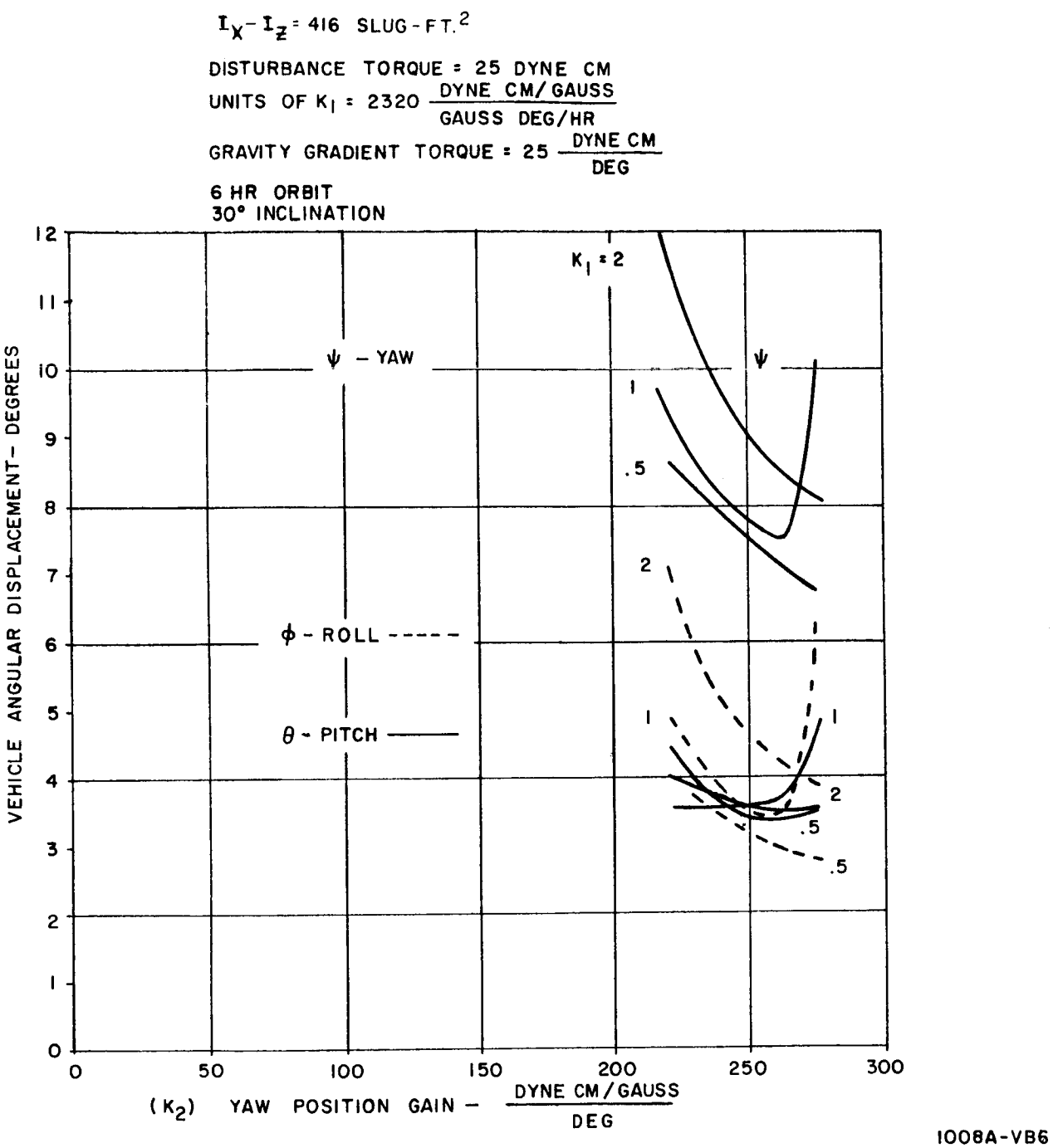

These curves are pessimistic in that they were prepared with the indicated level of disturbance torque applied constantly about each axis of the vehicle (in an actual space application, they are not constant, but sinusoidal) and the resultant errors are larger than a reasonably designed vehicle would experience. The object here was to evaluate the performance of the coils and gravity system under very adverse conditions.

Figure 4-4 Angular Errors vs. Position and Rate Gain

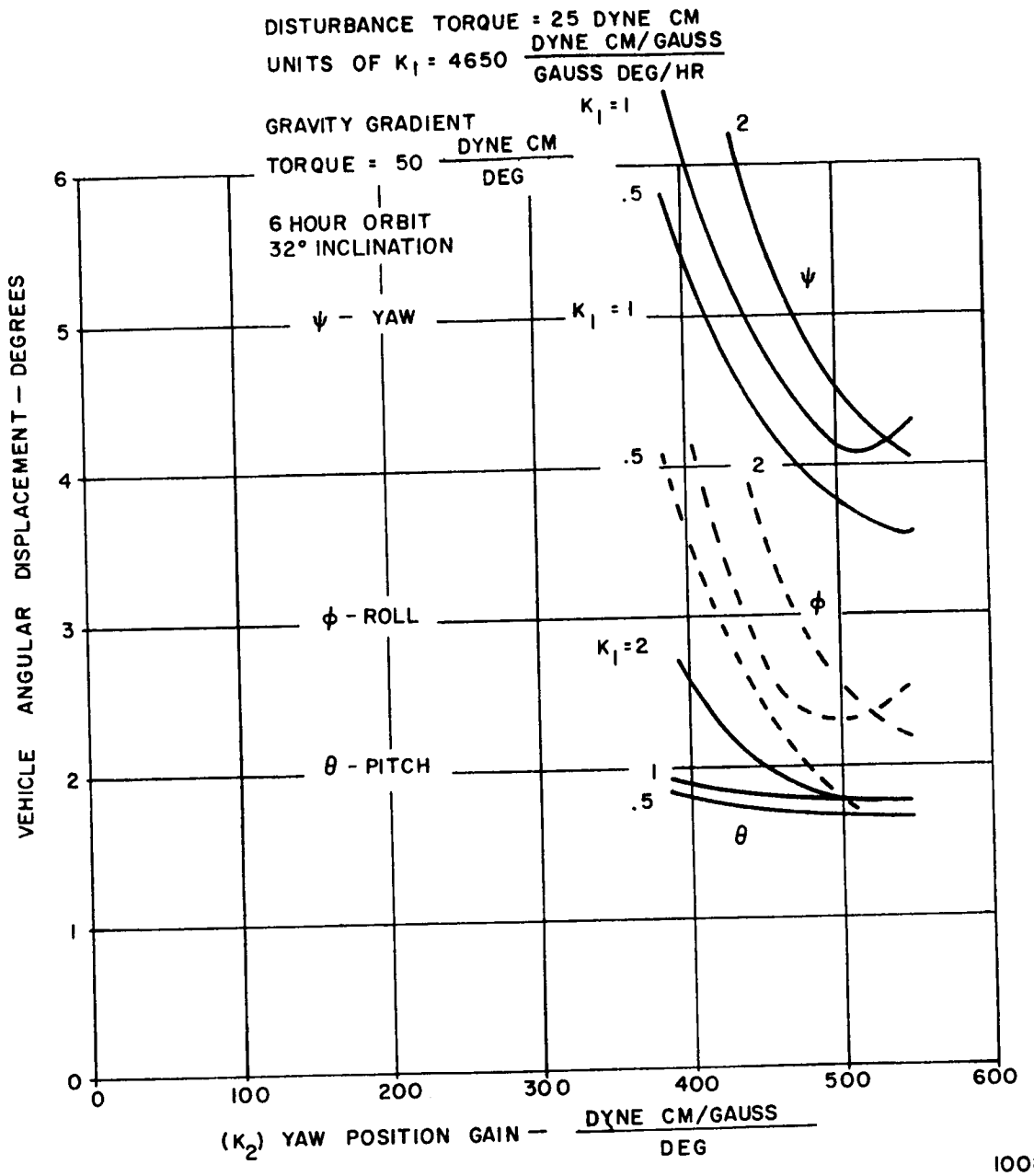

These curves are pessimistic in that they were prepared with the indicated level of disturbance torque applied constantly about each axis of the vehicle (in an actual space application, they are not constant, but sinusoidal) and the resultant errors are larger than a reasonably designed vehicle would experience. The object here was to evaluate the performance of the coils and gravity system under very adverse conditions.

Figure 4-5 Angular Errors vs. Position and Rate Gain

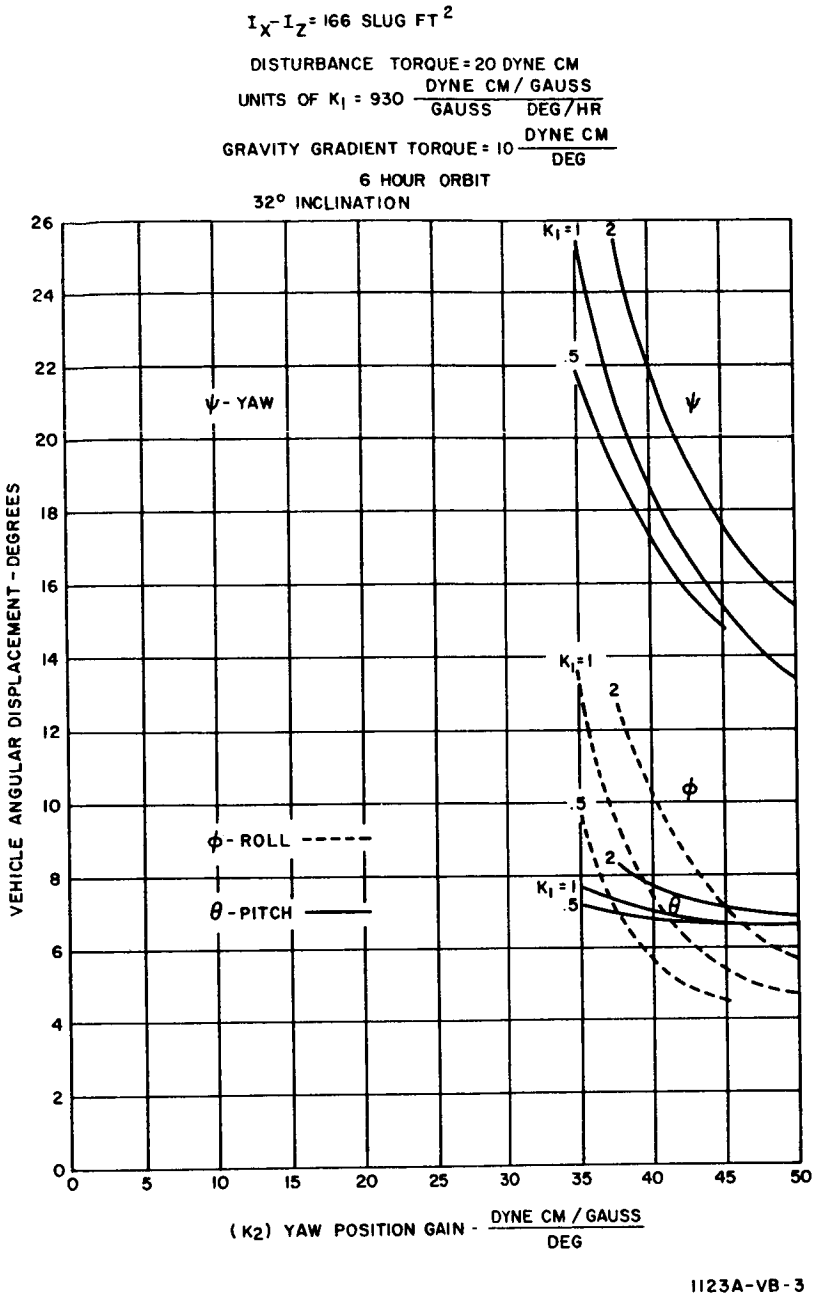

These curves are pessimistic in that they were prepared with the indicated level of disturbance torque applied constantly about each axis of the vehicle (in an actual space application, they are not constant, but sinusoidal) and the resultant errors are larger than a reasonably designed vehicle would experience. The object here was to evaluate the performance of the coils and gravity system under very adverse conditions.

Figure 4-6 Angular Errors vs. Position and Rate Gain

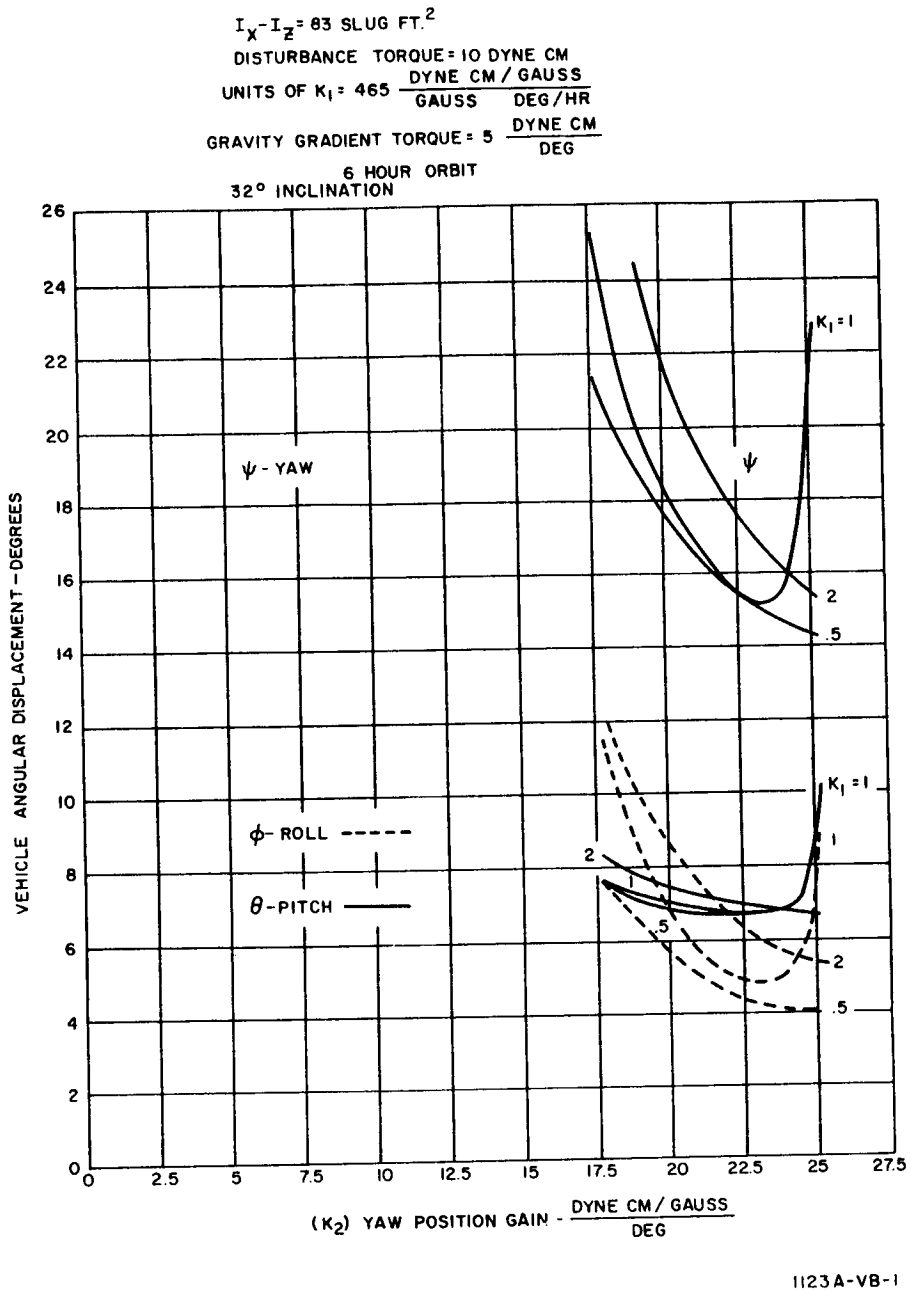

These curves are pessimistic in that they were prepared with the indicated level of disturbance torque applied constantly about each axis of the vehicle (in an actual space application, they are not constant, but sinusoidal and the resultant errors are larger than a reasonably designed vehicle would experience. The object here was to evaluate the performance of the coils and gravity system under very adverse conditions.

Figure 4-7 Angular Error vs. Position and Rate Gair

Using the data assembled in the preparation of the previous four illustrations, curves of the peak vehicle displacements as a function of disturbance torque were prepared for gravity gradient gains of 10, 25, and 50 dyne-cm in the six hour orbit as is shown in Figure 4-8. In the six hour orbit, the effects of magnetic disturbance torques is considerably reduced on any vehicle and, if care is exercised in the vehicle design to balance the solar pressure disturbance, then it should generally be possible to hold the total disturbance torque to less than ten dyne-cm. Thus, the peak roll and pitch position errors would be less than 1-1/2 degrees and the peak angular rates would be approximately 3.0 degrees per hour. The instantaneous values of the angular position errors and rate as a function of orbit position are shown in Figures 4-9 and 4-10 for gravity gradient gains of 25 and 50 dyne cm/degree, respectively, while a disturbance torque of 25 dyne-cm was applied continuously about each axis. However, for disturbances on the order of 10 dyne-cm, pointing errors can be held to approximately 1.5° and the angular rates to approximately 3.0 degrees/hour, and the way is made clear for the use of this technique in such applications as communications, meteorological, or reconnaissance vehicles where this combination of performance characteristics is generally required.

The response of the combination gravity gradient and electromagnetic actuation system to large initial errors was also examined and is shown in Figure 4-11, 4-12, and 4-13 for the six hour orbit. The damping action of the electromagnetic actuation system is clearly visible in these recordings. Approximately two days is required to damp out the initial rates of 50°/hour which were applied. This time can be shortened if it were desired by utilizing selective gain control rather than the linear system employed to obtain the recordings. Selective gain control would provide for higher loop gains when the direction of the earth's field is favorable.

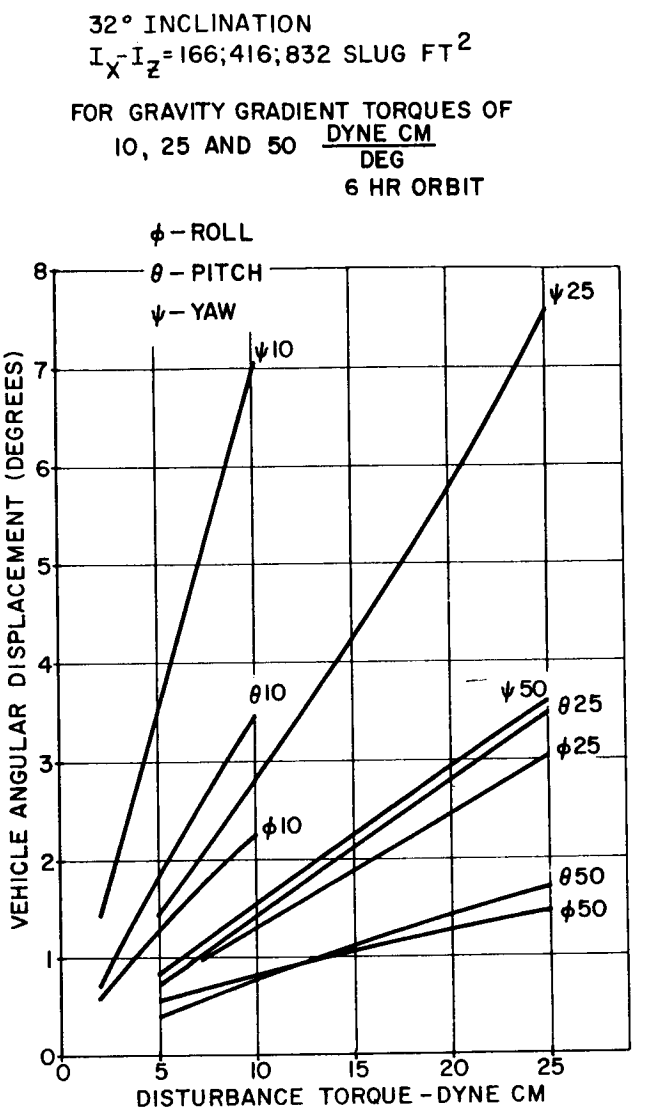

GRAVITY GRADIENT TORQUE (DYNE-CM / DEG)	K_1 DYNE-CM/GAUSS / GAUSS DEG/HR	K_2 DYNE-CM/GAUSS / DEG
10	465	478.8
25	1160	2622
50	2325	5244

1005A-VB-14

These curves are pessimistic in that they were prepared with the indicated level of disturbance torque applied constantly about each axis of the vehicle (in an actual space application, they are not constant, but sinusoidal) and the resultant errors are larger than a reasonably designed vehicle would experience. The object here was to evaluate the performance of the coils and gravity system under very adverse conditions.

Figure 4-8 Peak Position Errors vs. Disturbance

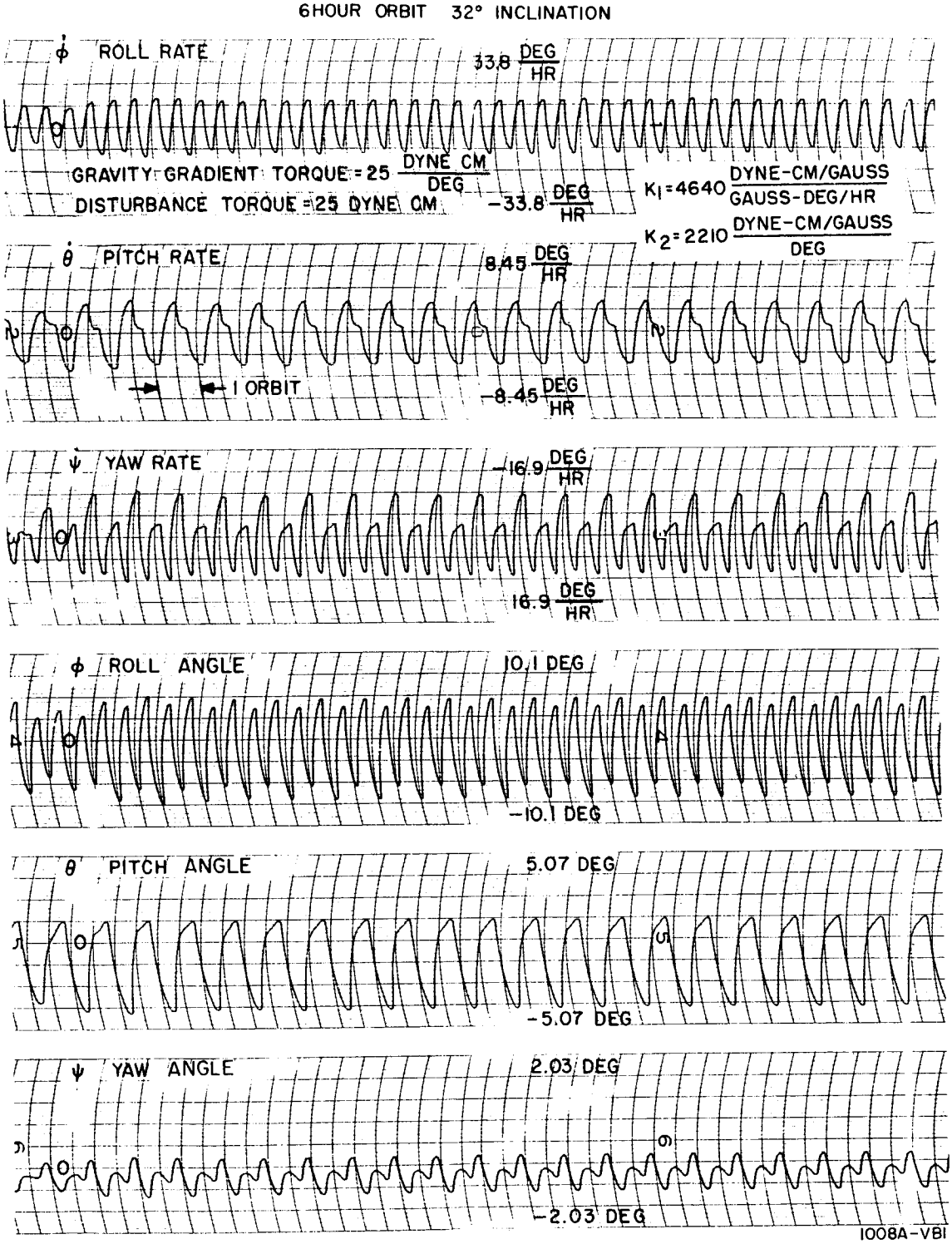

Figure 4-9 Position and Rate Errors as f(t)

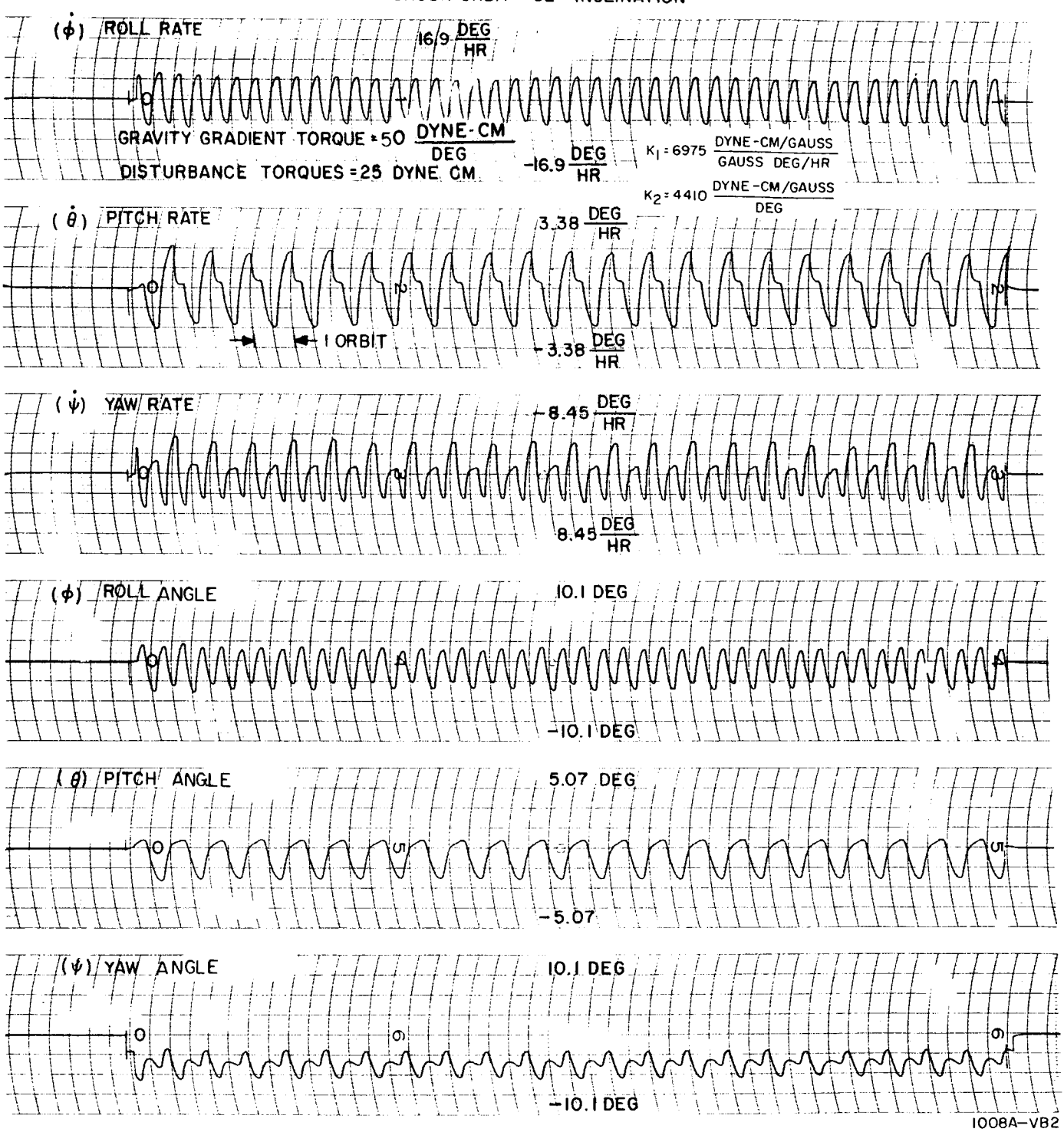

Figure 4-10 Position and Rate Errors as f(t)

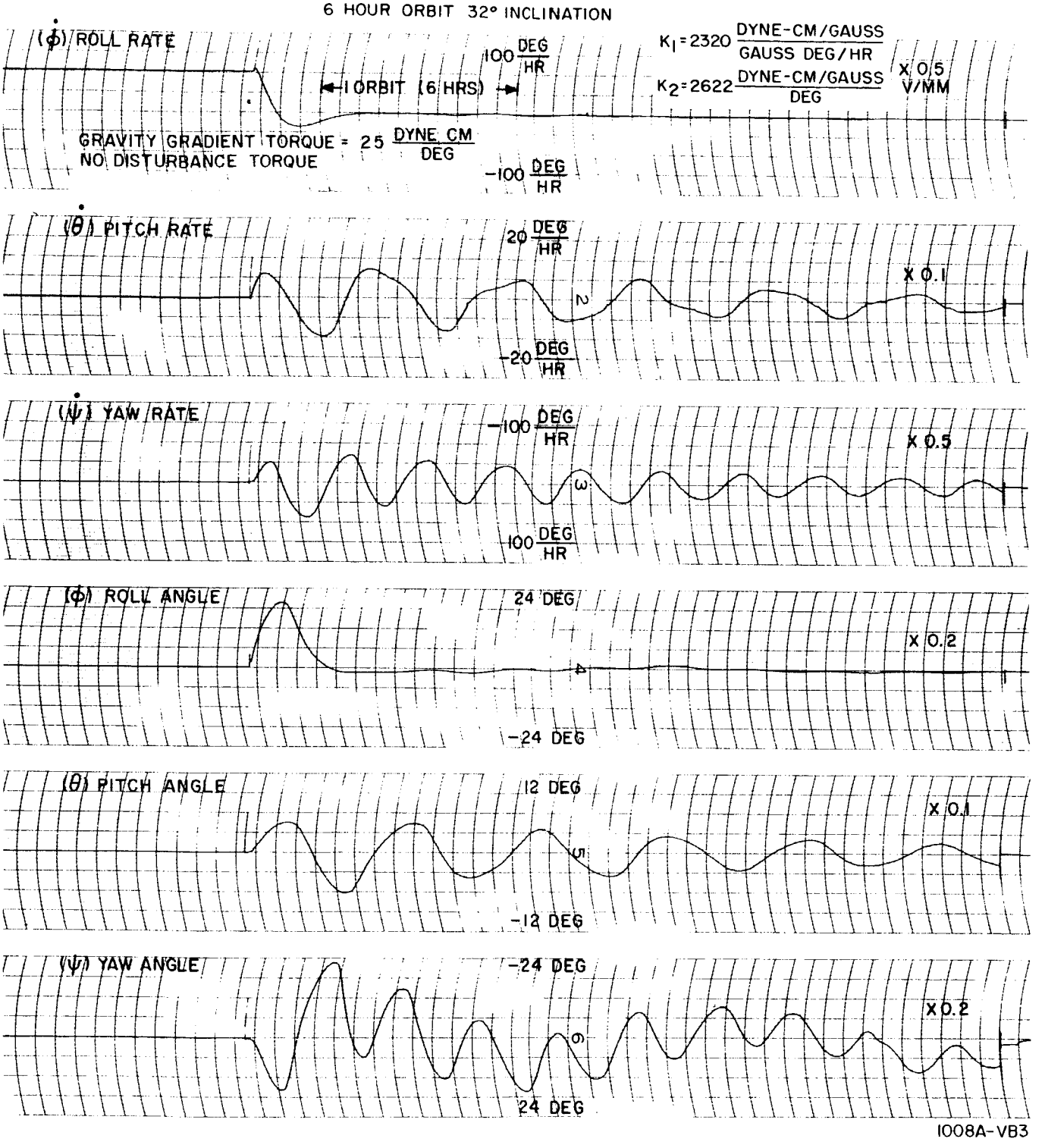

Figure 4-11 Response to Initial Roll Rate

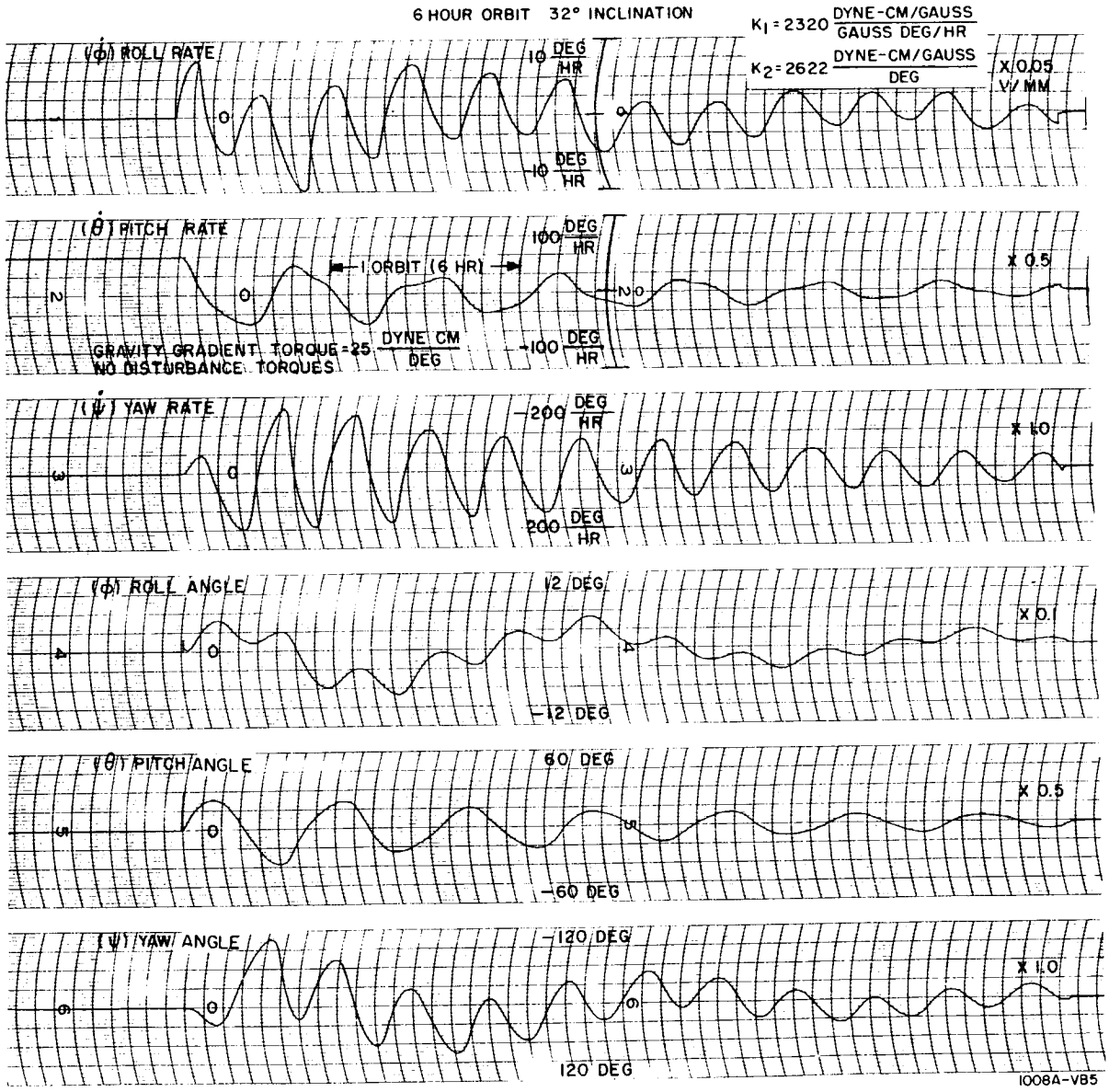

Figure 4-12 Response to Initial Pitch Rate

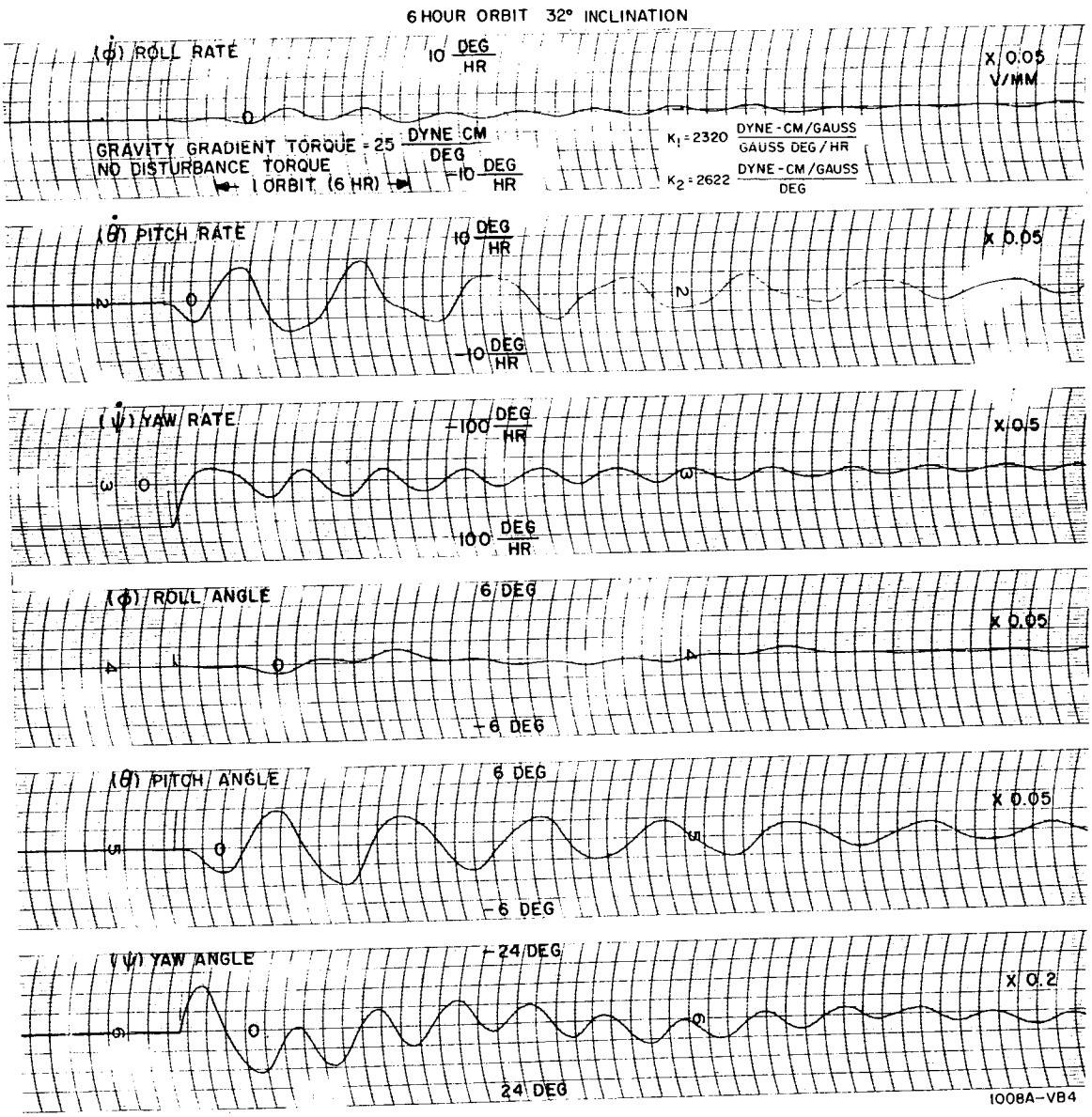

Figure 4-13 Response to Initial Yaw Rate

4.1.3 Detumbling

In order to eliminate completely the need for mass dispensing actuation systems, it was necessary that the ability of the electromagnetic actuation system to detumble the vehicle be demonstrated as well as its ability to satisfy the steady state pointing requirements. No simulation has been made of the gravity gradient and coils system in a detumbling operation. A typical vehicle was given initial rates and the time to detumble was determined as the system parameters were varied. In the case shown in Figure 4-14, the moments of inertia of the vehicle were 50 slug ft.^{2} about each axis and the rate change was from 1.0 degree/sec. about each axis down to a total vehicle rate of 50 degrees per hour. This amount of momentum change is typical of that undergone by a 500 pound vehicle during the initial detumbling phase. As is shown in Figure 4-14, the time to detumble can be reduced to less than one orbit if a sufficiently large coil is employed. However, a coil weight of three pounds will cause the vehicle to be detumbled in less than three orbits, which would be the more judicious selection of parameters in the interest of minimum system weight.

4.1.4 The Twelve-Hour Orbit

The steady state performance of the combination gravity gradient and electromagnetic actuation system was also examined in the 12 hour orbit. The vehicle displacements as a function of loop gain were determined for several vehicle configurations (i.e. gravity gradient gains) and disturbance torque levels. These characteristics are shown in Figures 4-15, 4-16, and 4-17. The gravity gradient gains employed were 12.5, 6.25, and 2.5 dyne-cm, respectively, while the disturbance torque levels were 25, 12.5 and 5 dyne-cm. The same general characteristics can be observed in the 12 hour orbit as prevail in the 6 hour orbit. Again, the vehicle displacements as a function of disturbance

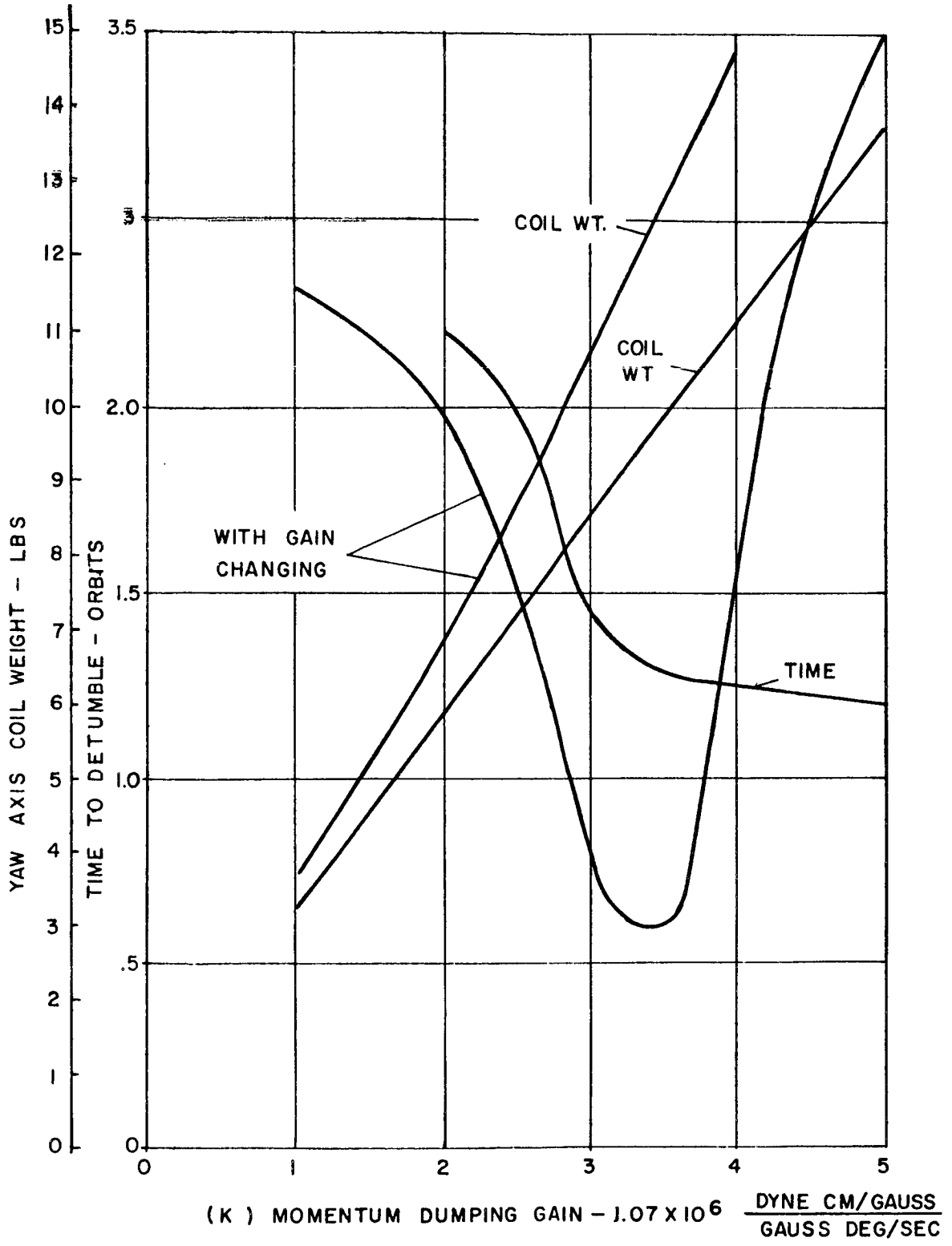

Figure 4-14 Detumbling Time vs. Actuator Weight

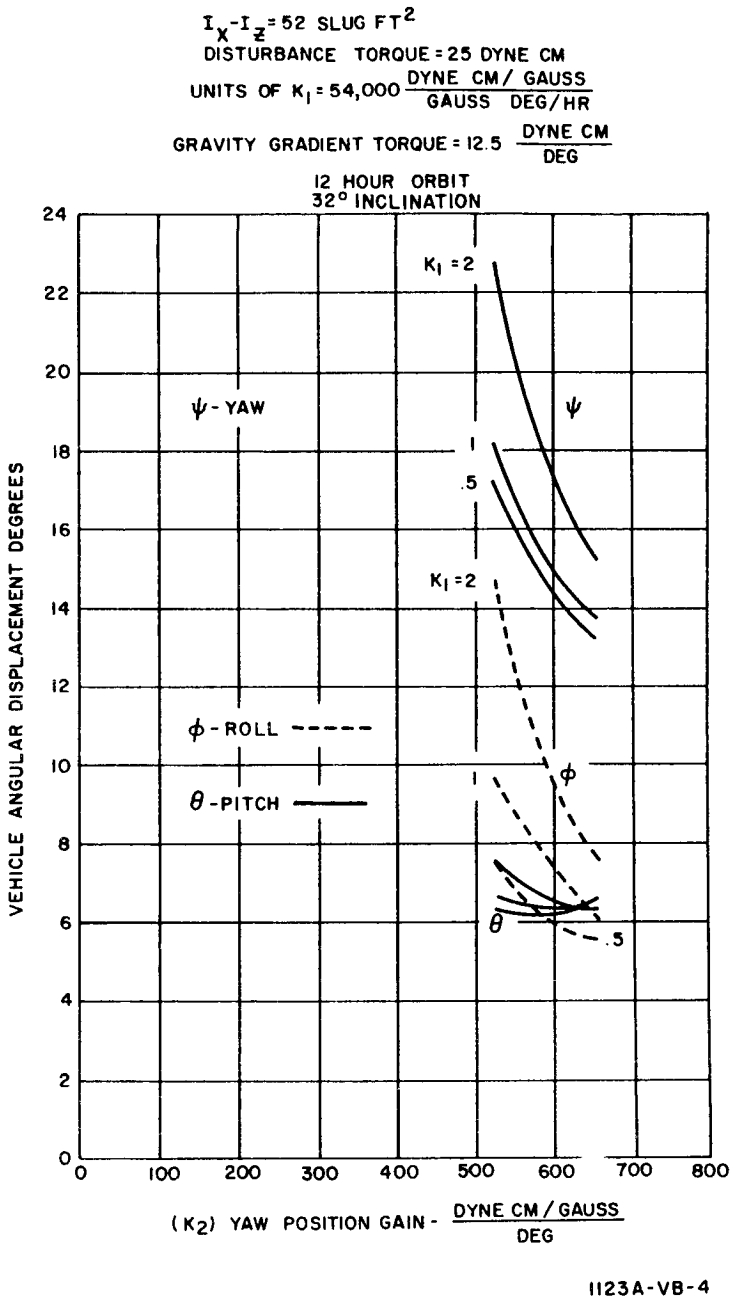

These curves are pessimistic in that they were prepared with the indicated level of disturbance torque applied constantly about each axis of the vehicle (in an actual space application, they are not constant, but sinusoidal) and the resultant errors are larger than a reasonably designed vehicle would experience. The object here was to evaluate the performance of the coils and gravity system under very adverse conditions.

Figure 4-15 Vehicle Displacement vs. Position and Rate Gain

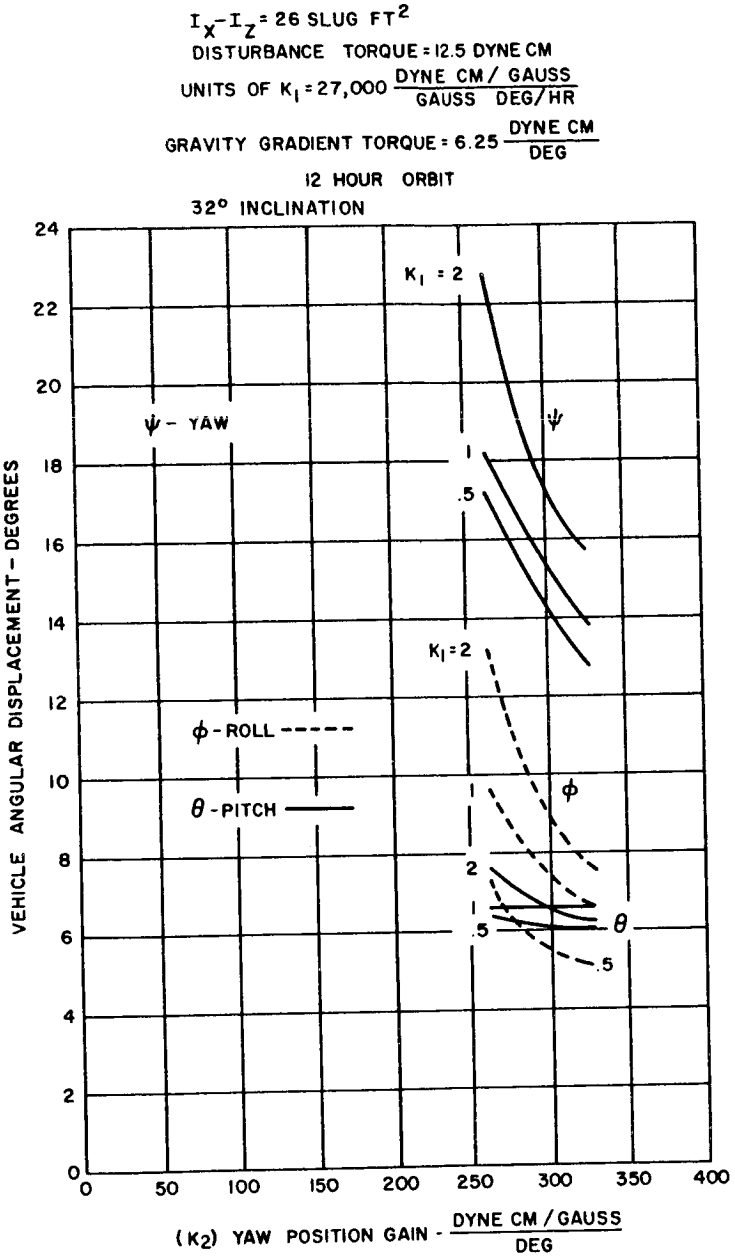

These curves are pessimistic in that they were prepared with the indicated level of disturbance torque applied constantly about each axis of the vehicle (in an actual space application, they are not constant, but sinusoidal) and the resultant errors are larger than a reasonably designed vehicle would experience. The object here was to evaluate the performance of the coils and gravity system under very adverse conditions.

Figure 4-16 Vehicle Displacement vs. Position and Rate Gain

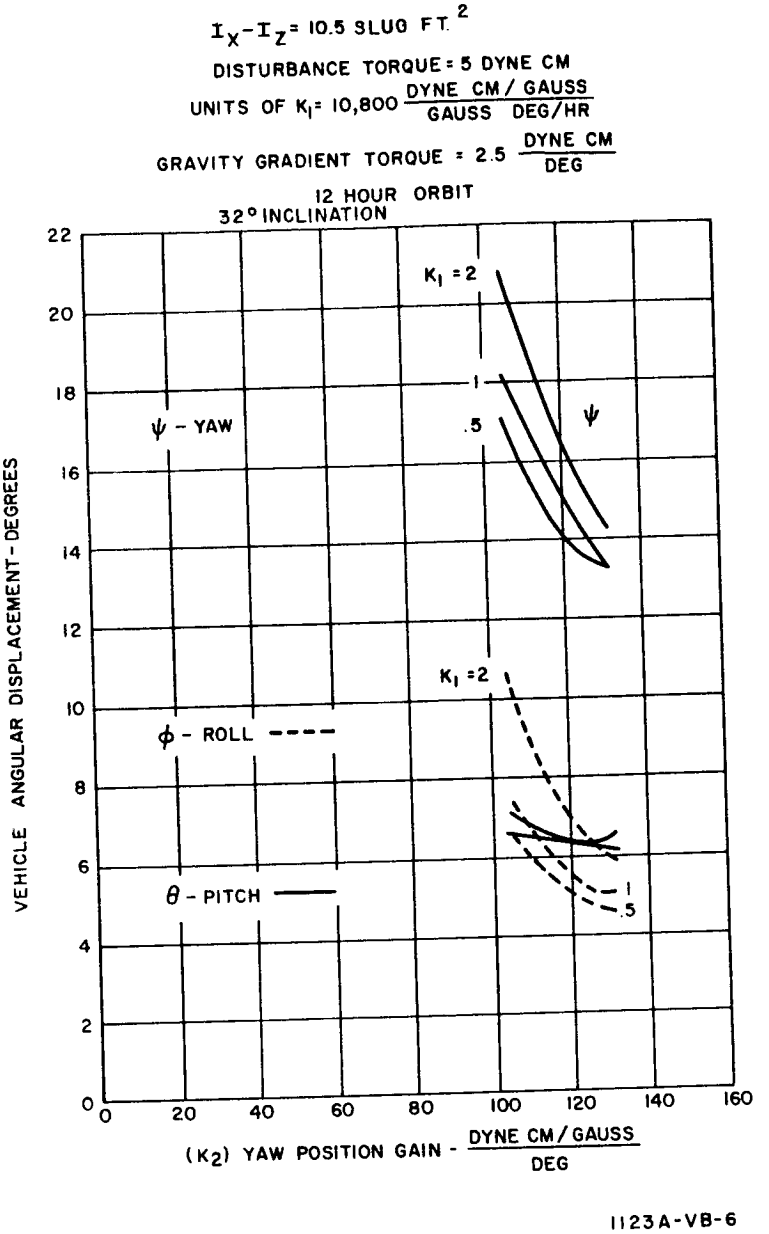

1123A-VB-6

These curves are pessimistic in that they were prepared with the indicated level of disturbance torque applied constantly about each axis of the vehicle (in an actual space application, they are not constant, but sinusoidal) and the resultant errors are larger than a reasonably designed vehicle would experience. The object here was to evaluate the performance of the coils and gravity system under very adverse conditions.

Figure 4-17 Vehicle Displacements vs. Position and Rate Gain

torque level were plotted as are shown in Figure 4-18 for each level of gravity gradient gain using the data from Figures 4-15, 4-16, 4-17. Figure 4-18 shows again that the accuracy of the technique is dependent upon the disturbance torque level and the gravity gradient gain. The instantaneous values of angular position error and rate as a function of orbit position error and rate as a function of orbit position are shown in Figures 4-19, 4-20, 4-21 for gravity gradient gains of 12.5, 6.25 and 2.5 dyne-cm per degree.

4.1.5 The Synchronous Orbit

In the synchronous equatorial orbit the control environment is considerably changed over that in subsynchronous orbits. For example, the magnitude of the gravity gradient torque is only 1/16th that in the six hour orbit and the direction of the earth's field remains essentially fixed with respect to the vehicle. Therefore, an alternate means must be provided for dumping the momentum about the axis parallel to the field direction and also damping the angular motion about that axis. One method of accomplishing this objective is to employ a reaction wheel control for damping in the one axis while the gravity gradient torque is utilized for momentum dumping. Although this is a departure from the "no moving parts" concept as was required in the synchronous orbit, the technique is feasible, and only one wheel is required.

An alternate technique of rate damping and dumping momentum in the pitch axis, which lies almost parallel to the earth's field, is the use of solar paddles as described in Section 8.3.

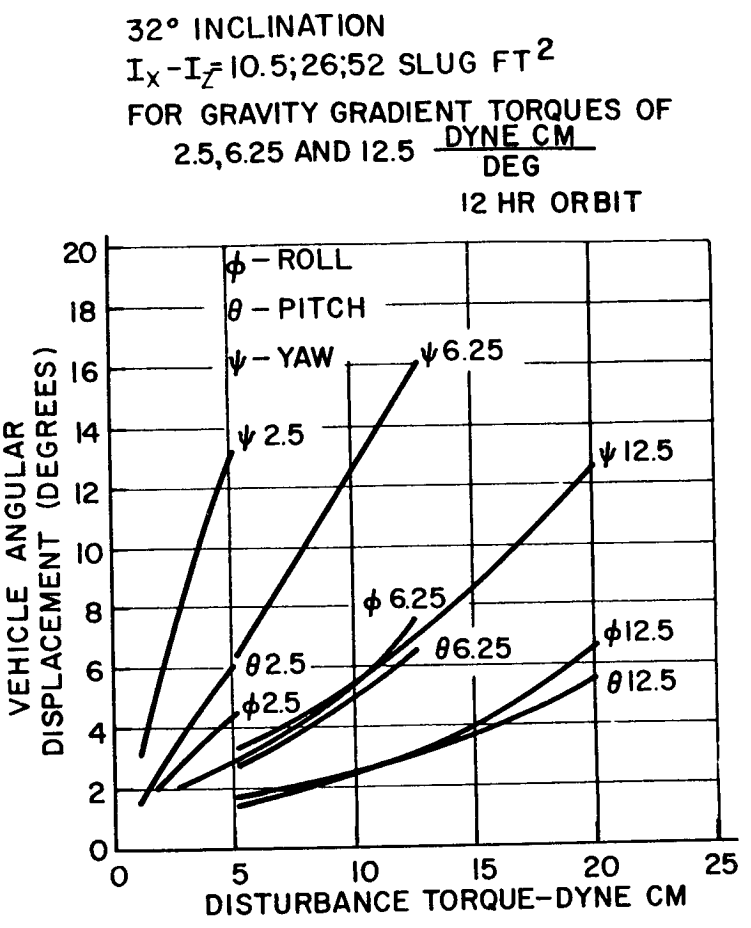

GRAVITY GRADIENT TORQUE $\left(\frac{\text{DYNE-CM}}{\text{DEG}}\right)$	K_1 $\frac{\text{DYNE-CM/GAUSS}}{\text{GAUSS DEG/HR}}$	K_2 $\frac{\text{DYNE-CM/GAUSS}}{\text{DEG}}$
2.5	5,400	126.4
6.25	13,500	316.4
12.5	27,000	332.7

1005A-VB-13

These curves are pessimistic in that they were prepared with the indicated level of disturbance torque applied constantly about each axis of the vehicle (in an actual space application, they are not constant, but sinusoidal) and the resultant errors are larger than a reasonably designed vehicle would experience. The object here was to evaluate the performance of the coils and gravity system under very adverse conditions.

Figure 4-18 Peak Position Errors vs. Disturbance

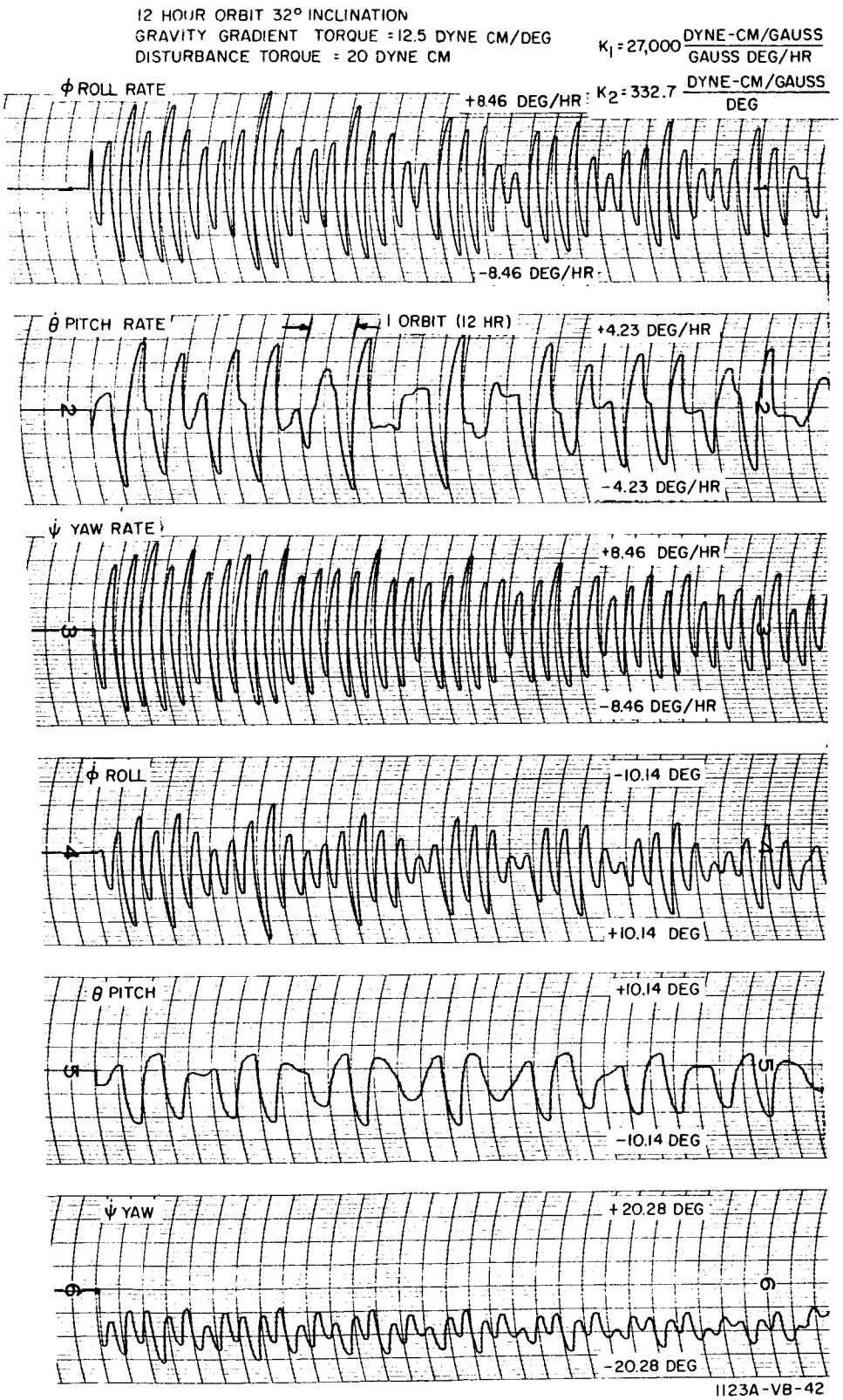

Figure 4-19 Position and Rate Errors as f(t)

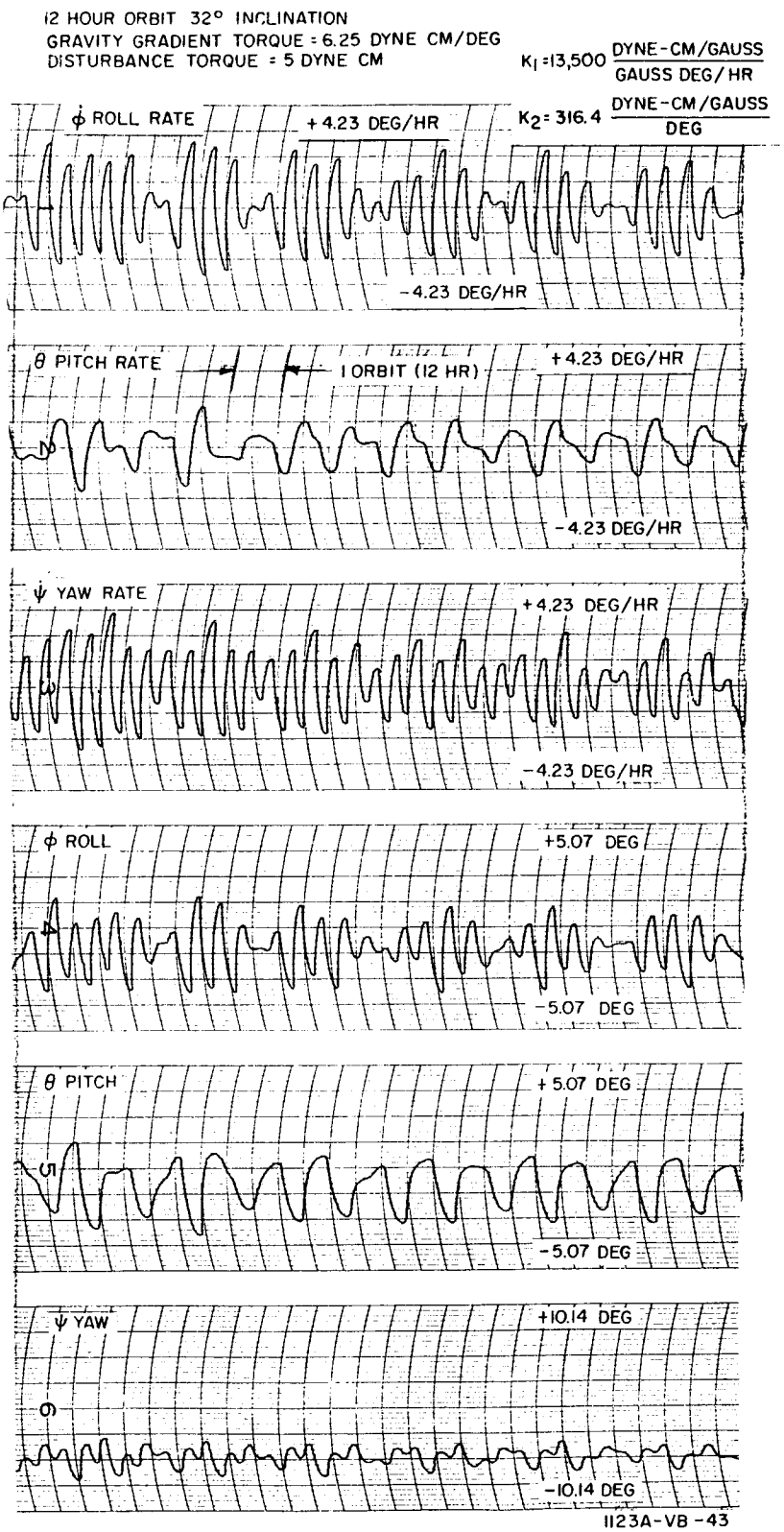

Figure 4-20 Position and Rate Errors as f(t)

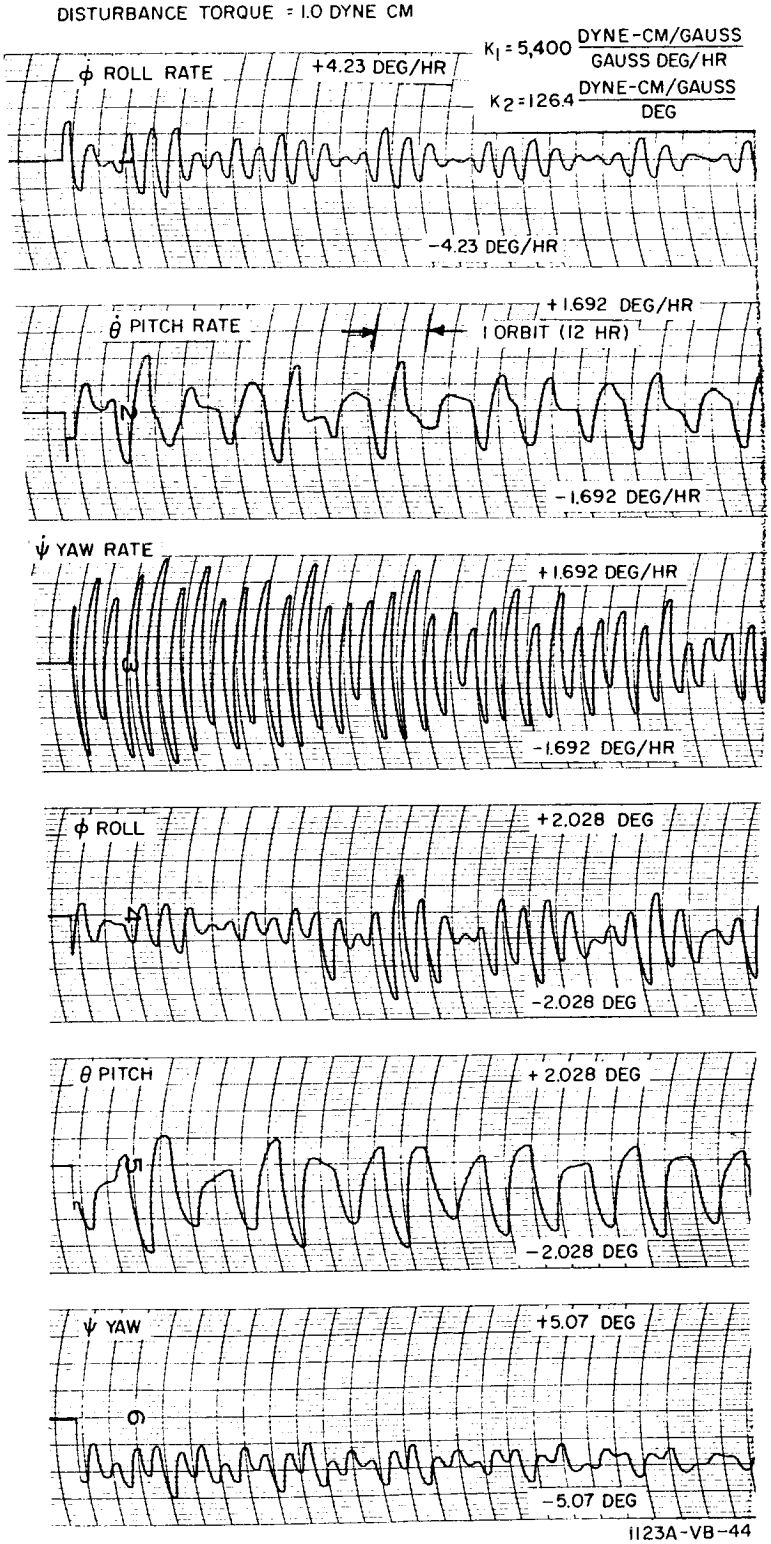

Figure 4-21 Position and Rate Errors as f(t)

4.1.6 Sample System Performance

In order to determine more realistic performance characteristics of the gravity-gradient and coils system a specific vehicle configuration was assumed and the simulations repeated. The expected disturbance torques were calculated for the vehicle configuration. These were based on careful vehicle design to reduce the disturbance torques. These disturbances were simulated by appropriate steady-state and sinusoidal components, which is more realistic than the constant disturbances assumed in the preceding simulations.

4.1.6.1 The Satellite Configuration and Disturbance Levels

4.1.6.1.1 Assumptions

A. It is assumed that adequate solar cell area is available on the satellite, to obtain 150 watts without requiring an oriented array.

B. The limiting dimensions for boost purposes are 55 in. dia., 132 in. long (Atlas-Agena). Dimensions greater than these are obtained by extending the main mass after shroud is discarded.

C. In order to make use of gravity gradients, the vehicle mass will be split into two main parts, and a dumbbell shape made, to get a ratio of about 10:1 in the yaw and pitch moments of inertia.

D. The weight will be assumed to be 500 lb., with a density of 10 lb/ft^3. (This is based on representative satellites, such as Explorer and Sputnik III.)

E. Satellite orbits will have 6, 12, and 24 hour periods.

4.1.6.1.2 Size and Shape

For these calculations, a configuration consisting of two spherical masses joined by light structural members is assumed. The radius of each sphere is calculated as follows.

$$\frac{250 \text{ lb}}{10 \text{ lb/ft}^3} = 25 \text{ ft}^3 = \frac{4\pi r^3}{3} = 4.189\, r^3 \; ; \; r^3 = 5.97$$

$$r = 1.815 \text{ ft.}$$

Allowable length is 132/12 = 11 ft.

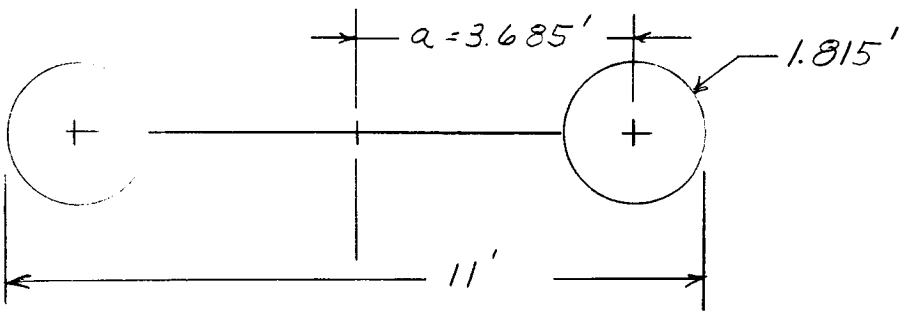

The moments of inertias are

$$I_p = \frac{2}{5} Mr^2 + Ma^2 = \frac{.4 \times 500}{32.2}(1.815)^2 + \frac{500}{32.2}(3.685)^2 = 232 \text{ slug-ft.}^2$$

$$I_y = \frac{2}{5} Mr^2 = 20.5$$

If the length of the satellite is increased from 11 ft. to 16 ft., then I_y will remain unchanged and Ip will increase to 655 slug-ft^2. In the control simulations to be described, it was found that this greater length was required in the 12 and 24-hour orbits in order to achieve an adequate gravity gradient effect.

Using the expression of page 4-1, and the length chosen above, the gravity gradient torques for the three cases are as below:

6-hr. orbit -- 363 sin 2α dyne-cm

12-hr. orbit -- 272 sin 2α dyne-cm

24-hr. orbit -- 68 sin 2α dyne-cm.

4.1.6.1.3 Disturbances

A. Internal Momentum Change

It is assumed that no motors, flaps, movable vanes, flowing coolant will be used aboard the vehicle, so that no disturbances from internal sources are present. Even compensation by contrarotating devices would leave high residual torques.

B. Aerodynamic

At altitudes above 1000 mi., aerodynamic drag forces are negligible. The lowest altitude to be considered is 5760 n.mi.

$T = \frac{\rho V^2}{2} \times A\ d \times 1.35 \times 10^7$, where T is torque, dyne-cm; ρ is density, slug/ft^3; V is velocity, feet/sec; A is area projected along velocity vector, sq. ft., and d is equivalent lever arm, ft.

At 1000 mi., ρ is 10^{-20} slug/ft^3,

$$T = \frac{(10^{-20})(2.3 \times 10^4)^2\ (24.4)(1/12)(1.35 \times 10^7)}{2} = 7.27 \times 10^{-5} \text{ dyne-cm}$$

This value is negligible.

C. Orbit Ellipticity

It is assumed that the orbit is circular. The equivalent maximum disturbance torque for an error of 10 miles at 6 hr. orbit is determined as follows.

$$\theta_M = \frac{10}{5760} = 1.735 \times 10^{-4} \text{ rad.}$$

where θ is orbital position and ω_o is the orbital rate.

$$T_{max} = \omega_o^2 I_p \varphi_M \sin\theta = (2.91 \times 10^{-4})^2 (232)(1.735 \times 10^{-4})(1.35 \times 10^7) \sin\theta$$

$$= .046 \sin\theta \text{ dyne-cm}$$

This also is negligible.

D. Solar Pressure

The maximum solar pressure possible for a unity reflectance plate normal to the sun would be 1.9×10^{-7} lb/ft^2. For a plate with zero reflectivity, the value would be half this value, or 9.5×10^{-8} lb/ft^2. If the satellite surface were carefully covered with a dull-finished non-metal, the reflectance can be made to be about .3 or less. By making the satellite as symmetrical as possible, and balancing it for coincidence of CG & CP, the solar pressure and its resulting torques can be reduced to very low levels. The reflectance can vary about 0.1 with age.

The total area is the area of two spheres plus the area of the struts, or approximately 24.4 ft^2. The total variation in reflectance will be about 0.1. If the average reflectance of one sphere exceeds that of the other by 0.04, the maximum torque would be, for pitch and roll,

$$T_{max} = (9.5 \times 10^{-8} \text{ lb/ft}^2)\left(\frac{24.4 \text{ ft}^2}{2}\right)(3.685 \text{ ft})(.04)\left(\frac{1.35 \times 10^7 \text{ dyne-cm}}{\text{lb-ft.}}\right)$$

$$= 2.2 \text{ dyne-cm.}$$

For roll, the maximum value is 2.2 sin 23.5 = 0.88 dyne cm.

For yaw, the value is

$$T_{max} = 9.5 \times 10^{-8} \times 12.2 \times .04 \times .77 \times 1.35 \times 10^7 = 0.48 \text{ dyne-cm.}$$

For the 12 and 24 hr. orbit vehicles, which are longer, the maximum values will be 3.6 dyne-cm for pitch, 1.4 dyne-cm for roll, and 0.48 dyne-cm for yaw. Note that the maximum values are given. The actual disturbances would take the form of $T = T_m \sin\theta$, where θ is the orbit angle. The exact equation would

include the shadowing of one sphere by the other occasionally, and the shadowing of the satellite by the earth occasionally.

E. Magnetic Torques

All magnetic materials will retain some residual magnetism. Since any satellite will contain some magnetic material, and the residual magnetism cannot be accurately determined for a satellite assembly, a composite test must be devised by which to determine the resultant magnetic torques. It is not practical to balance out the magnetic torques below about 100 dyne-cm on earth due to inherent test inaccuracies. It must be assumed, then, that the minimum torque in any axis may be 300 dyne-cm/gauss, in the test axis. If these values are taken, the maximum torques at the three altitudes will be

	6 hr., 30° Orbit Torque dyne-cm	12 hr., 30° Orbit Torque dyne-cm	24 hr., 0° Orbit Torque dyne-cm
Pitch	5.30	1.34	0.123
Roll	8.79	2.22	0.421
Yaw	6.65	1.69	0.371

F. Total Disturbances

The following maximum torques will be obtained if all maximum instantaneous torques add together simultaneously

	T_{max} 6 hr. orbit dyne-cm	T_{max} 12 hr. orbit dyne-cm	T_{max} 24 hr. orbit dyne-cm
Pitch	7.5	4.9	3.7
Roll	9.7	3.6	1.8
Yaw	7.1	2.2	0.9

Although the sinusoidal disturbances will rarely be in phase, the system must be capable of handling the worst combination which can occur during several year's orbiting. The worst-case time relationships are shown in Figure 4-22 for the 24-hour orbit.

4.1.6.2 Analysis

The gravity-gradient and electromagnetic coils system was simulated at 6, 12, and 24 hour orbits. The vehicle configuration assumed was dumbbell shaped as described in 4.1.6.1. The vehicle moments of inertia for the 6 hr. orbit were $I_x = I_y = 232$ slug-ft.^{2} and $I_z = 20.5$ slug-ft.^{2} For the 12 and 24 hour orbits the moment of inertia were $I_x = I_y = 655$ slug-ft.^{2} and $I_z = 20.5$ slug-ft.^{2} The disturbances were simulated appropriately with a steady-state component plus a sinusoid. This is more realistic than the constant disturbance torques used in previous simulations.

The magnetic field components used in this simulation were obtained from the Jensen-Whitaker magnetic field data. A stationary magnetic field was assumed for the synchronous orbit. This assumption is not strictly valid even though the vehicle does not move with respect to the earth. The magnetic field at high altitudes is in constant fluctuation because of extraterrestrial effects. These effects are not completely predictable; hence, their simulation is impossible. This assumption will not materially affect the results of the simulation. The simulation diagram is shown in Figure 4-23.

The generation of coil currents in the 6 hour orbit was based on the following equations:

$$I_{cx} = K_{1x}(q B_z - r B_y) + K_{2x}(\theta B_z - \psi B_y)$$

$$I_{cy} = K_{1y}(r B_x - p B_z) + K_{2y}(\psi B_x - \phi B_z)$$

$$I_{cz} = K_{1z}(p B_y - q B_x) + K_{2z}(\phi B_y - \theta B_x)$$

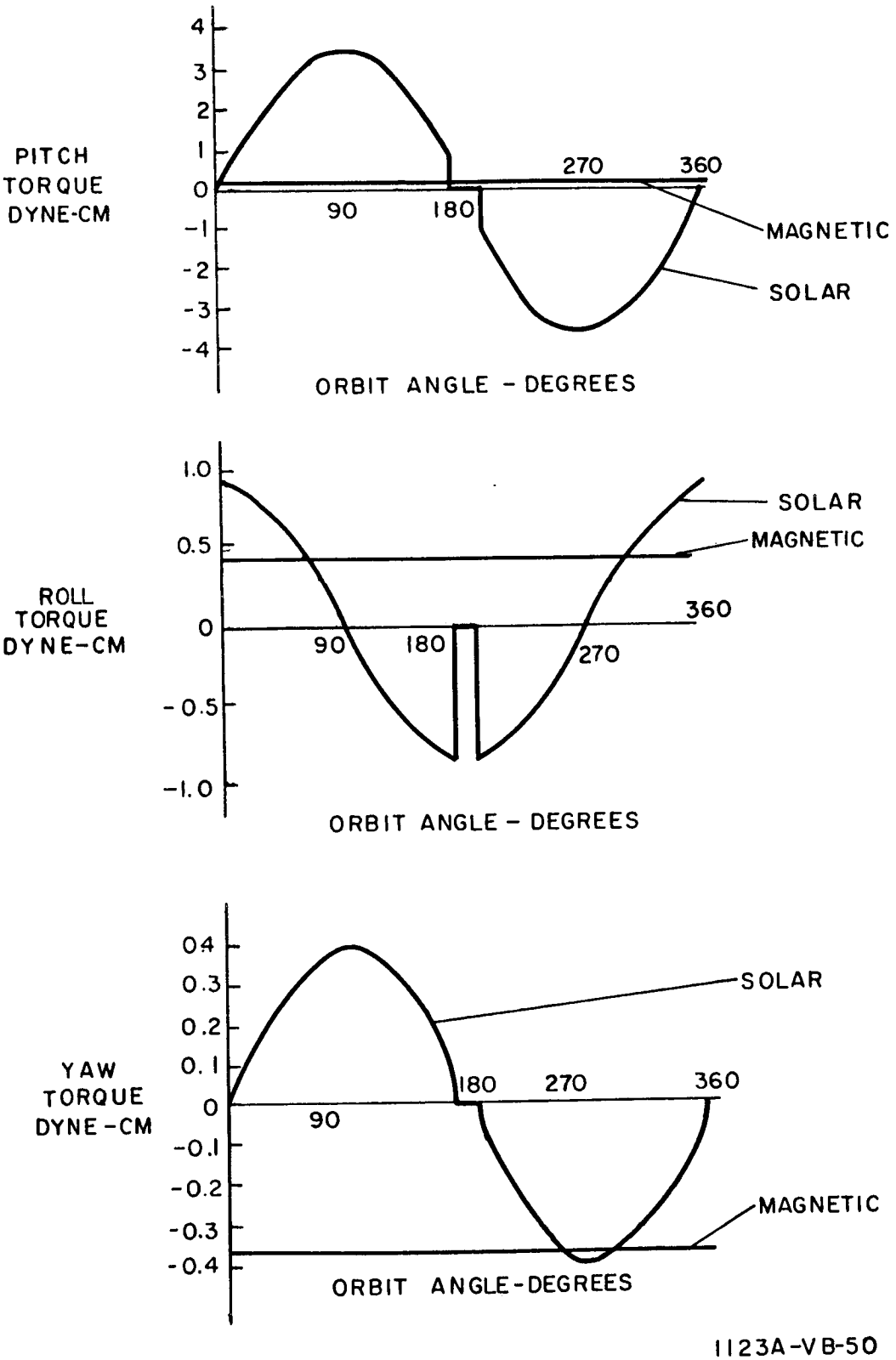

Figure 4-22 Approximate Satellite Disturbance Torques - 24 Hour Orbit

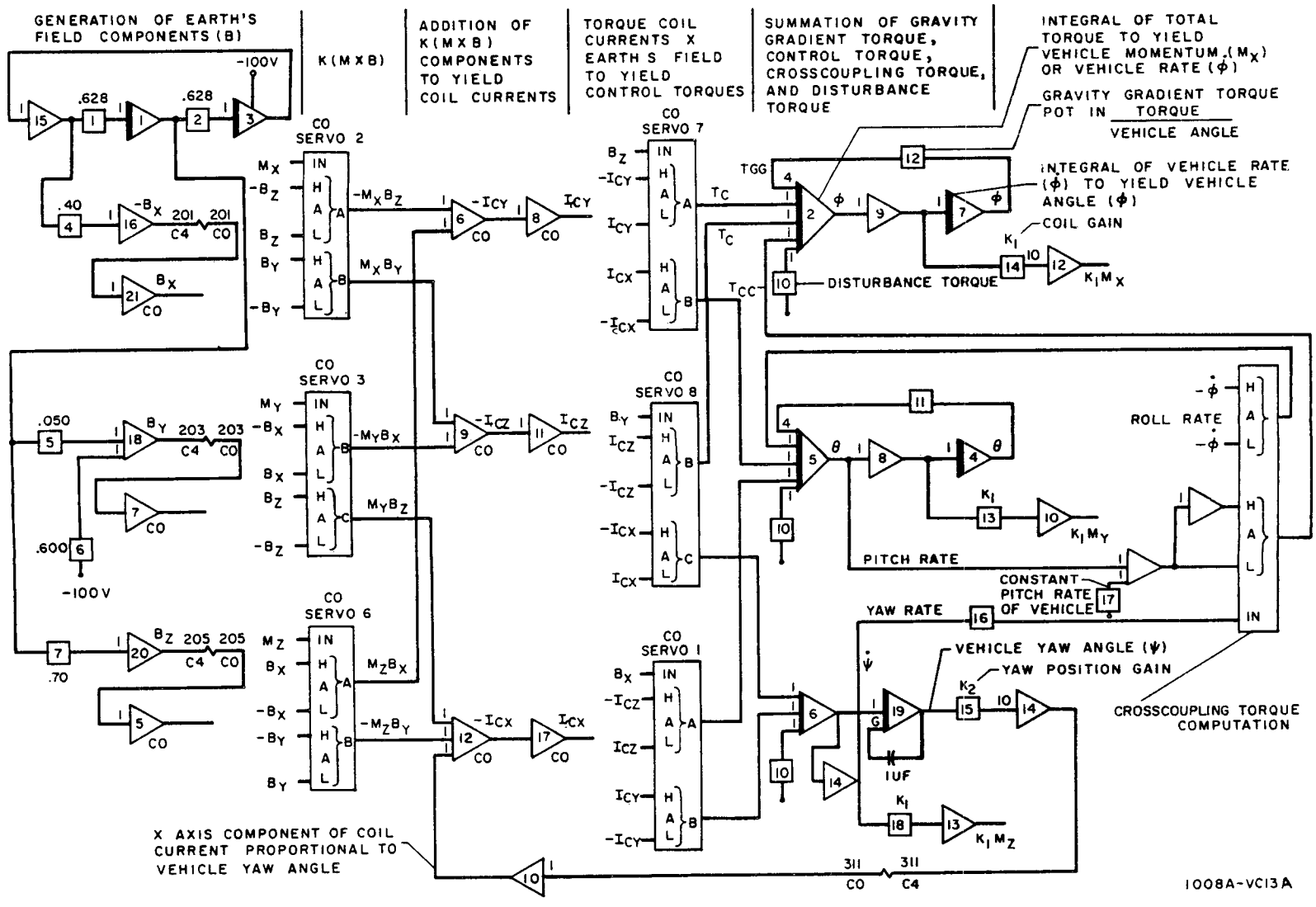

Figure 4-23 Analog Computer Simulation

Position information was used in the coil current equation to improve the accuracy of the system.

In the 12 hour orbit the large difference in moments of inertia resulted in large gyroscopic crosscoupling torques. System accuracy was improved by removing the position feedback through the magnetic actuators. The coil current equations were:

$$I_{cx} = K_{1x} (q B_z - r B_y) + K_{2x} \Psi$$

$$I_{cy} = K_{1y} (r B_x - p B_z)$$

$$I_{cz} = K_{1z} (p B_y - q B_x)$$

At synchronous orbit the system equations must be modified to include a pitch axis reaction wheel which will provide a torque proportional to vehicle rate. This reaction wheel is necessary to provide a torque about the pitch axis. The magnetic field direction is conservatively assumed to be constant and thus it can be used to produce torques about only 2 axes. Although external effects actually cause this direction to change, sufficient information is not available to assure that the variations will be great enough to enable its use in producing torques in more than two axes. The equation for coil current in the 24 hour orbit are:

$$I_{cx} = -K_{1x} (r B_y) - K_{2x} (\Psi B_y)$$

$$I_{cy} = K_{1y} (r B_x - p B_z) + K_{2y} (\Psi B_x - \emptyset B_z)$$

$$I_{cz} = K_{1z} (p B_y) + K_{2z} (\emptyset B_y)$$

The vehicle was assumed to be initially aligned to the vertical with the proper rates about all three axes ($p_o = 0$, q_o = orbital rate, $r = 0$). Ideal sensors (transfer function = K) were assumed throughout the simulation. Figures 4-24, 4-25, 4-26 illustrate the results of the simulation. The recordings

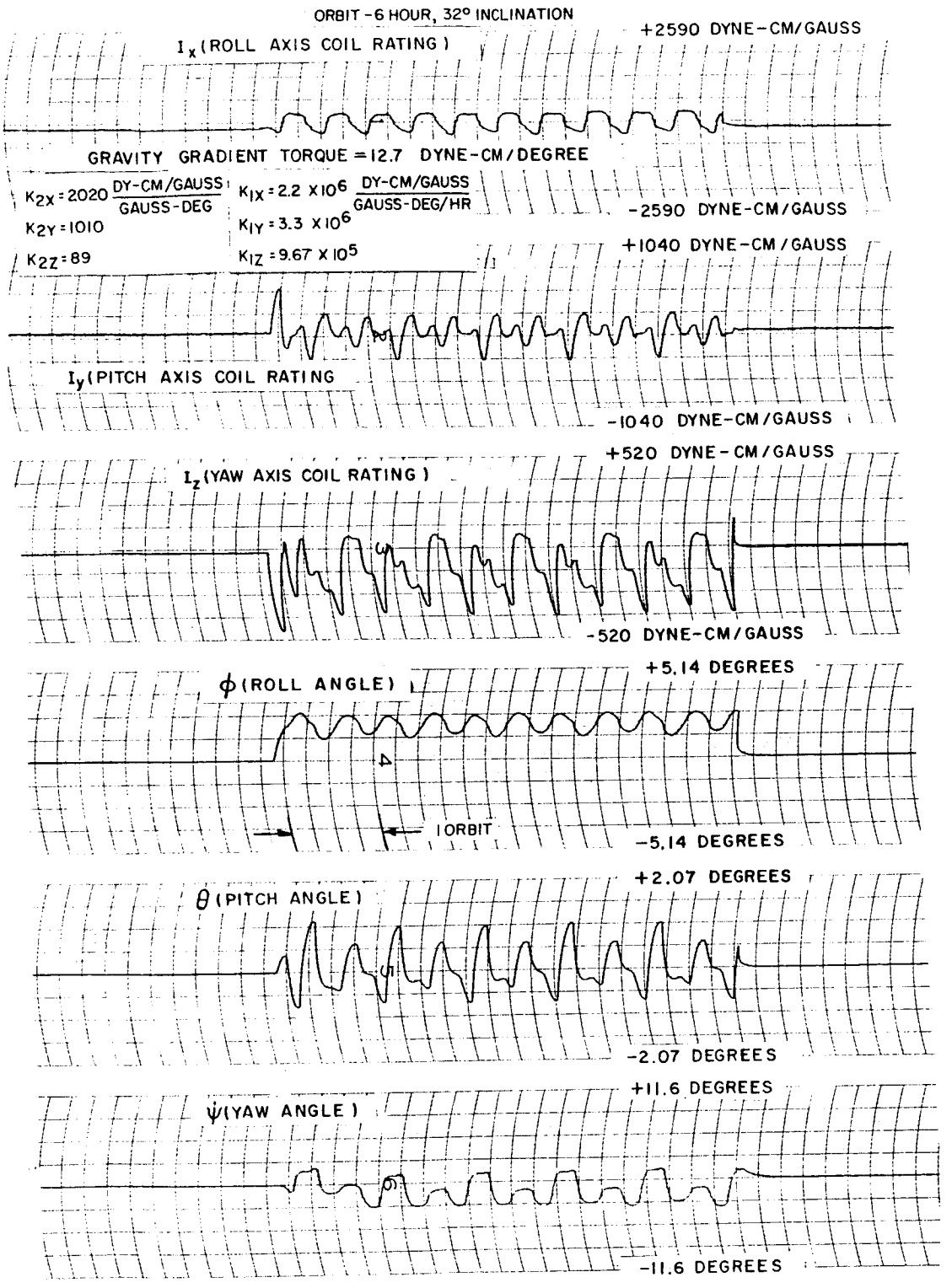

Figure 4-24 Simulation Results - 6 Hour Orbit

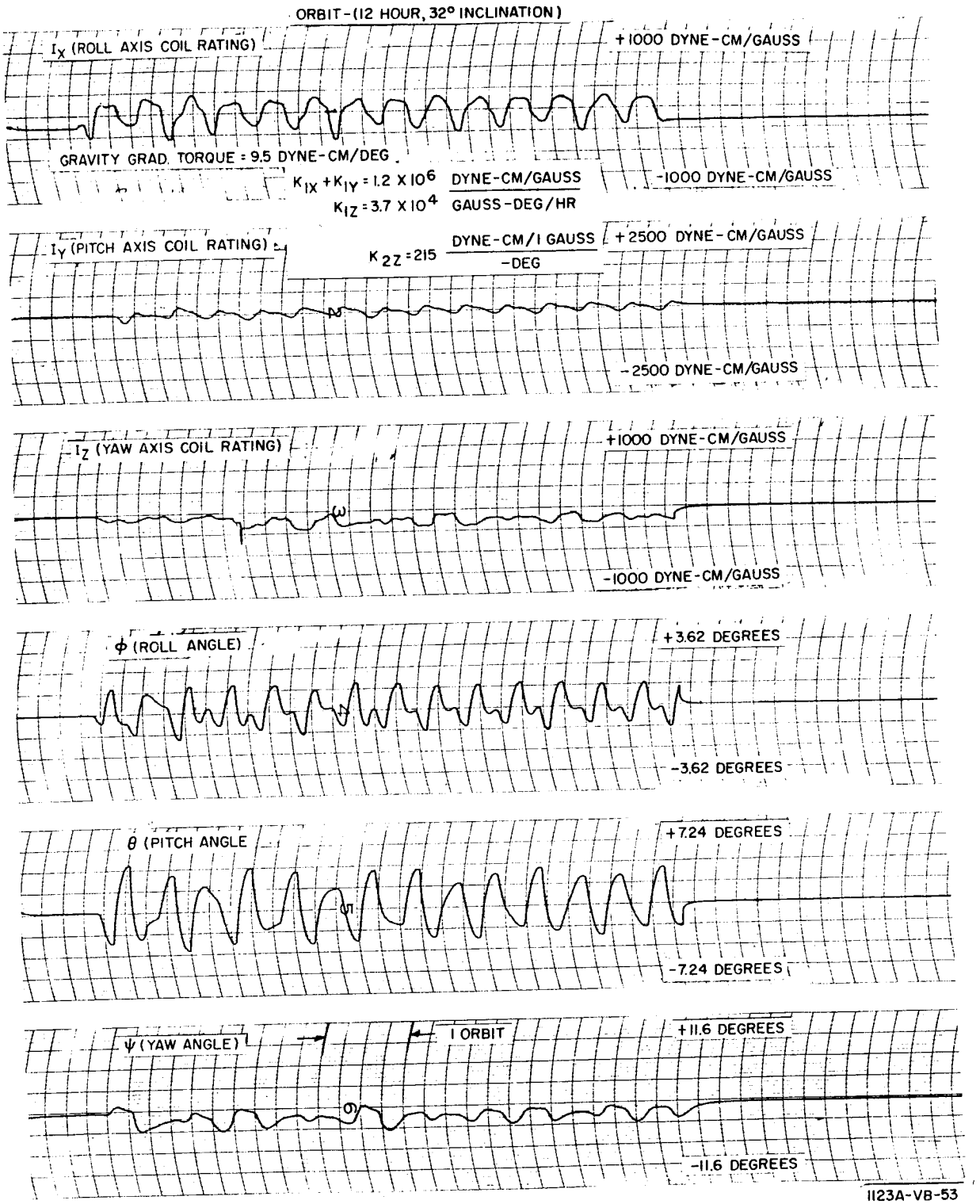

Figure 4-25 Simulation Results - 12 Hour Orbit

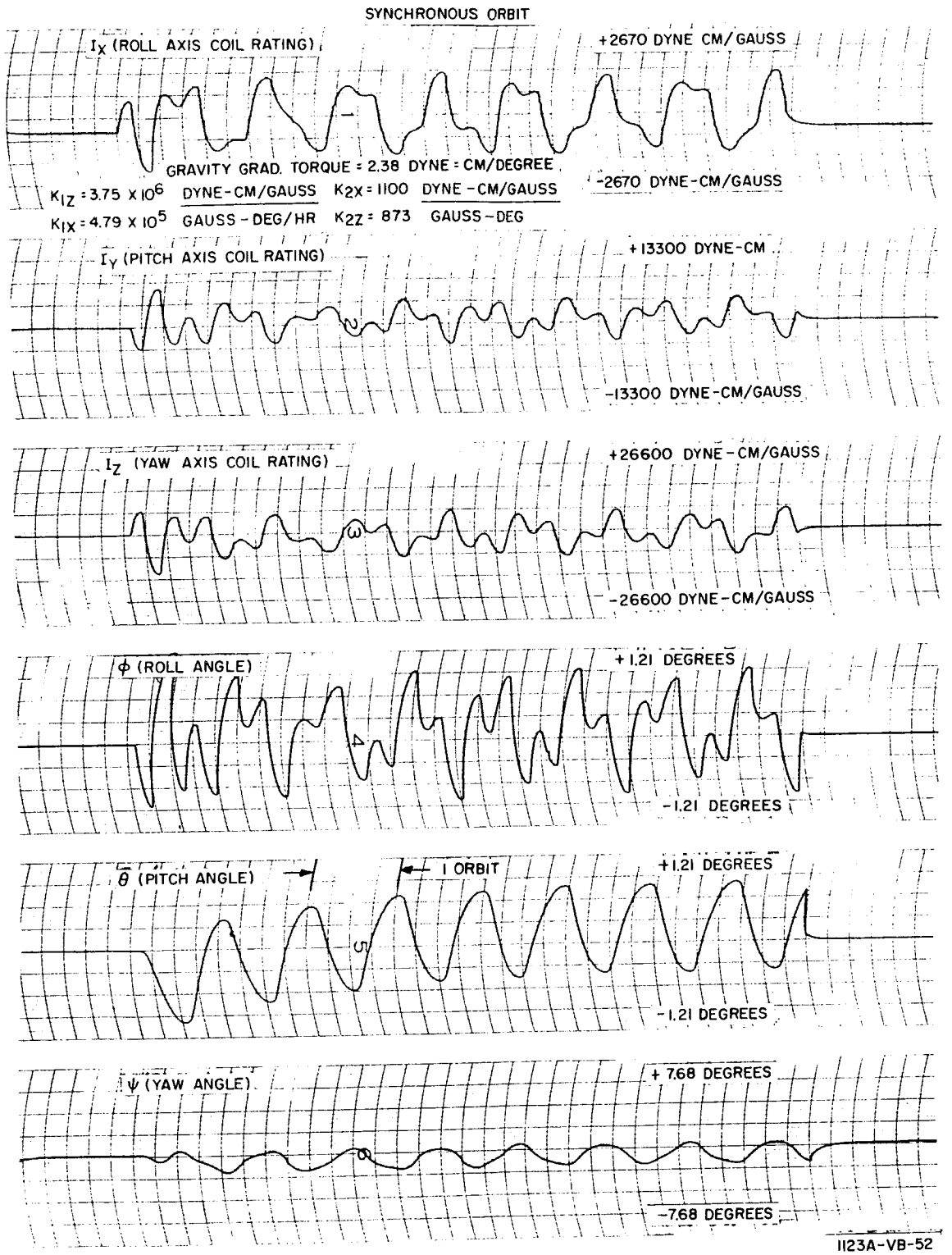

Figure 4-26 Simulation Results - Synchronous Orbit

include angular displacements and coil currents as a function of time. Table 4-A gives a summary of the results obtained for optimum gain settings at the three altitudes considered.

4.1.6.3 Conclusions

The results of the simulation show that the attitude of a vertically oriented satellite which is subjected to low disturbance torques may be held within the limits required by a communication satellite, by using a system composed of gravity - gradient and electromagnetic actuators. Since the gravitational field decreases with increasing altitude and the expected disturbances do not decrease proportionally it is logical that the size of the vehicle must increase as the orbital altitude is increased. This relationship does not hold at synchronous orbit because of the addition of a pitch axis reaction wheel.

A careful trade-off should be made in designing the satellite. Increasing the gravity-gradient torque by increasing the difference in moments of inertia ($I_X - I_Z$) results in an increased gyroscopic crosscoupling of the rates about the yaw and roll axes with the angular rate of the vehicle in the pitch axis. This fact was evident in the simulation of the 12 hour orbit where the addition of magnetic torques proportional to position error actually produced a detrimental effect on the system output. Increasing the gravity gradient torque to reduce the attitude errors will not always result in the desired reduction.

TABLE 4-A SIMULATION RESULTS

ORBIT	MAXIMUM ERRORS			VEHICLE LENGTH (Feet)	COIL SIZE (Dyne-Cm/Gauss)
	ROLL (Degrees)	PITCH (Degrees)	YAW (Degrees)		
6 hour	±2.6	±1.1	±3.5	10	389
12 hour	±1.1	±3.4	±2.9	16	300
24 hour	±.95	±.79	±1.5	16	1270 3660 7070

4.2 MECHANIZATION SUMMARY

4.2.1 System Plan

The purpose of this section is to determine the feasibility of the system combining magnetic actuation with the gravity gradient and depending entirely on satellite borne equipment for computation and control decisions.

This system would also require three rate gyros, a three-axis magnetometer, six multipliers, a horizon scanner, a stored gas actuation system for initial erection, an electronics assembly, and a yaw orientation system. A block diagram of this system is shown in Figure 4-27.

It was not assumed that such a system is optimum for any specific application, but rather, the aim was to establish reliability, weight, and potentialities of the system for use in future trade-offs against other attitude control systems. It was also assumed that the satellite must be oriented to the local vertical, and rotated about the yaw axis in order to orient a solar cell array. Injection of the satellite into orbit from the final stage will generate satellite tumbling rates, which must be reduced to zero prior to establishing its final attitude. The rate gyros generate signals which turn on the proper gas valve(s) to produce a decelerating torque. The roll axis is biased to produce a search rate for horizon acquisition. Once the satellite is erected to the vertical, the horizon scanner is disabled since the gravity gradient torque will keep the satellite yaw axis oriented to the vertical. The long axis of the satellite is considered to be the yaw axis. At the completion of this mode the vehicle will undergo a yaw search for the sun sensor to acquire its target.

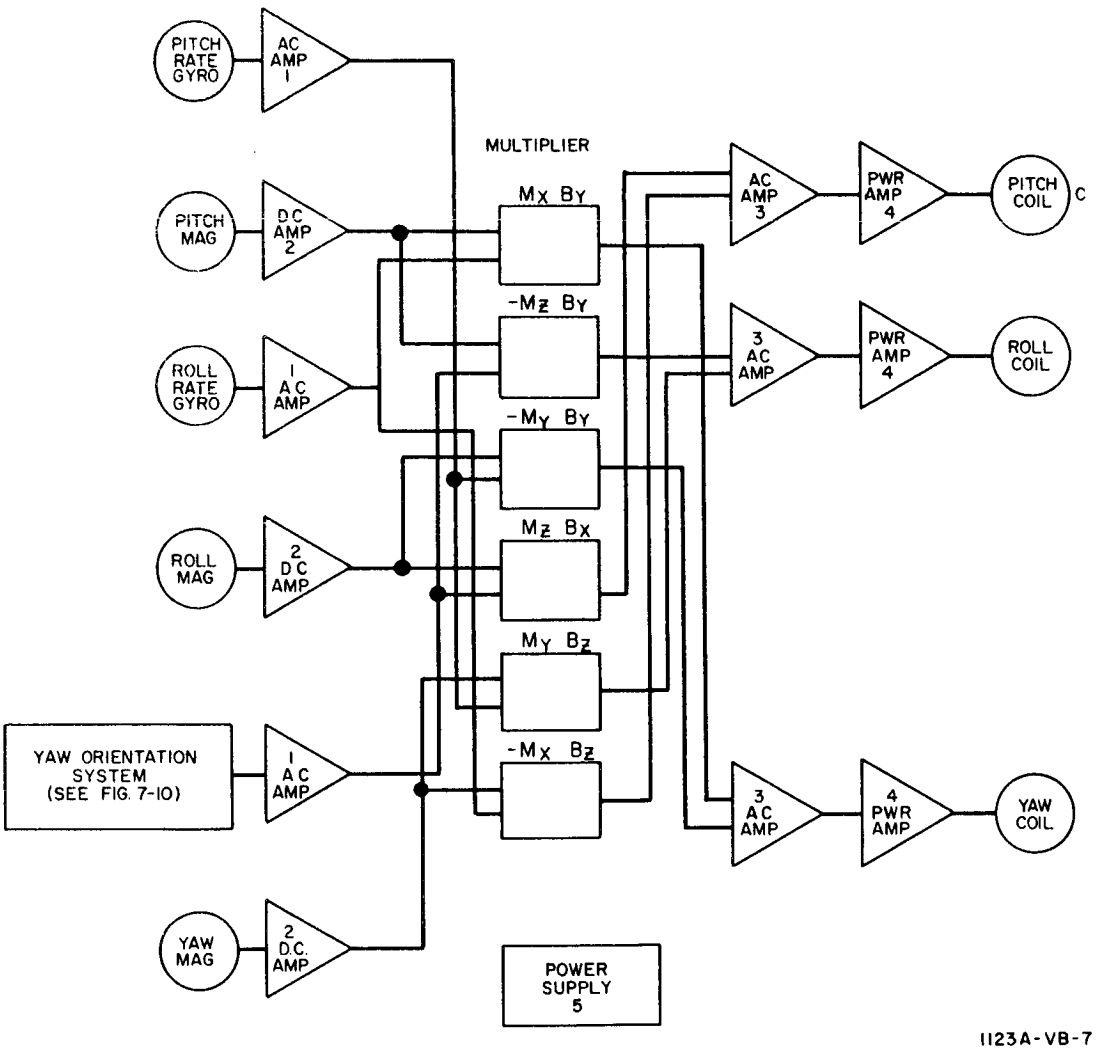

Figure 4-27 Gravity Gradient and Coils, On-Board Computation

The yaw search will be made by the yaw orientation system (see Figure 7-10 for a completion block diagram). The sun sensor of the yaw orientation system keeps the solar cell array oriented toward the sun by utilizing a yaw reaction wheel as torquer (see section 7.0). In routine operation, the magnetic actuators are used to torque the vehicle about the yaw axis and to damp the gravity gradient oscillations in the other two axes.

4.2.2 Reliability and Weight Analysis

The reliability analyses presented are based upon the use of Minuteman components wherever applicable. A breakdown of the electronic components used in the system is shown in Table 4-B. The number of components for each circuit is given, along with their failure rates. The block numbers refer to the blocks in Figure 4-27. This table is used to predict the reliability of the electronics portion of the system. The total failure rate for the electronics is 1.35 percent per 1000 hours, which yields a probability of success for 1 year of $P_S = e^{-0.0135 \times 8.76} = .888$.

The reliability of the electronics along with the other sub-systems is given in Table 4-C. The product of all these subsystem reliabilities will give the reliability of the entire system without redundancy. The gravity gradient and torque coils system without ground control has 0.0113 probability of success for 1 year. From Table 4-C, it is seen that the system reliability is heavily dependent on the reliability of the three rate gyros and hence redundancy may be used on this item to increase the system reliability. However, a complete departure from the use of rate gyros is obviously desirable, and such a system is discussed in Section 6.0.

The system weight is composed of the components as shown in Table D.

TABLE 4-B

Summary of Electronic Parts for the Gravity Gradient and Torque Coils Attitude Control System Without Ground Control

Block No.	No. of Blocks/ System	Signal Transistors	Power Transistors	Blocking Diodes	Zener Diodes	Tantulum Capacitors	Glass Capacitors	Resistors Wire Wound	Resistors Metal Film	Resistors Composition	Transformers	Potentiometers	Chokes
1	3	12					6		9	9			6
2	3	12							12	9			
3	3	9				9	3		18	15			
4	3	12		12		3			6	6	3		
5	1	4	2	12	2	4			4	4	5	2	
6	1			2			1		3			1	1
Total No. Components		49	2	26	2	16	10		52	43	8	3	7
Failure Rate %/1000 Hrs.		.049	.02	.026	.022	.024	.009		.0172	.00645	.8	.03	.35

Total Number of Components = 218

Total Failure Rate = 1.35%/1000 Hrs.

TABLE 4-C

Reliability of Subsystems

Subsystem	Probability of Success - 1 year
3 Rate Gyros	.0138
3 Axis Magnetometers	.990
6 Multipliers	.948
1 Gas System	.995 (1 hour)
1 Electronics Assembly	.888
3 Torque Coils	.997
1 Horizon Scanner	.999 (1 hour)
1 Yaw Orientation System	.988
	.0113

TABLE D

SYSTEM WEIGHT

	Weight (lbs.)
1 yaw orientation system	14.0
3 rate gyros	9.0
3 axis magnetometers	2.0
3 torque coils	1.0
6 multipliers	0.5
1 horizon scanner	6.0
1 sun sensor	3.0
1 gas system	4.0
1 electronics assembly	10.0
Total Weight	49.5 lbs.

4.2.3 Comparison to Other Systems

Table 4-E shows revised tabulations of the characteristics of the "wheels-and-coils" and "coils-only" systems of the May 1, 1962 report. They may be compared to the characteristics of two mechanizations of the "gravity gradient and coils" system as shown in Tables 4-C, 4-D, and 6-A.

TABLE 4-E

Comparison of System Parameters

A. Control by Wheels and Coils (Indirect System)

Component	WT lb.	VOLUME in^3	POWER watts	RELIABILITY P_s (1 yr.)
Wheels	9.0	42	2.5	0.999
Coils	1.0	8	0.7	0.997
Gas System (6 hrs.)	4.0	32	7.0	0.999
Rate Gyros (6 hrs.)	1.5	10	7.0	0.998
Magnetometer	2.5	97	2.0	0.990
Multipliers	0.5	15	0.1	0.948
Roll Rate Gyro	6.0	18	2.5	0.482
Scanner	6.0	120	6.0	0.557
Electronics	21.5	1300	20.0	0.730
TOTALS	52.0	1542	67.8	.183

B. Control by Coils Only (Direct on-board system)

Component	WT lb.	VOLUME in^3	POWER watts	RELIABILITY P_s (1 yr.)
Scanner	6.0	120	6.0	0.557
3 Rate Gyros	9.0	30	10.0	0.112
Magnetometer	2.0	97	2.0	0.990
Multipliers	0.5	15	1.0	0.948
Torque Coils	1.0	8	7.0	0.997
Electronics	21.5	1300	20.0	0.888
TOTALS	40.0	1570	38.8	.052

5.0 EARTH'S MAGNETIC FIELD AND SOLAR SENSING

5.1 Statement of the Problem

The development of reliable attitude control systems is in large measure a problem of attitude sensor reliabilities. Present methods for earth-oriented vehicles use horizon scanners and/or celestial trackers and gyros. The reliability of these devices is limited by the state-of-the-art in bearing design and by their general complexity. Attitude sensing using the magnetic field and the sun has interesting possibilities since less complex, non-rotating sensors may be used. These sensors are required to have 4π steradian coverage.

Data are available on the sun and on the magnetic field for altitudes up to perhaps 5,000 miles which would enable one to determine the orientation of a satellite if the direction of the sun and the magnetic field vector are known. Methods of determining these directions are discussed in the following section. The validity of the method depends, of course, on the constancy of the magnetic field, (see Section 9).

Two-axis information may be obtained from either a magnetometer or a sun sensor. Both are required to obtain three-axis attitude errors. Whenever possible the sun sensor will be used to provide two-axis information to the control system because the position of the sun is known much more accurately than the magnetic field vector. Except for very special orbits, the sun will not be visible to the vehicle for the entire orbit. The amount of shadow varies inversely with altitude (approximately 5% of the orbit at synchronous altitude to approximately 15% for 6 hr. orbit). Three-axis information will not be obtained during the portion of the orbit that the vehicle is shadowed from the sun.

Necessary requirements for three-axis information from the sun and magnetic field are that the sun is visible and that the "sun vector" does not coincide with the magnetic field vector. In general, these vectors will coincide for short periods of time. Since the magnetic field vector is changing rapidly in any but synchronous orbits, the time of coincidence is negligible.

The inclusion of an on-board computer to determine the attitude of the vehicle is not in keeping with the desire for high reliability. Therefore, the information from the sun sensor and magnetic field sensor will be sent to the ground station where all computation will be performed and appropriate commands relayed to the vehicle.

5.2 Magnetic Field Sensing

The magnetic field direction can be determined by three-axis magnetometer measurement. This method may be used for all inclinations and is limited in altitude only by the ability of magnetometers to measure very small fields accurately. The requirements for accuracy and range have been calculated for 6, 12, and 24 orbits. The average values of the magnetic field were obtained by extrapolation of available data at 2,500 and 10,000 miles.

B_{6} hour .029 gauss

B_{12} hour .0096 gauss

B_{24} hour .0013 gauss

The required threshold of the magnetometer was specified by the ability of the magnetometer to read B cos 89° (Figure 5-1). The magnetometer must range from B cos 89° to B. The accuracy was calculated from the requirement that the magnetometers must be able to measure the differences between B cos 44° and B cos 45°. The magnetometer requirements for $\pm$ 1° accuracy of measurement are listed in Table 5-A for 6, 12, and 24 hour orbits. The requirements for synchronous orbit are particularly stringent.

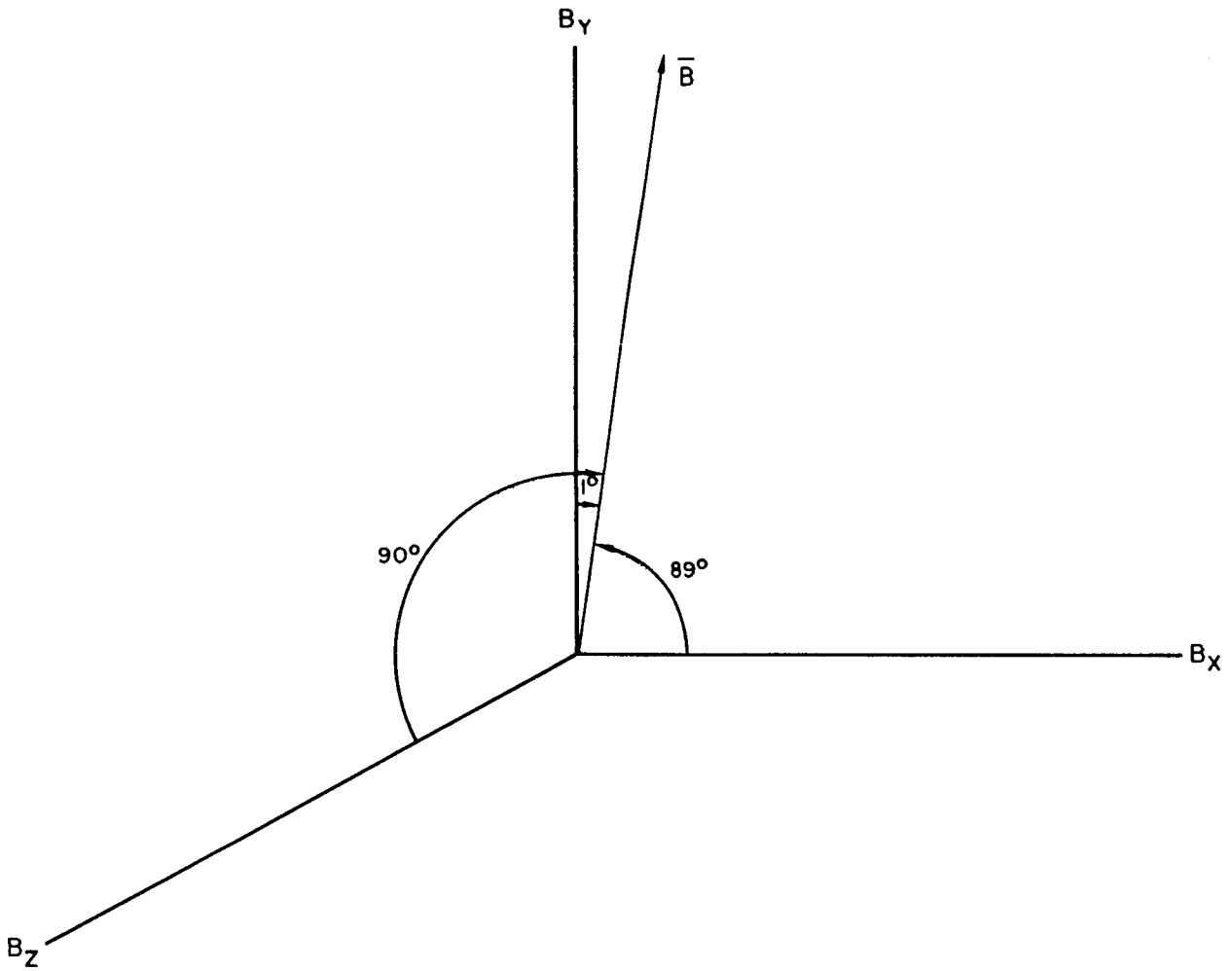

Figure 5-1. Magnetic Field Position for Determining Magnetometer Threshold

TABLE 5-A - Magnetometer Requirements

	Approx. B. Field (Gamma)	Threshold (Gamma)	Range (Gamma)	Accuracy (Gamma)
6 hour orbit	3300	58	58-3500	± 43
12 hour orbit	820	14	14-880	± 11
24 hour orbit	200	3.5	3.5-210	± 2.5

The Dalmo-Victor Company has under development a flux-gate magnetometer having a range of 1-20 gamma and an accuracy of $\pm$ 1 gamma (10^{-5} gauss). A unit similar to this unit could be used in this application. The physical data on a three-axis magnetometer for sensing in a 12 hour orbit are:

Size: Approx. 7" x 2" x 3"

Weight: 2 lbs.

Power: 2 watts

The accuracy of present data on the magnetic field direction may present a problem. Present data, such as the Jensen-Whitaker program is believed to be accurate within 1 degree at lower altitudes.

However, the effect of daily variations and sunspots on the magnetic field at high altitudes is not completely defined, and these variations are sizeable. This subject is discussed further in Section 9.

Careful selection of the materials comprising the satellite is necessary to assure that the magnetic field will not be disturbed. Any warping of the field will result in erroneous magnetometer measurements.

5.3 Sun Sensing

The problem of sensing the attitude of an earth-oriented vehicle by using a sun sensor is complicated by the fact that the earth is rotating around the sun. For a satellite in a non-equatorial orbit the sun may appear in any octant during the course of a year. This requires that the sun sensor be able to sense the sun's position accurately and reliably through 4π steradians. If an equatorial orbit is assumed the angular coverage is reduced to approximately 1.6π steradians. Angular coverage of this magnitude might immediately suggest the use of some type of rotating or gimballed device to follow the sun. Devices of this type are, however, inherently unreliable.

Therefore, every effort was made to conceive a sun sensor having no moving parts of any type. Several different devices were considered and a few representative ones are described.

The requirements for the sun sensor considered in this report were $\pm 1°$ accuracy with maximum vehicle rates of one degree per second, minimum size and weight, and maximum reliability.

The sun sensor which was chosen is a passive device which measures the direction angles of the line of sight to the sun. A simplified drawing of one unit of the sensor is shown in Figure 5-2. Each unit consists of an aluminum core (on which the solar cells are mounted), a set of black anodized aluminum leaves, shaped as truncated cones and solar cells which are located on the core between the leaves. The aluminum leaves are used to reduce the field of view of the solar cell to six degrees about the axes (secondary axes) normal to the unit's principal axis. Four units of the type shown in Figure 5-2 will provide complete spherical coverage. Figure 5-3 illustrates the geometric principle which is the basis of the sun sensor. Since the sum of the squares of the direction cosines equals one,

$$\cos^2\alpha + \cos^2\beta + \cos^2\gamma = 1$$

By measuring α and β,

$$\cos^2\gamma = 1 - \cos^2\alpha - \cos^2\beta$$

$$\gamma = \cos^{-1}\left(\pm\sqrt{1 - \cos^2\alpha - \cos^2\beta} \right)$$

If it is known in which octant the line-of-sight is, then γ is known and the line is completely defined. The octant containing the line can be determined if a dividing plane is passed through two of the units which are directly opposite each other. This dividing plane is perpendicular to the planes formed by the mounting surfaces of the four units. Thus two of the units contain 23 solar cells and two units contain 45.

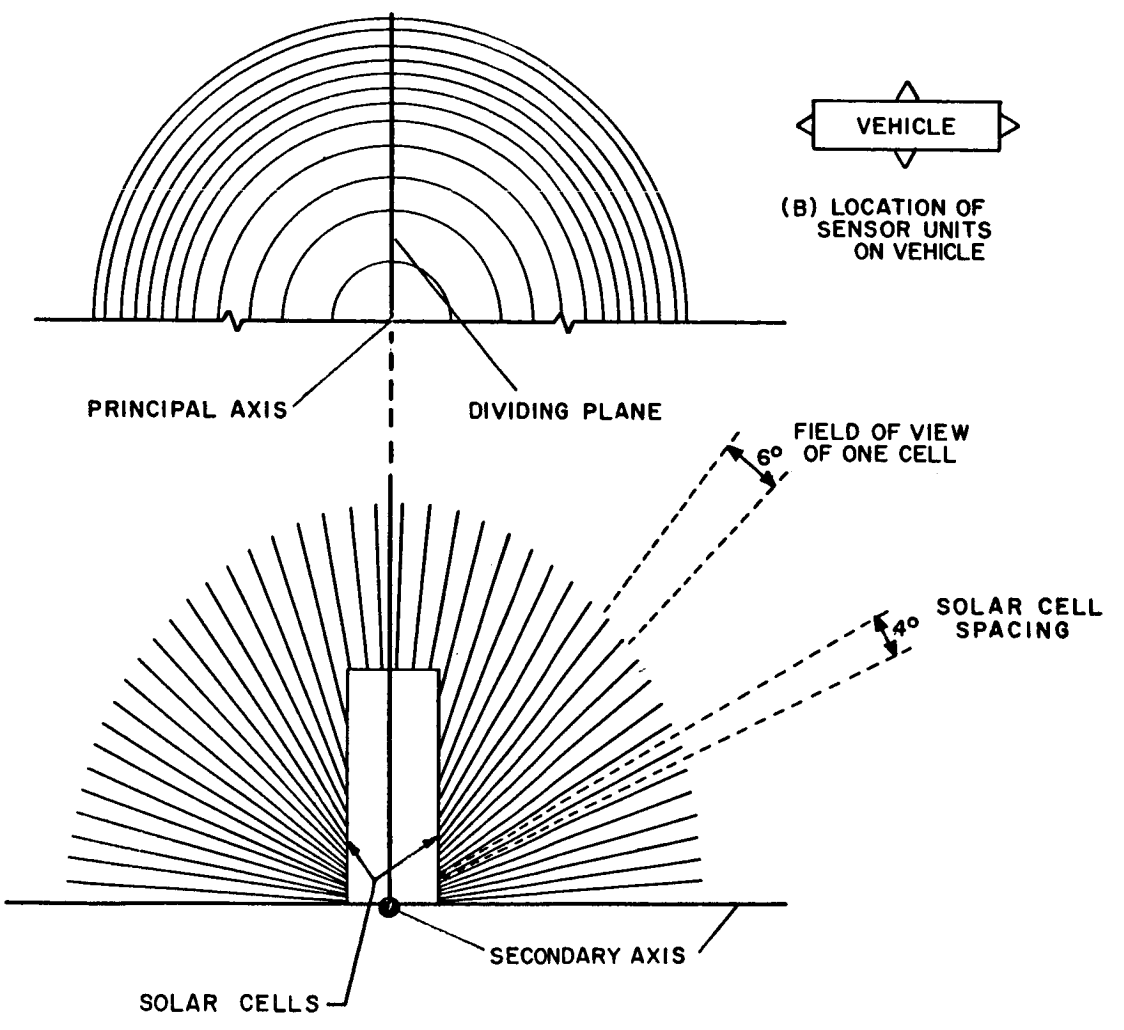

Figure 5-2. Cross Section and Top View of Sensor Unit

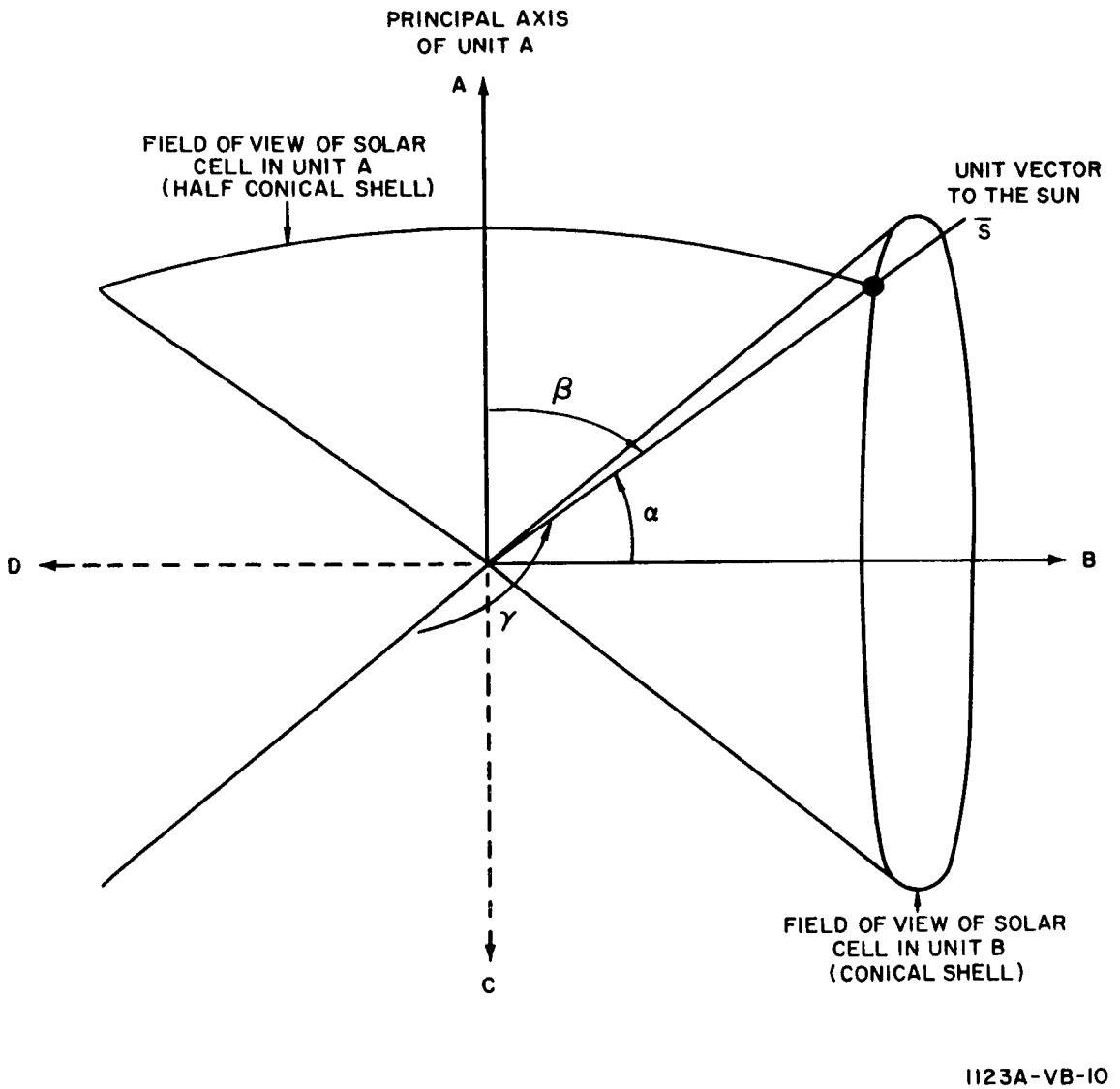

Figure 5-3. Geometric Principle of Sensor

The four units necessary to provide spherical coverage will require 136 solar cells. The solar cells will be spaced every 4 degrees about the secondary axes and the field of view of each will be a conical shell (half a conical shell for those cells which are in the two units which have been divided by the dividing plane) 6 degrees in width. Each solar cell will be required to give only an on-off indication as to whether or not it "sees" the sun. These on-off signals will be compared on the ground to the known positions of the sun and solar cells and the vehicle attitude will be computed.

Overlapping fields-of-view are designed into the sensor to provide the required accuracy with a minimum number of cells. Figure 5-4 illustrates the fields-of-view of typical cells and the method of obtaining $\pm$ 1° accuracy from cells having 6° fields-of-view.

Interrogation of the cells will be accomplished by designating each cell by a binary number. When the sensor is interrogated the binary numbers of the cells which are "on" will be obtained. Figure 5-5 shows a typical circuit for obtaining the binary number of the sunlit cell.

Reliability is of primary importance in the sun sensor described here. Table 5-B shows the number of parts required for the sun sensor, including the interrogator circuits. The reliability calculation disregards the inherent redundancy of the sensor. Failure of any one solar cell would only decrease the accuracy of the sensor in a particular area. Thus the reliability of the sensor would actually be higher than indicated in Table 5-B.

The information which must be transmitted to the ground station consists of 22 on-off signals. This compares very favorably with the information transmission required by other types of sensors.

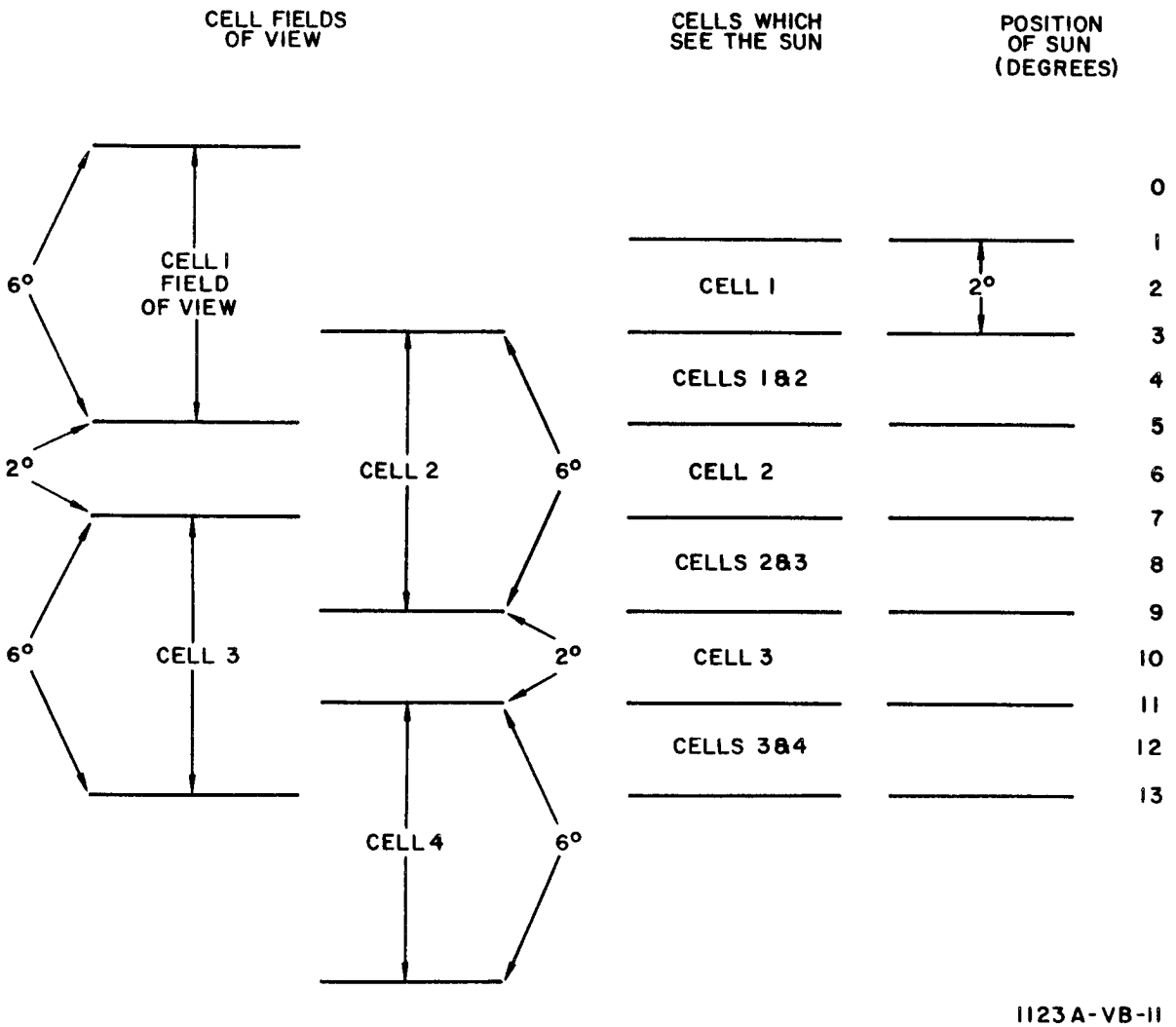

Figure 5-4. Overlapping of Solar Cell Fields-of-View

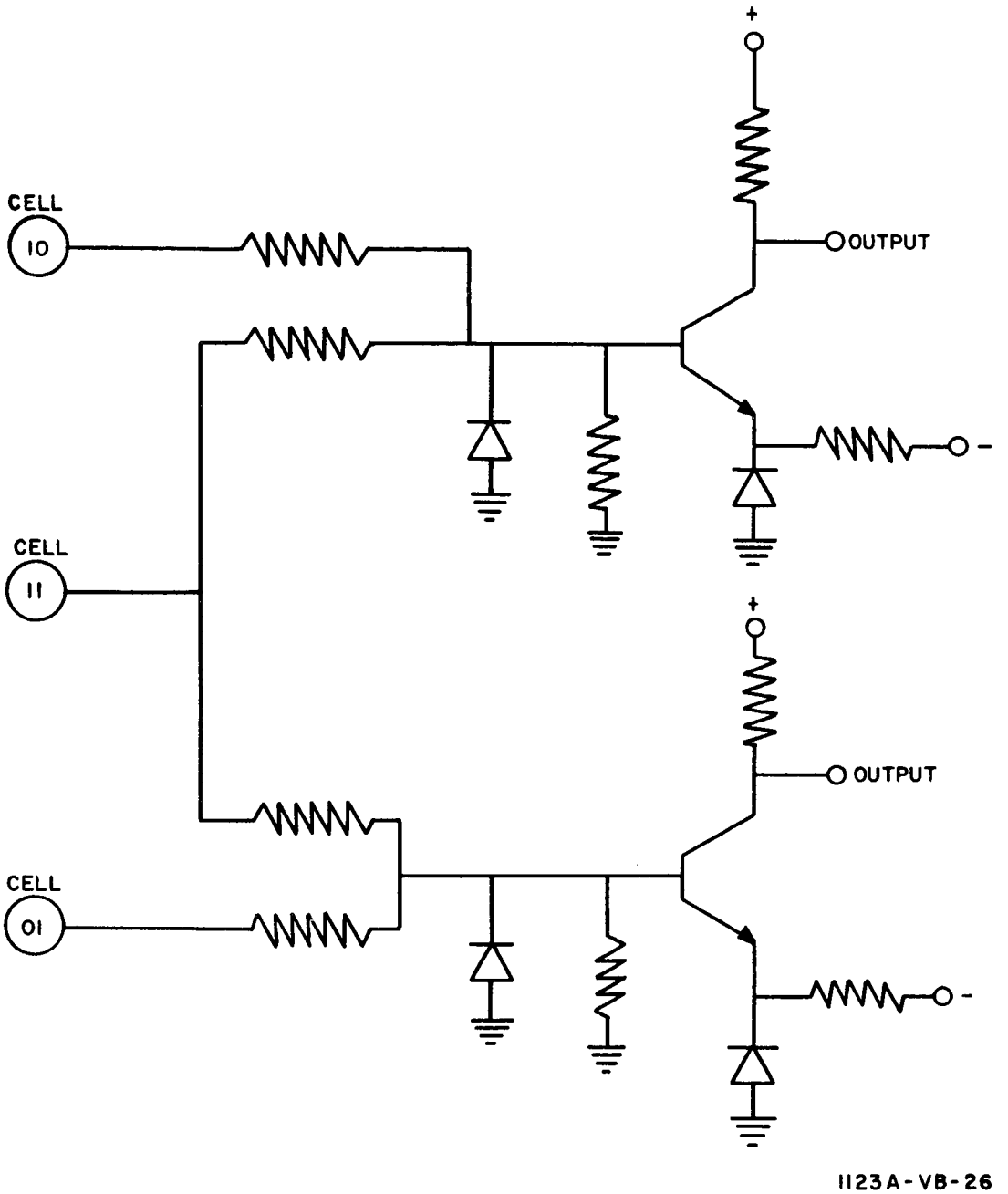

Figure 5-5. Interrogation Circuit

TABLE 5-B RELIABILITY COMPUTATION

Component	No	%Failures/1000 hrs/unit	Failure Rate (%/1000 hrs)
Transistors	38	.001	.038
Resistors	410	.00015	.062
Diodes	76	.001	.076
Solar Cells	138	.001	.138
TOTAL			.314

$$\text{Reliability} = e^{-8.76 \times .00314} = .97$$

Physical data on the sun sensor and interrogator circuit is

Size: Interrogator -- approx. 6" x 6" x 6"

4 Sensor Units -- approx. 4" x 4" x 4" each

Total Wt.: Interrogator and 4 Units -- approx. 4.5 lbs.

Power: Interrogator only -- approx. 2 watts

The four sensor units are mounted on the vehicle such that their center lines lie in a common plane and their pointing directions are at right angles.

Placement of the units on the vehicle should be such that reflections will not occur. If the vehicle contains solar paddles which might produce reflections or block the view of the sensor, the units may be mounted on the end of the paddles (although maintaining alignment would then become critical). The only requirement is that their relative orientation remain unchanged. The sensor combines long life and high reliability with low weight, making it extremely attractive for long life missions.

5.4 Alternate Sun Sensors

Several alternate sun sensors were considered but were not chosen because of reliability or size considerations. Two representative ones are briefly described below. One of these methods (a linearized sun sensor) consists of a solar cell covered by a hemispheric dome containing holes. The density of the holes decreases as the angle from the center line of the sun sensor increases. The net result is to linearize the solar cell characteristic as shown in Figure 5-6.

Two problems were encountered in a sensor of this type. The primary problem is that the sensor is dependent on the solar cell characteristic remaining constant. Solar cell characteristics do vary with temperature, radiation and shock. Some of these effects are not well known, and it would be extremely difficult to compensate for these changes. In addition, sublimation of the hemispheric

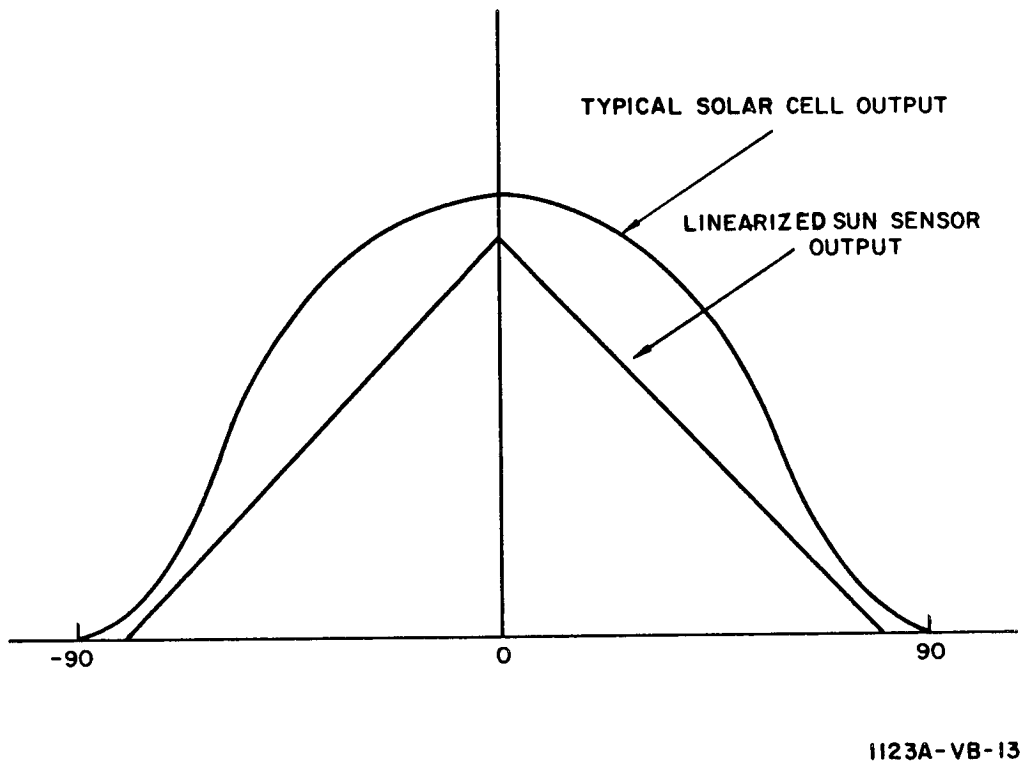

Figure 5-6. Output of Linearized Sun Sensor

dome would cause nonlinearities in the sun sensor output which could not be compensated.

Another sun sensor considered contains a rotating part. This sensor consists of a constant-speed motor driving a small dome covering a solar cell, which dome contains an opening which varies in width with the angle from the centerline of the sensor. As the dome rotates the sun sensor produces a pulse whenever the sun is sighted. The time of occurrence of the pulse is compared with the output of a synchro to determine the horizontal angle to the sun and the width of the pulse determines the vertical angle of the sun. Two of these sensors are required for 4π steradian coverage. A sensor of this type has reliability problems. It is extremely difficult to obtain 8,000 hours life from a bearing operating on earth. Since the two sensors necessary to provide spherical coverage contain two motors and two synchros, it is easy to see the problems which arise. This sensor is considered useful for short-life missions but will not meet the requirements for long life (1 to 3 years).

5.5 Conclusions

The selected sensors described in this section are reliable and relatively simple. They contain no moving parts. Their accuracy is limited, however. The sun sensor is particularly applicable to the high altitude, long life mission of a communication satellite. At lower altitudes, below 6 hour orbit, the use of a sun sensor is restricted because the vehicle is in the earth's shadow for a large portion (over 15% of the orbit for most inclinations), of each orbit. The sun sensor could be reduced in scope for synchronous orbit or for reduced accuracy requirements.

The use of a magnetometer for sensing vehicle attitude is also attractive for long life missions. At the present time high accuracies are not obtainable. The maximum magnetometer error is approximately 1° and the maximum error in defining the earth's field is thought to be approximately 1° at the altitude of a 6-hr. orbit. In addition some error (approx. 1%) will be introduced in the telemetry system. The total maximum error will be approximately 3°.

The total system error will probably be 1° - 3° in a 6-hour orbit. The worst case occurs when the vehicle is shadowed from the sun and the errors in magnetic sensing add. If the ground computer is programmed to give proper consideration to the relative accuracies of the two sensors the total system error should be reduced to less than $\pm 2°$. For systems in which these accuracies are sufficient the sensing of attitude by magnetic field and solar sensors offers high reliability and long life.

6. GROUND CONTROL

6.1 System Plan

The purpose of ground computation of coil currents is to minimize the complexity of the equipment carried on board the satellite, and consequently, enhance the reliability of the overall system.

The basic system chosen is a coils and gravity gradient configuration, where the gravity gradient effect is used to provide torques which tend to align the vehicle yaw axis with the local vertical and the coil currents are used to generate directional and damping torques. The function of the ground computer is to generate the coil current command signals in accordance with the equations relating on-board sensor data and stored values of reference sensor information (in vehicle coordinates for proper alignment in the orbital plane).

6.1.1 Coil Current Equations

The basic equations of coil current necessary to generate the directional alignment and damping torques are:

$$I_{cx} = K_1 (M_z B_{ay} - M_y B_{az}) + P_\psi B_{ay}$$

$$I_{cy} = K_1 (M_x B_{az} - M_z B_{ax})$$

$$I_{cz} = K_1 (M_y B_{ax} - M_x B_{ay})$$

where

I_{cx}, I_{cy}, I_{cz} are currents in the coils whose axes are parallel to the x, y, and z axes respectively.

K_1 is a gain constant relating the net product of momentum times field and the coil current.

P_ψ is proportional to the sine of the yaw angular error

B_{ax}, B_{ay}, B_{az} are earth's magnetic field components as measured by magnetometer elements along the x, y, and z axes of the vehicle.

x, y, and z are the roll, pitch, and yaw axes of the vehicle.

These equations differ from those developed in paragraph 2.2 of the final report of the basic contract (dated 1 May 1962) in that no terms incorporating pitch and roll angular errors appear. In the system described here, the alignment torques about the pitch and roll axes are generated by the gravity gradient effect operating on the long, slender vehicle..

Since direct measurement of the three components of the momentum vector would require the use of three accurate rate gyros mounted on board the vehicle, and since this would degrade the reliability to an intolerable degree, the momentum vectors must be measured by changes in the components of earth's magnetic field strength and changes in the components of one other directional vector. In the system studied for this report, the second vector used is the sunline directional vector. Two independent directional vectors must be used to resolve the components of angular velocity about the axes coincident with each vector, since angular motion about the magnetic field vector axis will not result in any change in field strength as measured by the three-axis magnetometer.

The yaw angular error signal must be generated by using ephemeris data, comparing it with the measured data, and developing an error signal about the z-azis.

6.1.2 Computation of Angular Velocities

Using Figure 6-1 as a reference, motion about the three axes will result in changes of field strength as follows:

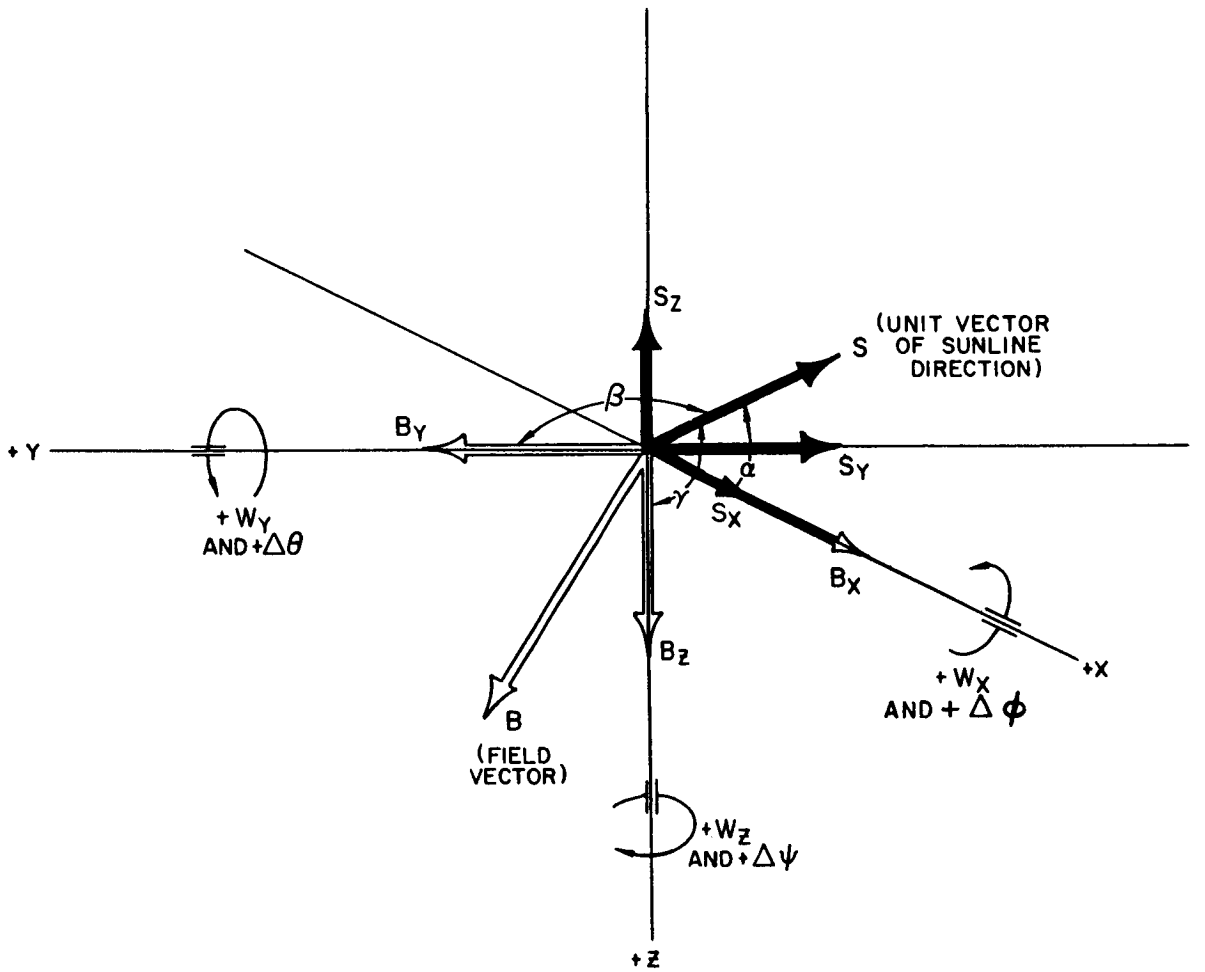

B_X, B_Y, B_Z ARE MAGNETIC FIELD COMPONENTS

S_X, S_Y, S_Z ARE SOLAR DIRECTIONAL VECTOR COMPONENTS

1123A-VB-14

Figure 6-1 Sunline and Magnetic Field Vectors in Vehicle Coordinates as Measured by On-Board Sensors

$$\Delta B_y = B_x (\Delta \psi) - B_z (\Delta \phi)$$

$$\Delta B_x = B_z (\Delta \theta) - B_y (\Delta \psi)$$

$$\Delta B_z = B_y (\Delta \phi) - B_x (\Delta \theta)$$

where

$\Delta \phi, \Delta \theta, \Delta \psi$ are incremental angular motions about the vehicle's x, y, and z axes.

ΔB_x, ΔB_y, ΔB_z are incremental changes in the measured components of field strength along the vehicle's x, y, and z axes.

B_x, B_y, and B_z are instantaneous values of field strength along the vehicle's x, y, and z axes.

Dividing by Δt (increment of time) and allowing the Δ increments to approach zero, we obtain:

$$\dot{B}_y = B_x \omega_z - B_z \omega_x$$

$$\dot{B}_x = B_z \omega_y - B_y \omega_z$$

$$\dot{B}_z = B_y \omega_x - B_x \omega_y$$

These three equations are not independent (the matrix of the coefficients of ω equals zero) and this results from the fact that motion about an axis coincident with the field vector will not yield changes in any of the three axis components. Since the solutions for ω_x, ω_y, and ω_z cannot be computed from these three equations alone, a second set of three equations is developed from the sunline directional vector in a similar manner:

$$\dot{S}_y = S_x \omega_z - S_z \omega_x$$

$$\dot{S}_x = S_z \omega_y - S_y \omega_z$$

$$\dot{S}_z = S_y \omega_x - S_x \omega_y$$

where

$$S_x = \cos\alpha$$

$$S_y = \cos\beta$$

$$S_z = \cos\gamma$$

Solving for ω_x, ω_y, and ω_z by eliminating the unwanted velocity between a pair of equations containing the same two velocities, the result is a set of six equations, two for each axial component of angular velocity. The presence of two independent solutions permits computation of ω when the denominator of one of the equations approaches zero. The six equations are:

$$\omega_x = \frac{S_x \dot{B}_y - \dot{S}_y B_x}{S_z B_x - S_x B_z}$$

$\frac{d\phi}{dt}$

$$\omega_x = \frac{S_x \dot{B}_z - \dot{S}_z B_x}{S_x B_y - S_y B_x}$$

$$\omega_x = \frac{S_y \dot{B}_z - \dot{S}_z B_y}{S_x B_y - S_y B_x}$$

$\frac{d\theta}{dt}$

$$\omega_y = \frac{S_y \dot{B}_x - \dot{S}_x B_y}{S_y B_z - S_z B_y}$$

$$\omega_z = \frac{S_z \dot{B}_x - \dot{S}_x B_z}{S_y B_z - S_z B_y}$$

$\frac{d\psi}{dt}$

$$\omega_z = \frac{S_z \dot{B}_y - \dot{S}_y B_z}{S_z B_x - S_x B_z}$$

The momentum in each axis can then be computed by multiplying the angular velocity about that axis times the moment of inertia.

6 1.3 Computation of Yaw Angular Error

The signal proportional to the yaw angular error can be computed from either the combination of stored and measured magnetic field data in vehicle coordinates or the combination of stored and measured sunline directional vectors in vehicle coordinates. Using Figures 6-2 and 6-3 as references, the yaw angular error is defined as the angular difference $(\Delta\psi_1, \Delta\psi_2)$ between the projections on the x-y plane of reference and measured directional vectors. In developing the yaw angular error signal, P_ψ, the components contributed by the difference in sunline vectors and difference in magnetic field vectors will be weighed according to the accuracy to which they can be measured and the value of the denominator in each equation.

The yaw angular error signal is computed from the cross product of the components which lie in the x-y plane and is numerically proportional to the sine of the angular error. The two components are:

$$P_{\psi s} = \frac{K_3 \left[\overline{S_r\ (x\text{-}y)} \times \overline{S_a\ (x\text{-}y)}\right]}{|S_r\ (x\text{-}y)|\ |S_a\ (x\text{-}y)|}$$

$$= \frac{K_3 \left[S_{rx}\, S_{ay} - S_{ry}\, S_{ax}\right]}{\sqrt{S_{rx}^2 + S_{ry}^2} \times \sqrt{S_{ax}^2 + S_{ay}^2}}$$

$$= \frac{K_3 \left[S_{rx}\, S_{ay} - S_{ry}\, S_{ax}\right]}{\sqrt{(S_{rx}^2 + S_{ry}^2) \times (S_{ax}^2 + S_{ay}^2)}}$$

$$P_{\psi B} = \frac{K_2 \left[\overline{B_r\ (x\text{-}y)} \times \overline{B_a\ (x\text{-}y)}\right]}{|B_r\ (x\text{-}y)|\ |B_a\ (x\text{-}y)|}$$

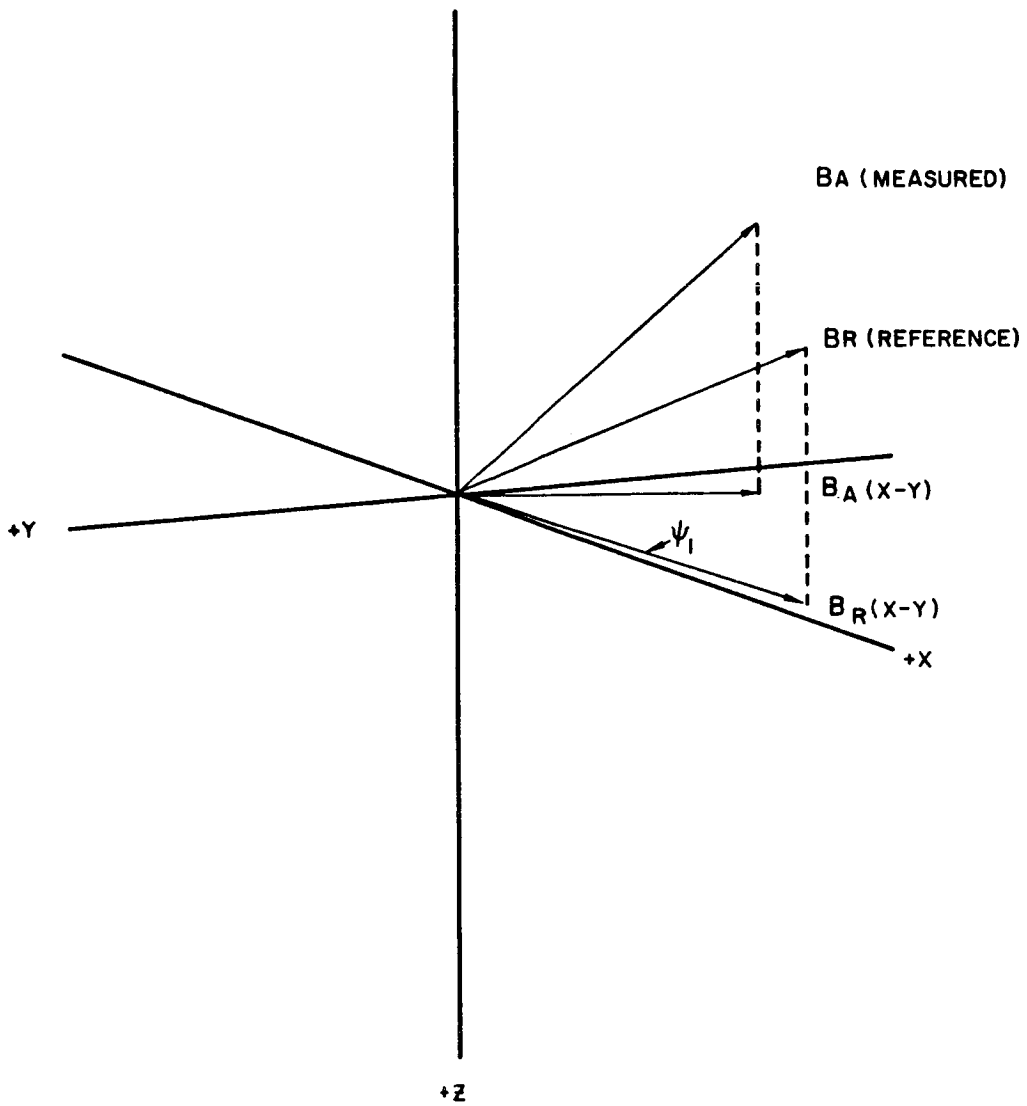

Figure 6-2 Reference and Measured Magnetic Field Vectors

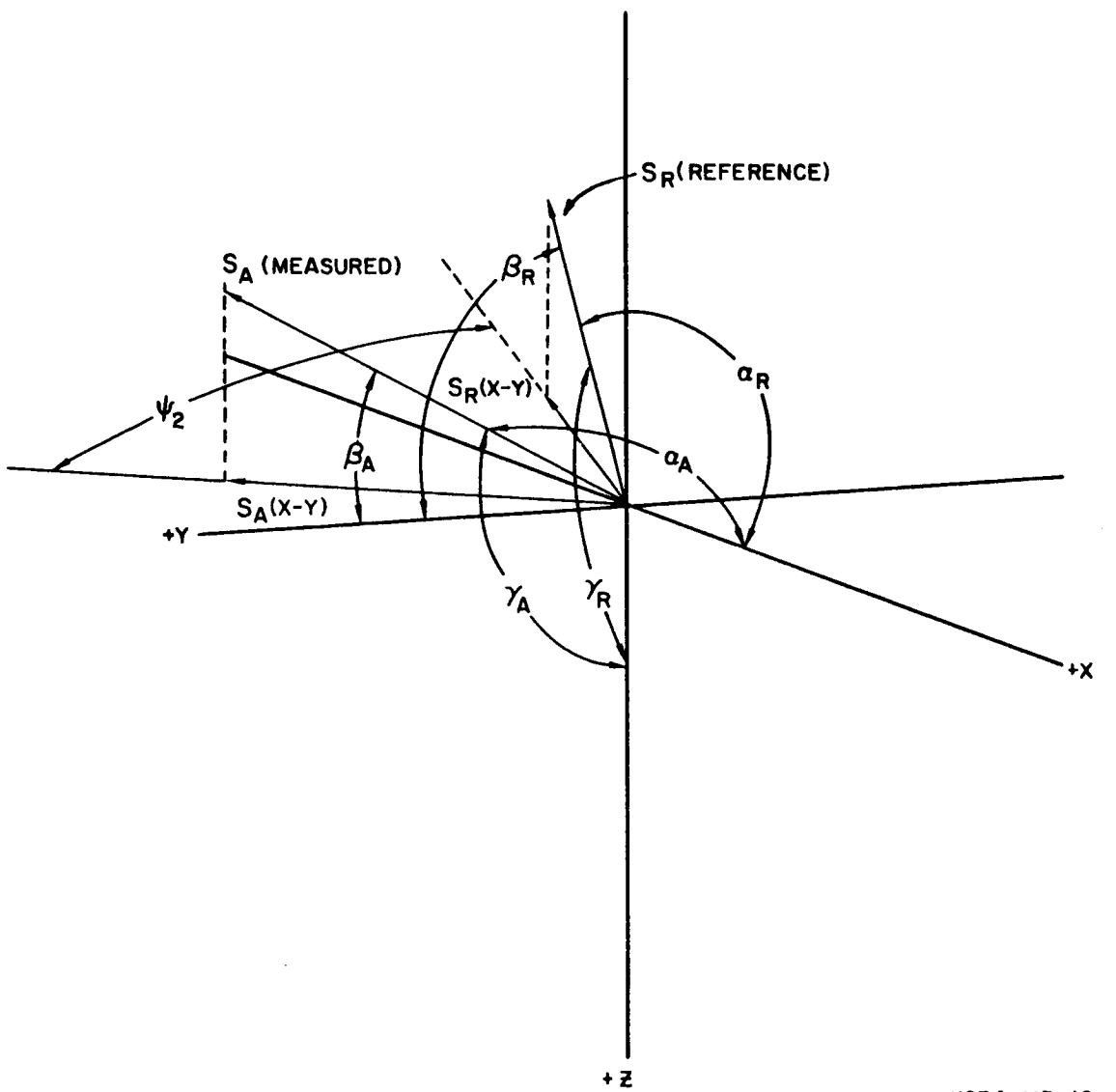

Figure 6-3 Reference and Measured Solar Direction Vectors

$$P_{\psi_B} = \frac{K_2 \left[B_{rx} B_{ay} - B_{ry} B_{ax}\right]}{\sqrt{(B_{rx}^2 + B_{ry}^2)(B_{ax}^2 + B_{ay}^2)}}$$

$$P_{\psi} = P_{\psi s} + P_{\psi B}$$

where:

$S_r\ (x\text{-}y) = i\ S_{rx} + j\ S_{ry}$ = component of stored sunline directional vector lying in the x-y plane. The subscript r refers to the reference function and indicates the direction, in vehicle coordinates, which the vector will assume for proper vehicle alignment.

$S_a\ (x\text{-}y) = i\ S_{ax} + j\ S_{ay}$ = component of measured (note subscript a) sunline directional vector lying in the x-y plane.

$S_{rx} = \cos \alpha_R$

$S_{ry} = \cos \beta_R$

$S_{rz} = \cos \gamma_R$

$S_{ax} = \cos \alpha_A$

$S_{ay} = \cos \beta_A$

$S_{az} = \cos \gamma_A$

$B_r(x\text{-}y)$, $B_a(x\text{-}y)$, B_{rx} etc. are magnetic field vector components corresponding in subscript notation to similar components of the S_a and S_r vectors.

6.1.4 The Complete Loop

Figure 6-4 illustrates the complete loop in block diagram form.

In paragraphs 6.2 and 6.3, the on-board and ground mechanization studies are discussed. The measured sunline and magnetic field component information is transmitted from the satellite, received and decoded, and used to compute the vehicle momentum and yaw error signal. The computation is performed by a digital computer which utilizes measured and stored (reference) vector information to develop the P_ψ (yaw error) signal and only the measured data to develop the momentum vector signals. Both the vector and position signals are then cross multiplied with the measured field vectors to generate signals proportional to the currents to be commanded in the three-axis coils.

Since it is desirable to use discrete-tone command transmission of current command information, the only feasible method of encoding is pulse-width modulation of the linear signal. This is performed in the blocks just preceding the tone command and transmitter block. Each pulse modulator energizes one of two tone signals depending on the sign of the current signal. The duty-cycle of the tone command signal is proportional to the magnitude of the current, and the satellite receiver decodes the signal in real time so that the average coil current is proportional to the I_x, I_y and I_z signals from the digital computer.

6.2 On-Board Equipment Mechanization

The purpose behind the development of a ground control for satellite orientation is, of course, to simplify the equipment on board the satellite, thus improving reliability; however, this simplification must be made within the framework of a feasible ground installation. The on-board and ground control equipment will now be assessed, the former with respect to reliability and weight, the

latter with respect to feasibility and availability.

The on-board equipment will consist of four solar sensor units, a solar sensor interrogation unit, a three-axis magnetometer, a telemetry system, a command receiver, a decoding and switching unit, three magnetic torquers and a power and connection unit. A general block diagram is shown in Figure 6-5. The individual components are described below:

6.2.1 Solar Sensing

The solar sensing units and its associated interrogation circuitry are described in section 5.3. The information unit will provide a 22-bit word representing the sun's location to the telemetry system.

6.2.2 Three-Axis Magnetometer

The magnetometer and its operation are described in section 5.2. It will provide three -2V to +2V analog signals representing the earth's field components to the telemetry system.

6.2.3 Telemetry

The approach presented to the telemetry communications problem for this control system assumes a data acquisition system whose capability equals that of the Fairbanks, Alaska or Goldstone stations. The space-borne system units and techniques have been proven in several space programs.

The data to be transmitted will be one 22-bit digital word from the solar sensor interrogation unit and three -2 to +2 volt analog signals from the magnetometer. The data will be transmitted in real time; no storage of data aboard the vehicle will be required.

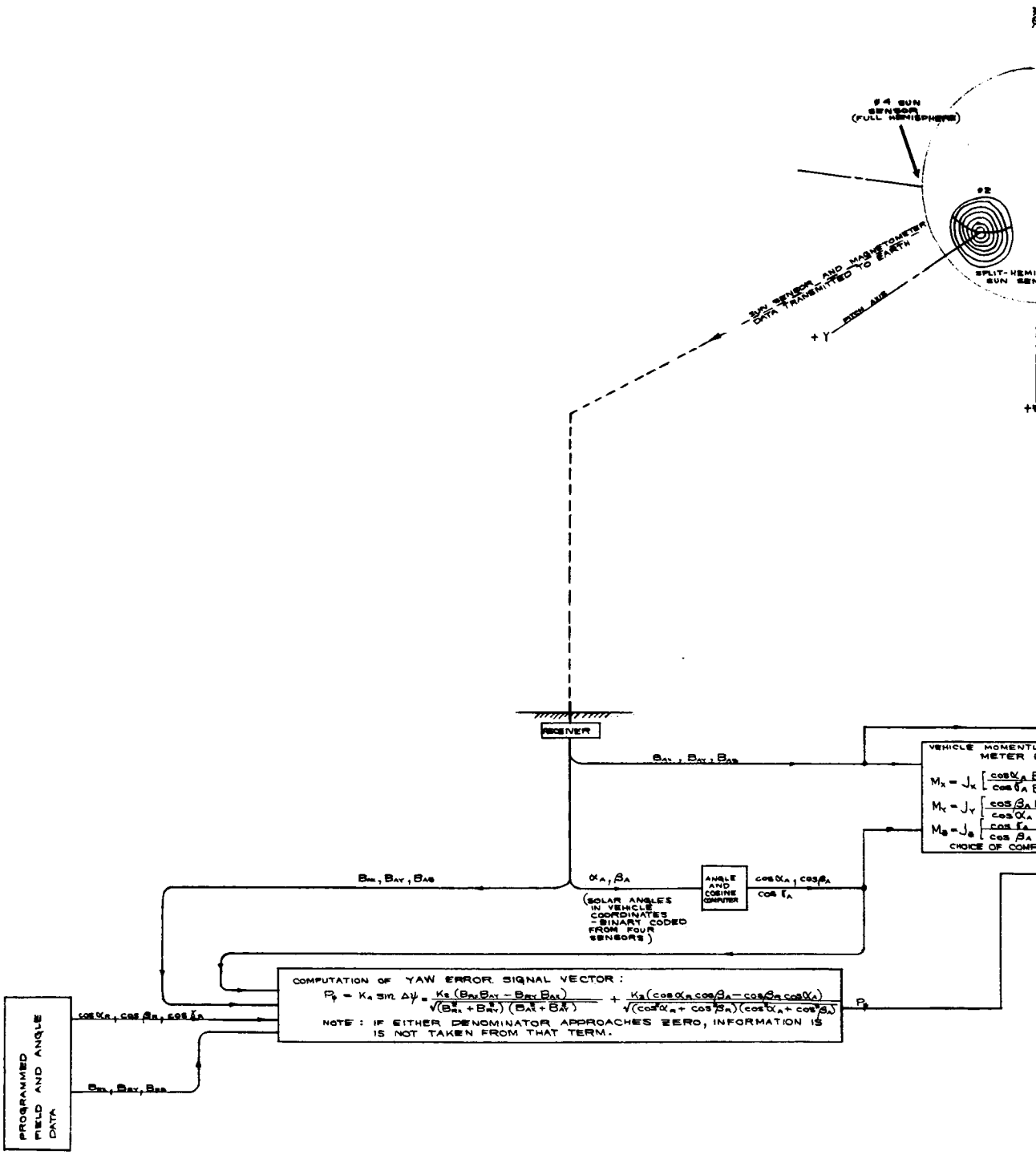
#4 SUN SENSOR (FULL HEMISPHERE)
#2
SUN SENSOR AND MAGNETOMETER DATA TRANSMITTED TO EARTH
+Y
ROLL AXIS
SPLIT-HEMI SUN SEN
RECEIVER
B_{AX}, B_{AY}, B_{AS}
VEHICLE MOMENTU METER
$M_X = J_X$
$M_Y = J_Y$
$M_S = J_S$
CHOICE OF COMP
B_{RX}, B_{RY}, B_{RS}
α_A, β_A
(SOLAR ANGLES IN VEHICLE COORDINATES - BINARY CODED FROM FOUR SENSORS)
ANGLE AND COSINE COMPUTER
$\cos\alpha_A, \cos\beta_A$
$\cos\gamma_A$
COMPUTATION OF YAW ERROR SIGNAL VECTOR:
$P_\psi = K_A \sin\Delta\psi = \frac{K_B (B_{RX}B_{AY} - B_{RY}B_{AX})}{\sqrt{(B_{RX}^2 + B_{RY}^2)(B_{AX}^2 + B_{AY}^2)}} + \frac{K_B(\cos\alpha_R\cos\beta_A - \cos\beta_R\cos\alpha_A)}{\sqrt{(\cos^2\alpha_R + \cos^2\beta_R)(\cos^2\alpha_A + \cos^2\beta_A)}}$
P_ψ
NOTE: IF EITHER DENOMINATOR APPROACHES ZERO, INFORMATION IS IS NOT TAKEN FROM THAT TERM.
PROGRAMMED FIELD AND ANGLE DATA
$\cos\alpha_R, \cos\beta_R, \cos\gamma_R$
B_{RX}, B_{RY}, B_{RS}

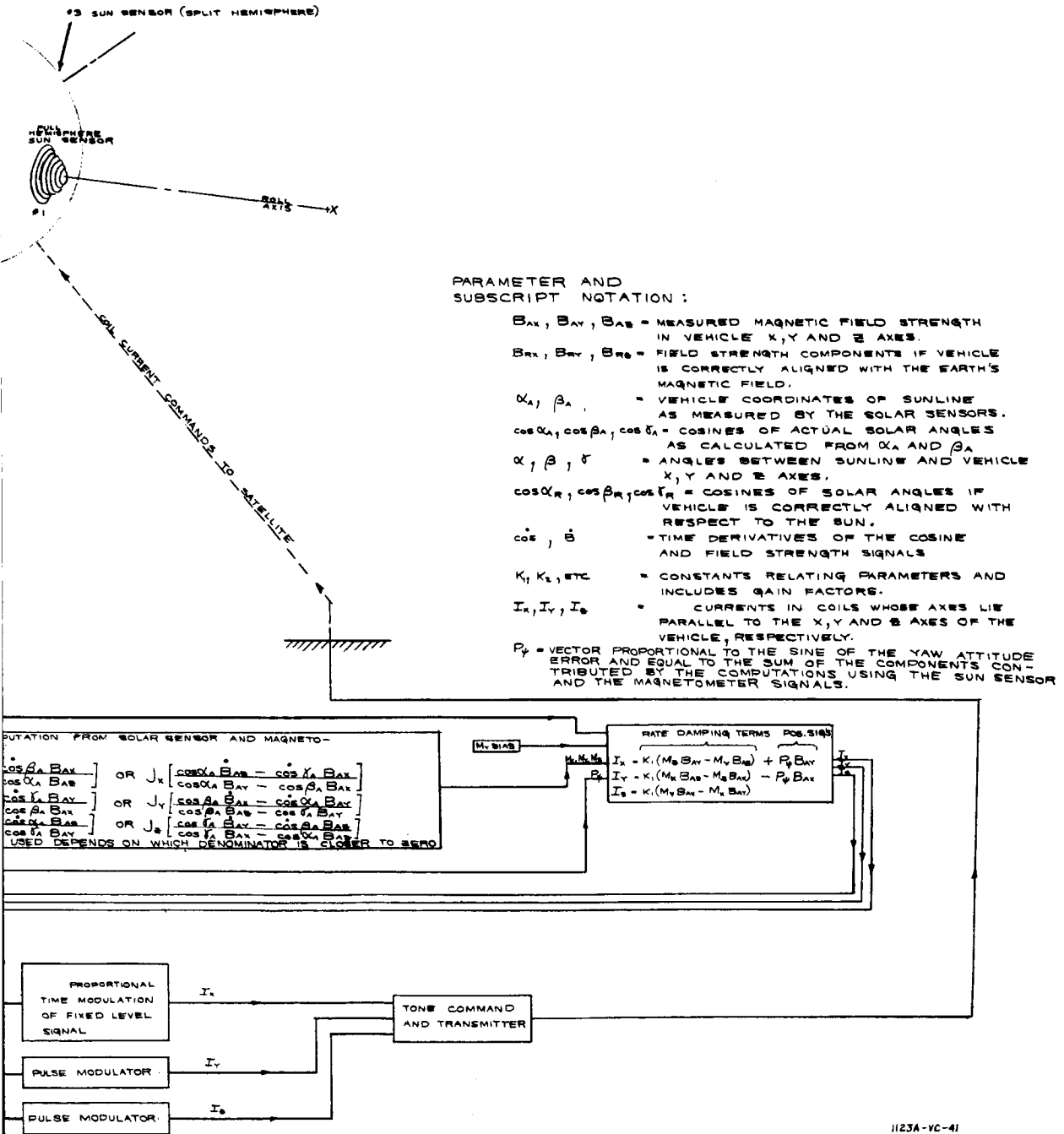

FIGURE 6.4
BLOCK DIAGRAM - GROUND COMPUTER REQUIREMENTS
REMOTE COMPUTER SATELLITE CONFIGURATION
Page 6-11 / 6-12

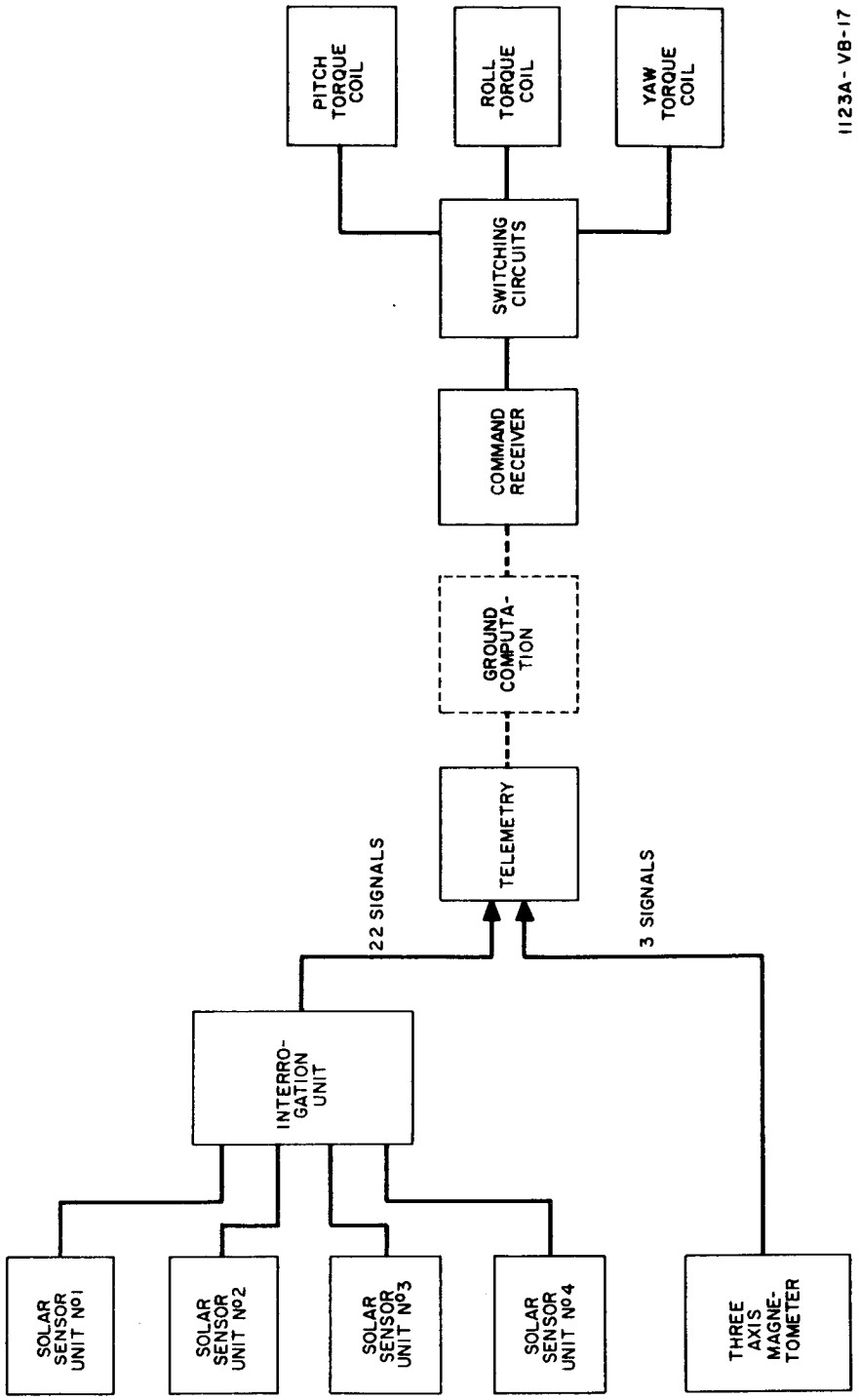

Figure 6-5

Block Diagram - On Board Control Equipment

The spaceborne telemetry system will consist of a PCM telemetry transmitter operating at a carrier frequency of 1700 mc with an r-f power output of 1 watt; an analog-to-digital converter which changes the three magnetometer signals into three seven-bit words; and a commutator containing a synchronizing channel and four data channels. The data will be sampled at 5 cps and the system data rate for all signals will be 215 bits per second. Utilizing the N.A.S.A. data acquisition station equipment, including the 85 foot parabolic receiving antenna, a carrier-to-noise ratio of 40.07 db can be obtained in a 6-hour orbit.

The probability for success for one year for the above system is 0.864, a figure arrived at by combining information from Radiation, Inc. on the transmitter with estimates on the commutator and A-D converter. In order to obtain good reliability, two fully redundant systems will be used in parallel. This gives a probability of success for one year of 0.982. The weights indicated later (in Table 6-A) include all redundancy.

6.2.4 Command System

The command system will utilize pulse duration bursts of one of 30 audio frequency tones which are coded and arranged by a format that can provide up to 70 distinct, secure commands. The system will operate in the 120-150 Mc band, and similar systems have been proven thoroughly in actual satellites.

Tone bursts are transmitted from NASA Digital Command Console in 5-word frames. The frames consist of two address and three command words. If either of the first two words and any of the last three words are received, the command is executed. Each word consists of 10 bits; a blank bit, a synchronizer bit, and 8 data bits. A complete frame is transmitted every 686 milliseconds. Although 70 commands are available from the 8 data bits, the only commands used will be the positive and negative torque commands for the pitch, roll and yaw channels.

Using the standard NASA command transmitters, a carrier-to-noise ratio of 35.15 db can be obtained for a 6 hour orbit.

The receiver output will operate a decoder and switching circuit. All commands will be coupled directly to the torque coils by means of electronic switches. Multiple levels of command are not necessary.

In order to obtain high reliability, two parallel receivers and a redundant 7-channel decoder will be used, to give an overall probability of success for one year of 0.975, according to a manufacturer.

6.2.5 Magnetic Torque Coils

Three magnetic torque coils are aligned along the three vehicle axes. Each coil need produce only a 200 dyne-cm torque to counteract the disturbance expected and provide damping for the vehicle. With a suitable design margin applied the coils must have a length of 10 inches and a diameter of 0.6 inches to produce the desired torques. In order to simplify the control equipment, the torques will be pulse modulated to obtain the desired proportionality. Currents will be constant-level, but reversible by means of the command switching.

6.2.6 Miscellaneous Electronics

A power supply is required to provide regulated voltages to the various components. It will consist of inverters and voltage regulators. In addition to the power supply, a junction center is needed with which to connect the various components, and provide test capability. Redundancy is required to obtain adequate reliability. The reliability shown below was determined from ar. S-52 power supply breakdown and added connection data.

6.2.7 Summary of On-Board Equipment Characteristics

Table 6-A tabulates the control system data.

Table 6-A

Component	Weight lb.	Volume in.3	Power Watts	Reliability Ps/1 year
Solar Sensors	4.5	471	2.0	.973
Magnetometers	2.0	42	2.0	.990
Telemetry	3.0	100	5.0	.982
Command System	7.0	130	3.0	.975
Magnetic Torquers	2.0	12	1.0	.997
Misc. Electronics	3.0	75	5.0	.991
TOTALS	21.5	830	18.0	.912

It should be noted that there are no moving parts and the wearout life of each component part is practically unlimited. For a three-year period the success probability would be 0.774.

This reliability result is far superior to those obtained in realistic evaluations of more conventional attitude control techniques.

6.3 ANALYSIS OF GROUND BASED COMPUTER REQUIREMENTS

6.3.1 General Capabilities

The ground based computer must have the following capabilities:

1. Arithmetic (multiply, divide, add, subtract).
2. Logical operations (masking, shifting, tests, etc.).
3. Floating point (hardware or routines).
4. Sin-Cos routines (fixed and floating).
5. Square root routines (fixed and floating).
6. Flexible input/output.
7. Magnetic tape handling (two drives).

8. Card or punched paper tape I/O.

9. Printer or typewriter output.

6.3.2 Memory

In order to facilitate tape searching and to provide a memory buffer for incoming satellite data and outgoing commands it is estimated that a minimum of 4096 words of core storage will be required. The memory should be used to store the sine, square root, floating point, input/output routines, and main program as well as the data, commands and tables. A suggested minimum word size of 18 bits will be needed for packing, numerical resolution, and efficient storage.

6.3.3 Feed-Through Time

The feed-through time or time from transmission of data from satellite to reception of commands by satellite will be almost entirely dependent on the extent of data handling required to provide an interface between the telemetry equipment and the computer's memory as well as the tape handling time to retrieve tabular information from the magnetic tape drives. However, the computations themselves will require some time. It is estimated that the computations will require approximately 6000 machine cycles. This figure was arrived at by determining the average number of computations that would be necessary and assigning weights to each type of computation. The weights that were used were selected as being representative of many commerically available computers as opposed to applying specifically to any particular computer.

6.3.4 Input/Output Requirements

A buffered input/output is required to provide an interface with the P.C.M. data handling equipment. This input/output should be flexible and programmable. The standard peripheral equipment should include card or paper tape input and output equipment and at least two magnetic tapes for program and table storage. A printer, typewriter or flexowriter will be needed for "hard copy" output.

6.3.5 Applicable Systems

A digital computer capable of handling the requirements ranges in price from $150,000 up to a few millions of dollars. The following computer systems (approximately in the price range of $150,000 to $220,000, including tape drives) will be applicable for the purpose, listed in the order of their degree of suitability for the task:

1. SDS 920	Scientific Data Systems
2. PDP-1	Digital Equipment Corp.
3. AD/ECS 37A	General Mills
4. PB-250	Packard Bell

The SDS-920 is a single address, serial machine with a basic memory of 4096 words. The fixed word length consists of 24 information bits plus one parity bit. The execution times vary from 16 micro sec. add and 32 micro-sec multiply for fixed point operations to 192 micro sec add and 184 micro sec multiply for floating point operations. All memory operations on this machine are parity checked as are all input/output characters. Flexible input/output is achieved by five independent input/output systems and two standard priority interrupts. Buffering is provided so that a number of input/output operations can be carried on simultaneously. Standard low-density tape format (200 bits/inch at 75 in/sec) can be read and written by this machine. A 300 character/second photoelectric paper tape reader and a 60 character/second tape punch is supplied as standard equipment with the SDS-920. A 300 line/minute, 132 character/line printer is supplied. Software support is supplied by the following programming systems:

1. SDS 900 FORTRAN II	(Mathematical language)
2. SYMBOL	(Symbolic language)
3. HELP	(Machine language)

In addition, a full library of subroutines as well as a special computer diagnostic program, EXAMINER, round out the programming aids and facilitate pinpointing marginal conditions if they should exist. Memory access time is 8 microseconds.

The PDP-1 is a single-address, serial machine with a basic memory of 4096 words, each word consisting of 18 bits. Fixed point execution times are add 5 microsec, multiply 300 microsec, divide 600 microsec. Input/output is serial and standard low-density tapes can be read or written. Supplied with the PDP-1 is a 300 character/sec. photoelectric reader and a 20 character per second paper tape punch. An assembly routine and a full library of subroutines are available to users. Memory access time is 5 microseconds.

The AD/ECS 37A packs two single address instructions in its 37 bit word. This serial machine has a basic memory of 4096 words fixed point add, multiply, and divide times are 80, 840, and 940 microsec, respectively. Buffered input/output and interrupt logic provide flexible interface capability, but tape handling capability is only fair. Standard peripheral equipment includes typewriter, 150 character/sec., paper tape reader and 12 character/sec tape punch. Very little software support is available for users of this machine. Memory access time is 8 microseconds.

The PB-250 is a fixed point, serial machine with a 22 bit word length. The basic memory consists of 1808 words which can be expanded in modules of 256 words to a maximum of 15,888. Add, multiply and divide times are 108 microseconds, 372 microseconds and 348 microseconds respectively. Standard peripheral equipment includes a flexowriter, 300 character/second paper tape reader and 110 character/second tape punch. Memory access time is 1540 microseconds.

6.4 CONCLUSIONS

The ground control system described in this study report has been shown to meet the requirements for attitude accuracy if the information supplied by the sensors is non-granulated, displacements are confined to small angles, and the computation of coil currents is performed in real time. Since the actual system which was chosen relies on granulated sunline vector information and digital computation of coil currents, it actually remains to be proven that the system will maintain the required attitude accuracy. It is recommended, therefore, that the program be extended to include a simulation which includes the following:

(a) Sun sensor information which is generated in discrete steps;

(b) Large angle, tumbling initial conditions;

(c) Transport lags to simulate digital computation.

However, there is every reason to expect that the ground-controlled system with granulated position signals and digital computation will exhibit a performance substantially like that obtained in section 4.2.

In addition, one can conclude that ground and control brings a marked improvement in satellite reliability, and that the ground computation task is quite feasible with existing equipment and at reasonable expense.

7.0 SOLAR ARRAY CONTROL

7.1 Description of Problem

A comparison of power supply systems utilizing non-oriented, yaw-oriented, and yaw-and-elevation-oriented solar arrays has been made for three different mission configurations. The following data were assumed as a working basis.

TABLE 7-A

Parameter	Mission		
Launch Date	1964	1966	1968
Circular orbit period, hr.	6	12	24
Orbit inclination angle, deg.	32	32	0
Power supply output, watts	250	270	330
Lifetime, years	1.5	3	3
Vehicle weight, lb.	500	500	750

The satellite configuration, assuming it to be compatible with the plan of Section 4.0, must allow the greatest possible use of gravity gradient stabilization, requiring the vehicle to have large pitch and roll moments of inertia, compared to the yaw moment of inertia. This configuration also implements a desire for low yaw control power. The satellite configuration shown in Figure 7-1 has been chosen as one which will have good gravity gradient qualities and have the flexibility necessary for most satellite programs.

The three solar array systems must be compared on the bases of:

(A) Size of the power supply for a given output;

(B) Complexity and weight of the array orientation means.

As the array is made more efficient by better orientation, the orientation equipment becomes heavier and less reliable. The best type of array for a given

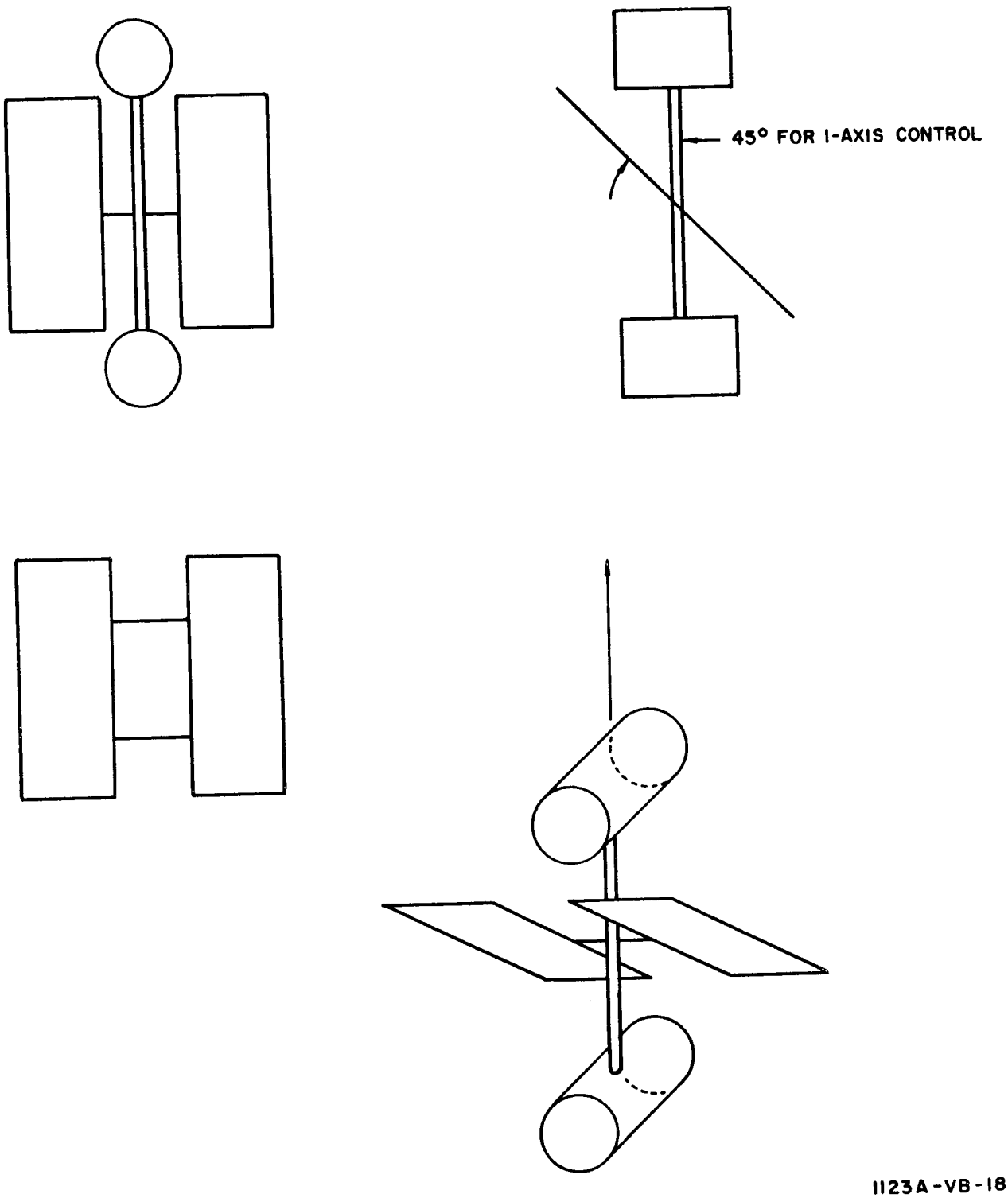

Figure 7-1: Vehicle Configuration

satellite application will depend on the relative importance assigned to the characteristics of power supply weight and system reliability. However, the basic elements of this tradeoff will be derived here by sizing the array for each orientation technique and by performing a preliminary mechanization study of the yaw and array (elevation) control systems for the purpose of sizing these systems and estimating their reliabilities.

7.2 Sunline Angle and Control Motions for Solar Arrays

In order to compare the various array plans, it is necessary first to develop the sunline angle for the partially oriented array (yaw control only). For the completely oriented array, the sunline angle is 90°, or the aspect ratio is unity, except at occultation. In this section the average aspect ratio for various declinations of the sun is given for a vehicle in a 32° inclined circular orbit. Three different orbital periods are used: 6 hr., 12 hr., and 24 hr. periods. The maximum possible occultation times are considered when developing the aspect ratio for these periods.

The vehicle has the yaw axis always aligned to the local vertical. The vehicle and associated solar paddles are allowed to turn about the yaw axis to arrive at the best possible aspect ratio. For the partially oriented method, the solar paddles are fixed at an angle of 45° to the yaw axis. These paddles have solar cells on both sides. In the completely oriented method, the solar paddles can have motion relative to the vehicle about an axis perpendicular to the yaw axis. Solar cells are needed only on one surface of the paddles in this latter case.

A general set of equations were developed with yaw and elevation control which will always keep the aspect ratio at unity. The results are modified to arrive at the aspect ratio for yaw control only. These equations are as follows:

Yaw

$$A = \tan^{-1}\left(\frac{-\tan \delta}{-\sin \alpha}\right)$$

Elevation

$$E = \sin^{-1}\left(\cos \alpha \cos \delta\right)$$

In Figure 7-2 the two parameters A and E are shown along with the other parameters necessary in the derivation of the equations. The term α is the satellite orbital position as measured from noon. The term δ is the angle between the orbital plane and the ecliptic plane. This angle will change with time and can be as high as 55.5°. This consists of two parts, which are the 23.5° maximum displacement of the sun from the equator and the 32° orbit inclination. It is not necessary for the development of the following curves to have a time history of declination.

The yaw (azimuth) and elevation control motions, illustrated in Figures 7-3 and 7-4 respectively are plotted as functions of orbit angle for various angles between the ecliptic and orbital planes. These are the motions through which the solar paddles must turn in order to keep the aspect ratio at unity.

Special use is made of Figures 7-3 and 7-4 for the case where there is yaw control only to arrive at the best possible aspect ratio. The solar paddles for this case have cells placed on both sides, and the paddles are fixed to the vehicle at an elevation angle of 45° to the yaw axis. In Figure 7-5 the azimuth or yaw angle for this case is plotted against orbit angle for various declinations. At 90° and 270° orbit angle, the paddles are rotated 180 degrees in yaw which will then expose to sunlight the solar cells on the opposite side of the paddles. In Figure 7-6, the elevation angle is shown as a function of orbit angle for various orbital declinations. In generating the curves, 45° was added to the elevation angle which was calculated from the elevation equation in order to

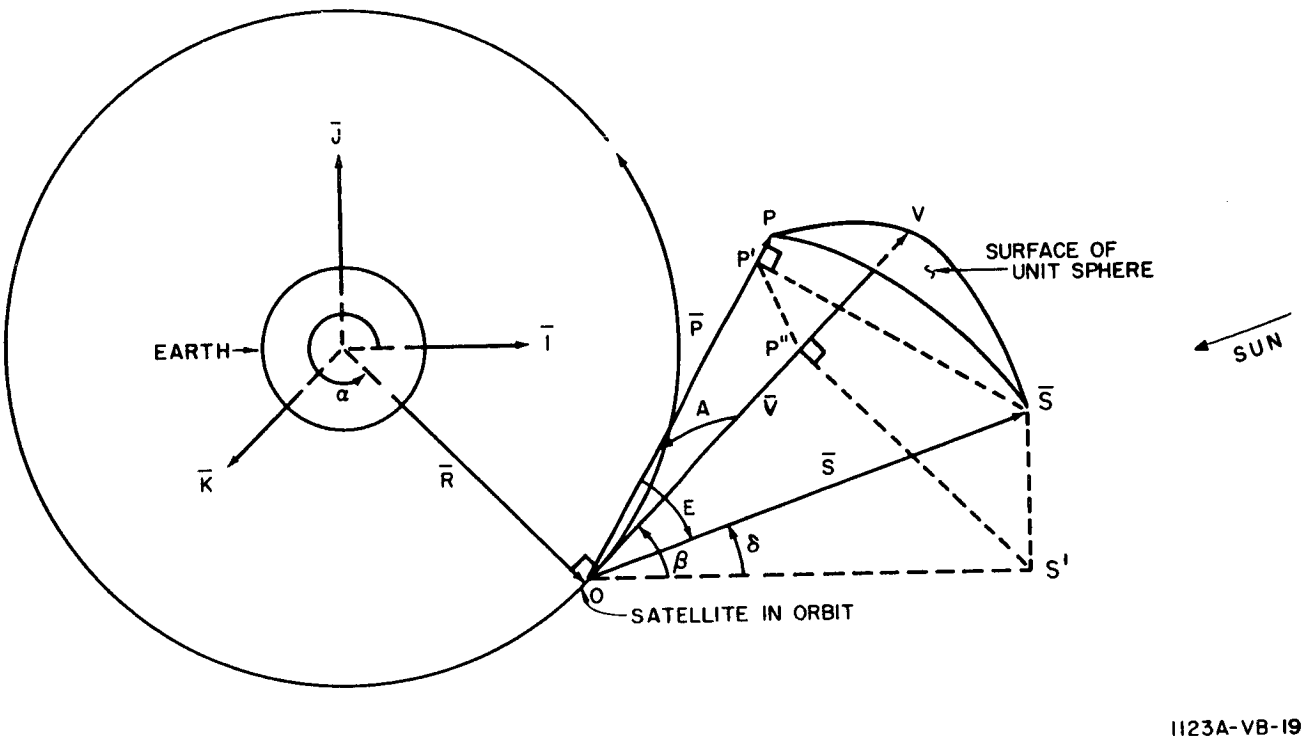

Figure 7-2: Diagram of Control Motions

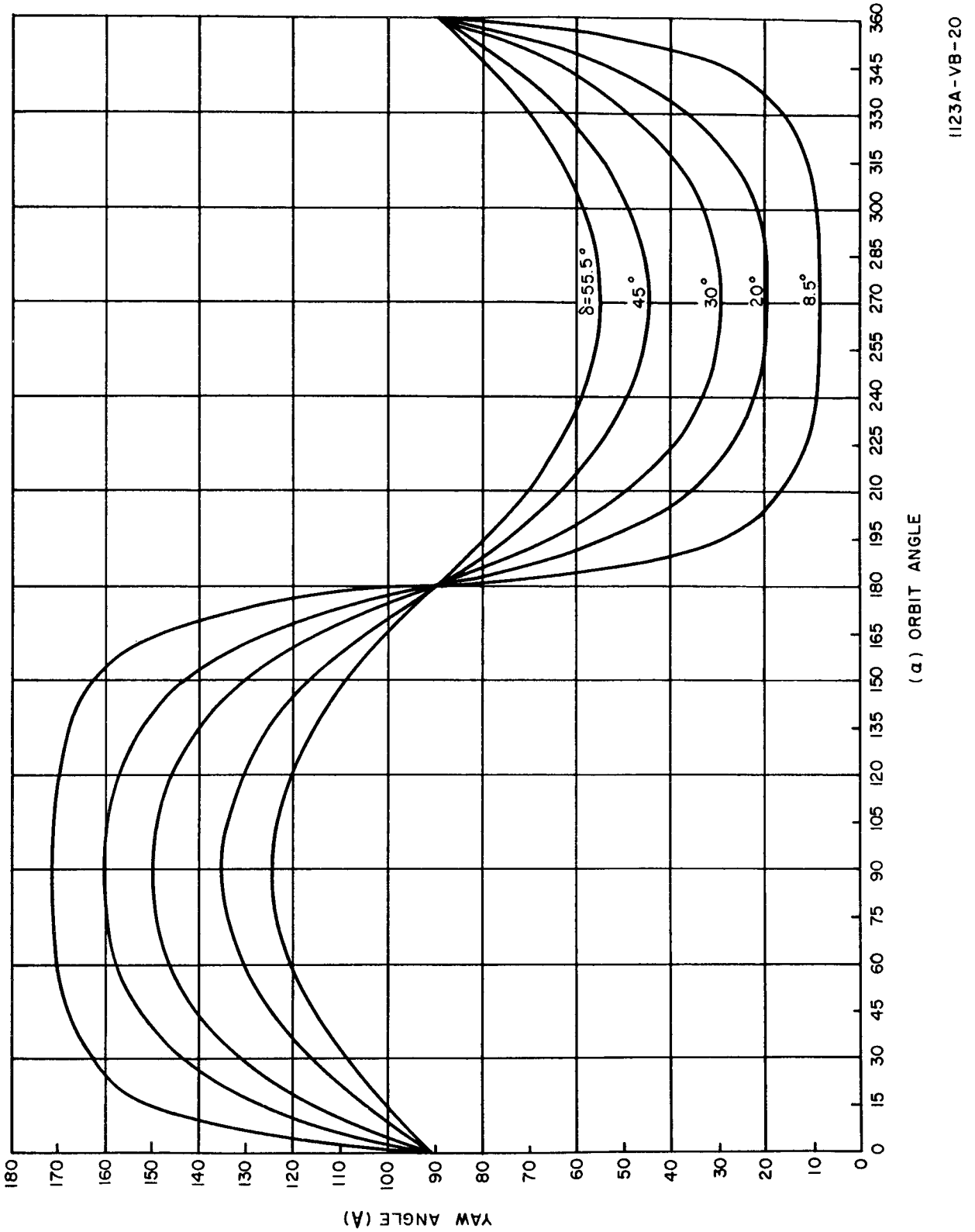

Figure 7-3: Yaw Angle vs. Orbit Angle

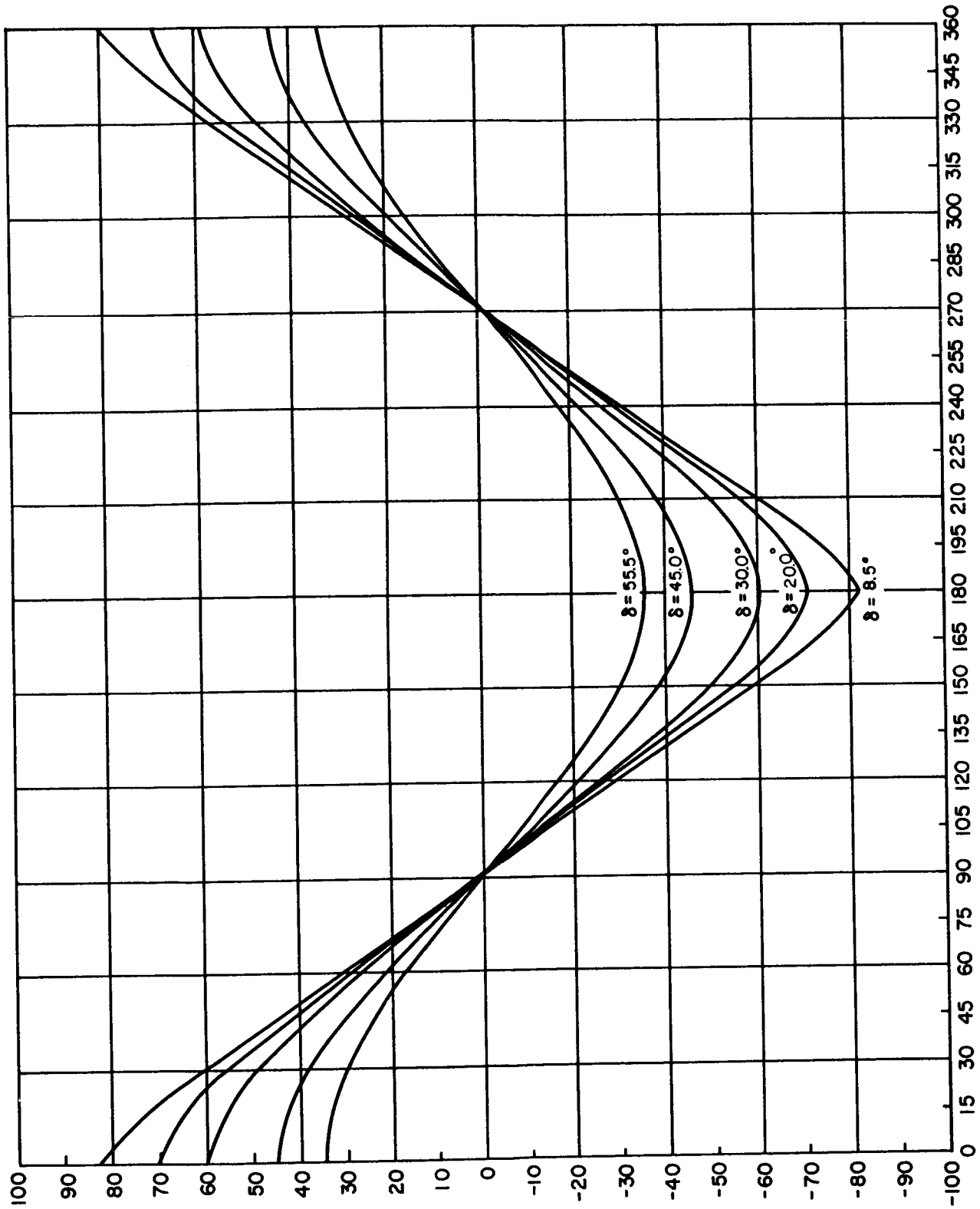

1123A-VB-21

Figure 7-4: Elevation Angle vs. Orbit Angle

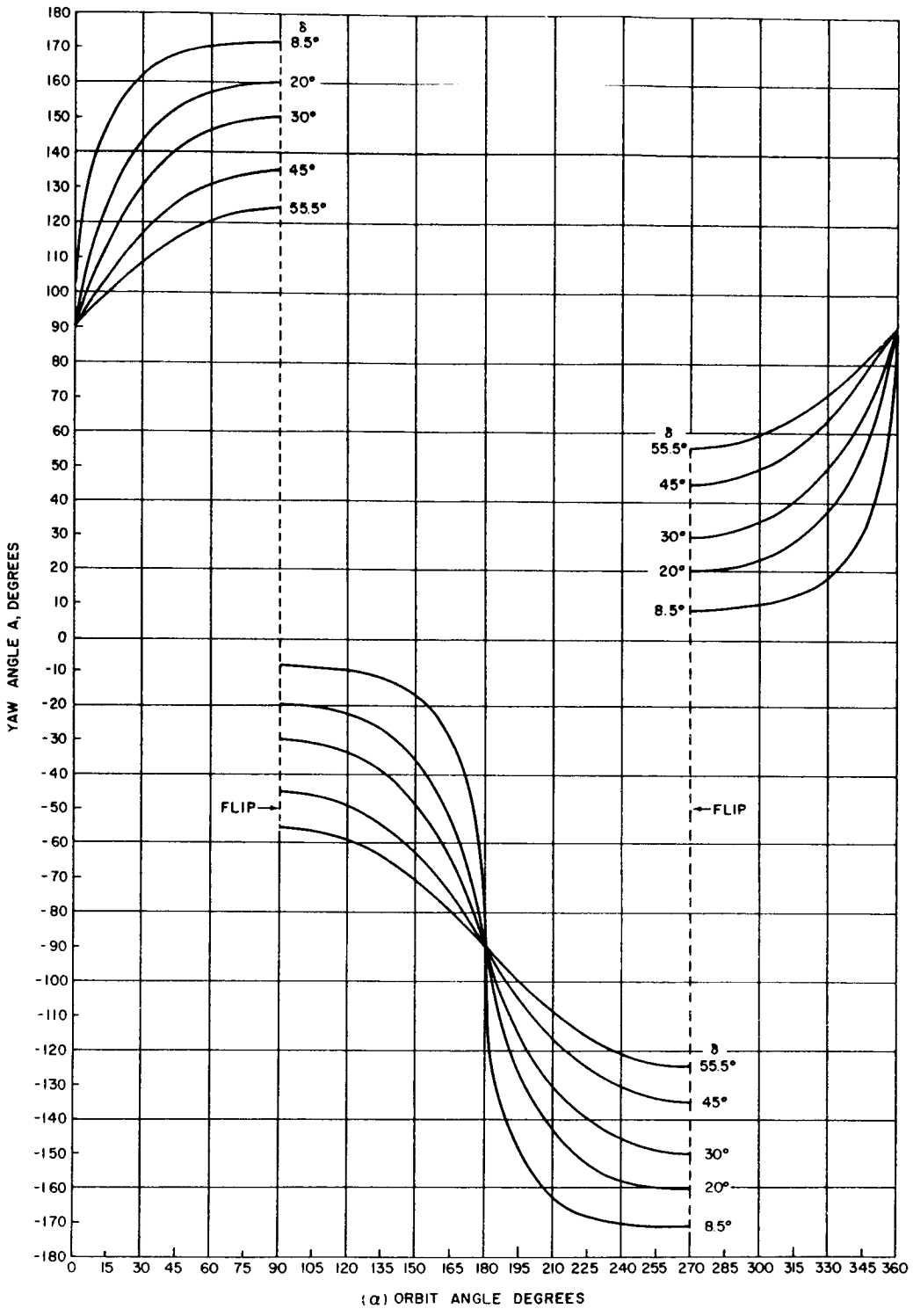

Figure 7-5: Yaw Angle vs. Orbit Angle, with 180° shifts

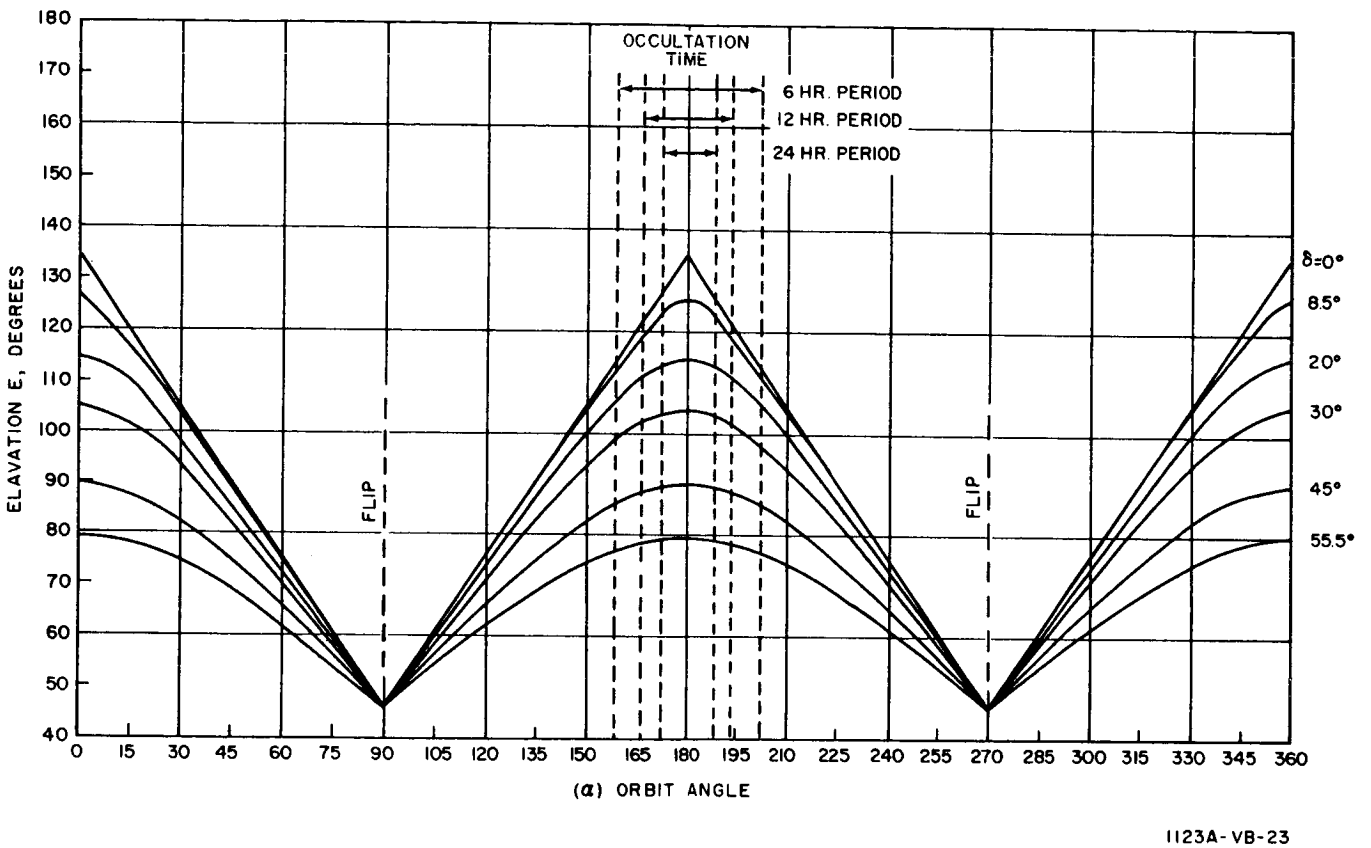

Figure 7-6: Elevation Angle vs. Orbit Angle, with 180° Shifts

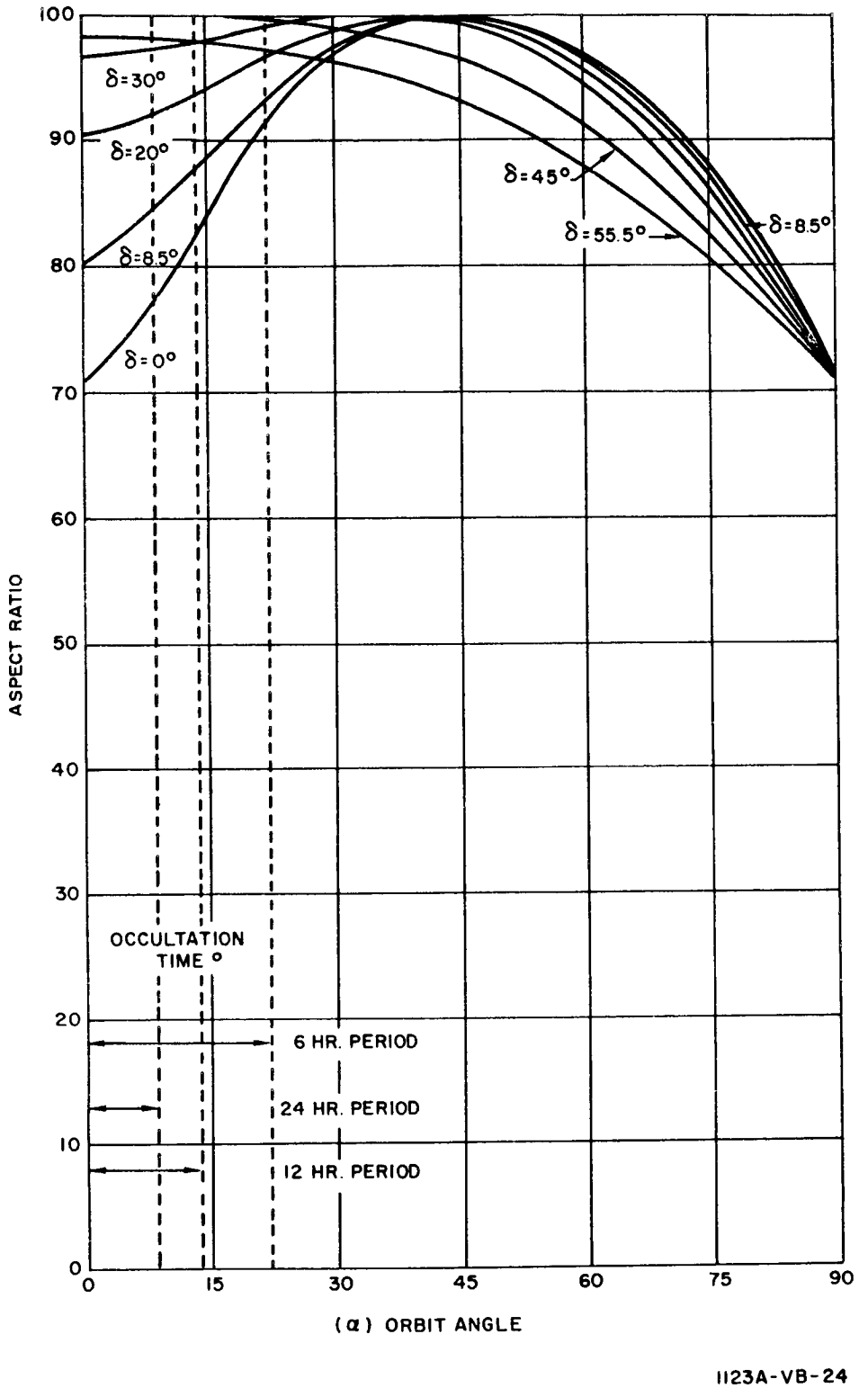

Figure 7-7: Aspect Ratio vs. Orbit Angle

account for the pre-set angle that the paddles make with the vehicle. When this procedure is followed, the aspect ratio of the cells facing the sun does not fall below cos 45°. Without the 180° flip, the aspect ratio would decrease to zero as the orbit angle increased from 90° toward 180°. The elevation angle in Figure 7-6 is then the angle that the sun makes with the paddles. For this portion of the study the aspect ratio for various orbits is more important than the control motion since the paddles can have no elevation motions. The aspect ratio is then plotted in Figure 7-7 for a quarter orbit for various declinations. Since this ratio repeats for a complete orbit except for occultation periods, a quarter orbit plot is sufficient. The occultation times are shown with vertical lines appropriately marked for orbit periods of 6 hr., 12 hr., and 24 hr. in both Figures 7-6 and 7-7. The curves of Figure 7-7 were graphically integrated to arrive at Figure 7-8, which is the average aspect ratio for a complete orbit taking into account the maximum occultation time for various declinations. As before, three orbits are considered. At declination angles above 8.5°, 13.6°, and 22°, there are no occultations in the 24-hour, 12-hour, and 6-hour orbits, respectively. The limits of the average aspect ratio for a complete orbit will be between the no-occultations curve and the 6 hr., 12 hr., or 24 hr. orbit curve, depending upon the period selected.

7.3 Yaw-Oriented Array Control System

In this system, the yaw axis is oriented such that the line X-X is always normal to the sun line, for the general configuration as shown in Figure 7-9. The array is positioned such that it makes a 45° angle to either the pitch or yaw axis. During one orbit, the elevation angle of the array varies between 45° and 135° as shown in Figure 7-5. Each curve is shown for the various possible angles of orbit inclination to the ecliptic plane. The vehicle is rotated through 180° twice during each orbit.

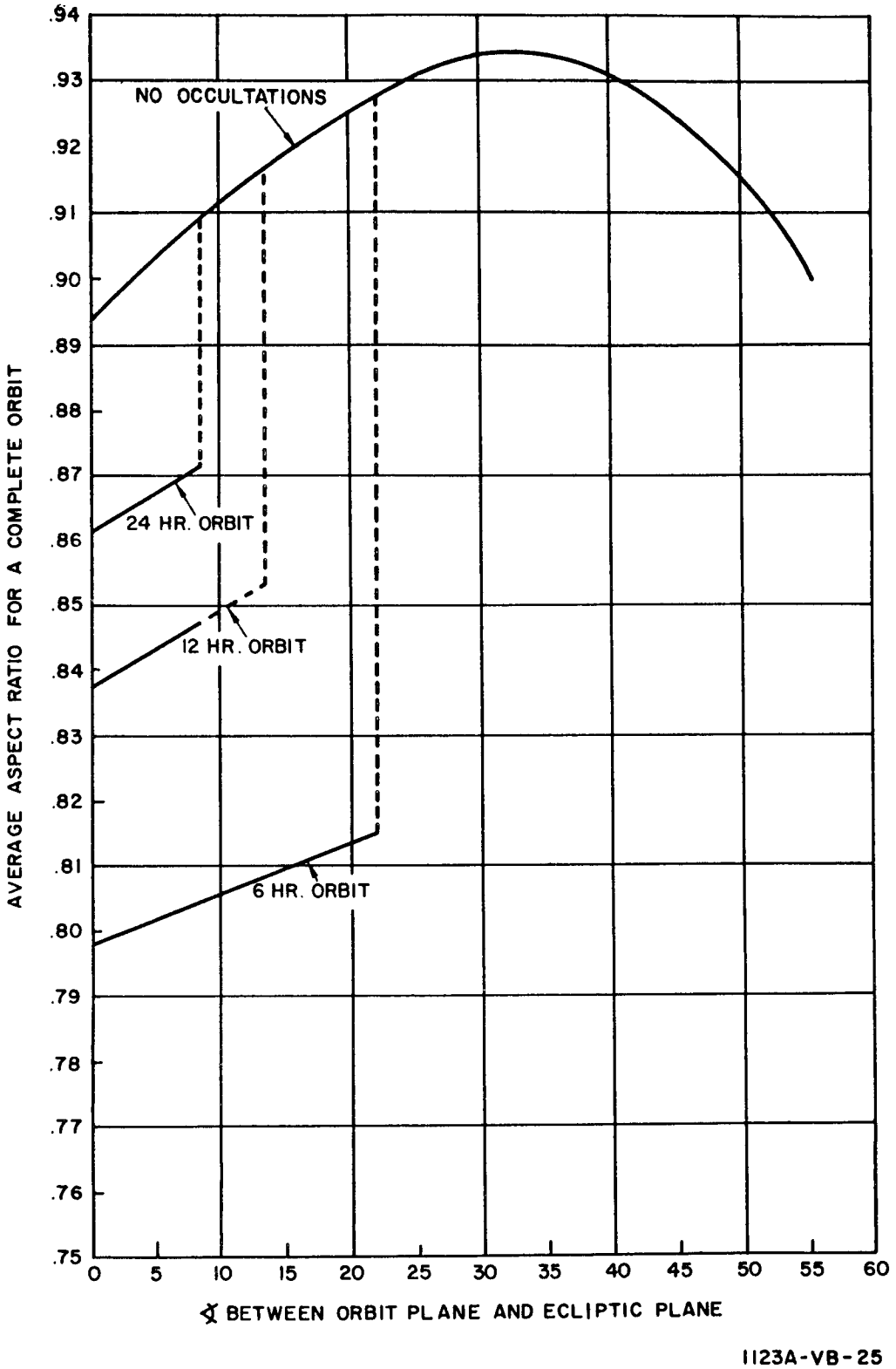

Figure 7-8: Average Aspect Ratio

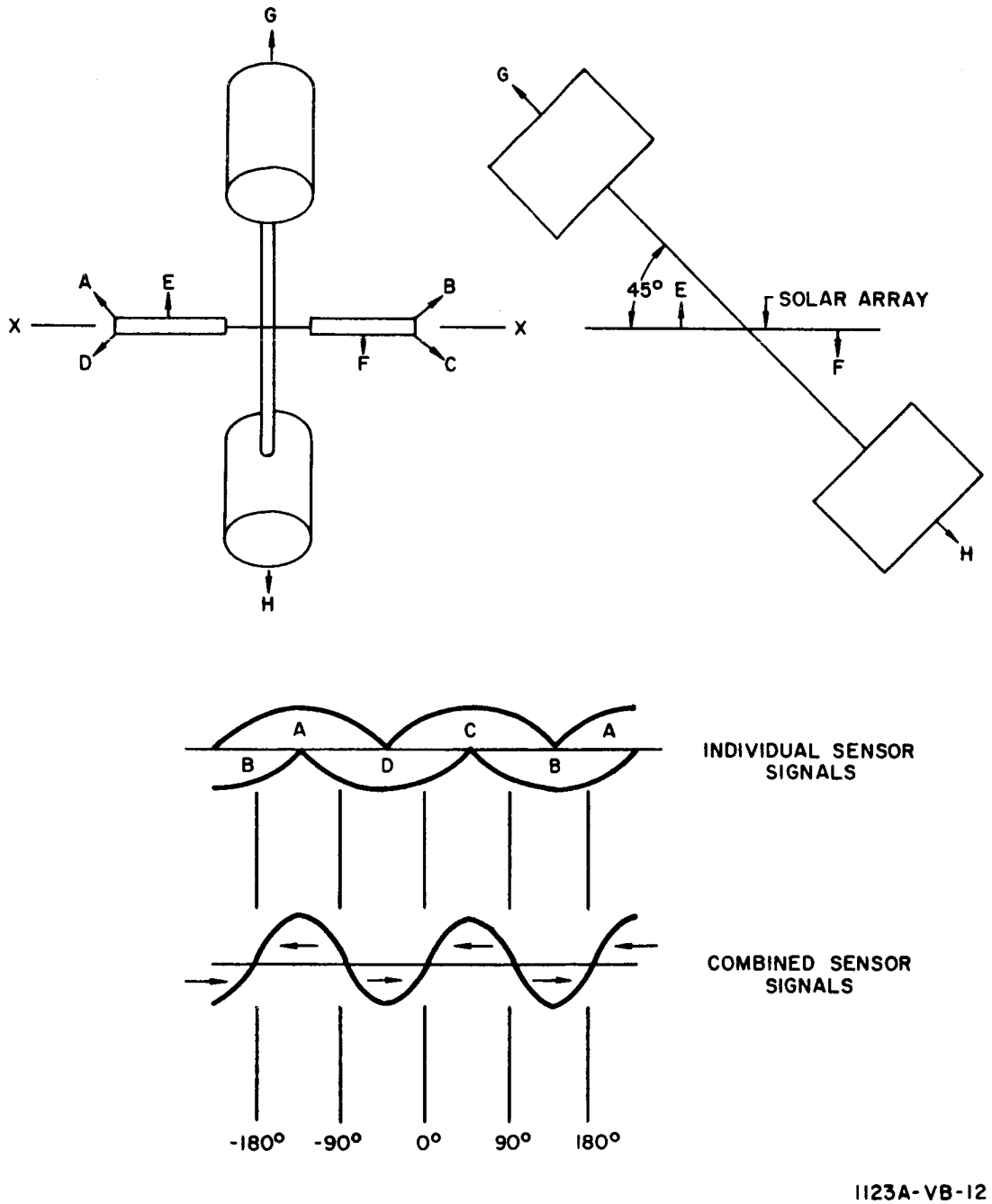

Figure 7-9: Solar Cell Configuration, Yaw Oriented Vehicle

The array control system is shown in Figure 7-10. Four solar cells A, B, C, and D are arranged, as shown in Figure 7-9, so as to give stable outputs when the yaw component of the angle between the sunline and the normal to the array is 0° or 180°. This method obviates the switching of sensor polarity periodically. The solar cell output is modulated to control the power amplifier which drives an inertia wheel. The inertia wheel, (with essentially constant torque vs. speed), has the capability of turning the vehicle through 180° in less than 4 minutes. As shown in Figure 7-6 if at 90° or 270°, a flip were not used, the solar cell aspect ratio would go to zero; i.e., the elevation angle would vary between 90° and -90° as shown in Figure 7-4, resulting in an average aspect ratio of less than 0.25. To prevent this, solar cells E and F, oriented as shown in Figure 7-9 are used to determine when the sun angle becomes less than 45°. If the cell output goes below 0.7 V max, a 30-second time delay is initiated. If during the 30 seconds the output falls below 0.1 V max, the time delay relay is reset, and no control is initiated since the satellite is in the earth's shadow. The main solar cells are switched out until the E-F solar cell voltage exceeds 0.1 V max. If the E-F cell output remains between 0.1 V_{max} and 0.70 V_{max} for 30 seconds, a timer is energized, and provides a control signal which torques the reaction wheel in a direction such as to reduce its speed for 100 seconds, then torques it in the opposite direction for the same length of time.

This effectively rotates the vehicle 180° in yaw, ending with zero velocity. A tachometer in the reaction wheel drives a switch which indicates initial wheel direction.

Solar sensors G and H, aligned with the yaw axis and having a 10 degree field of view, inhibit control when the yaw axis is within 5 degrees of the sun line, since in this area, no yaw control can improve the aspect ratio, and very small perturbations could require complete rotation of the vehicle.

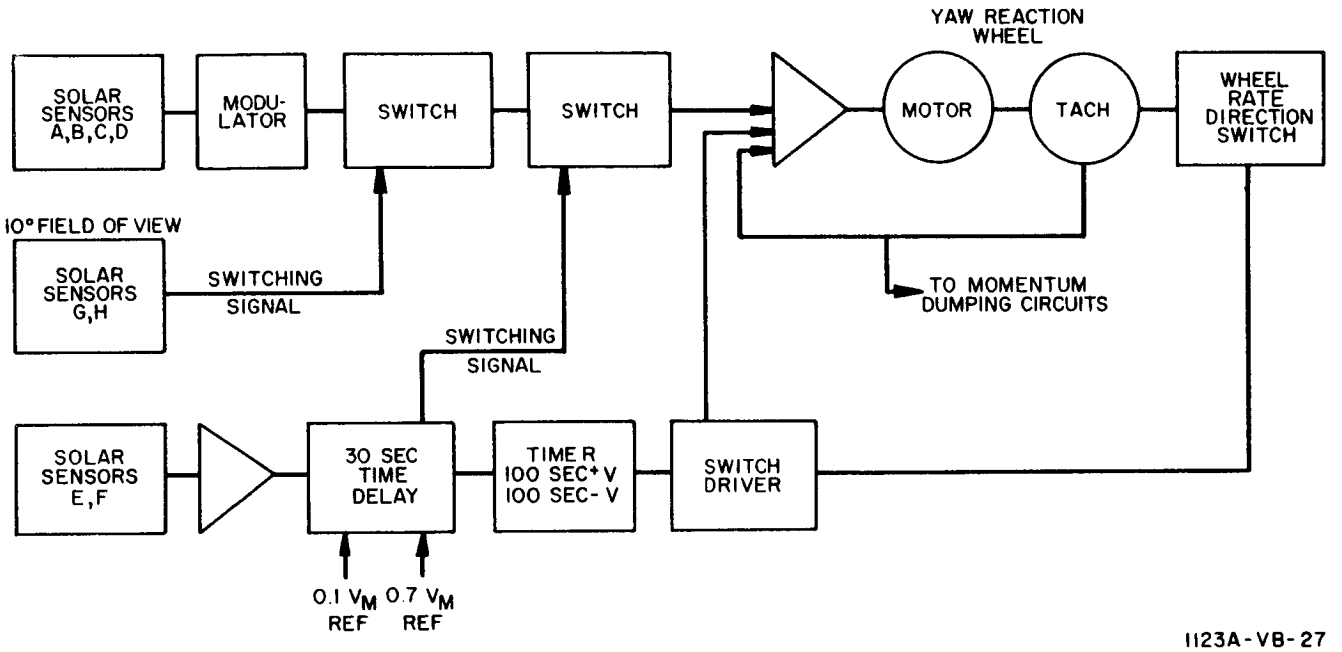

Figure 7-10: Block Diagram Yaw Orientation System

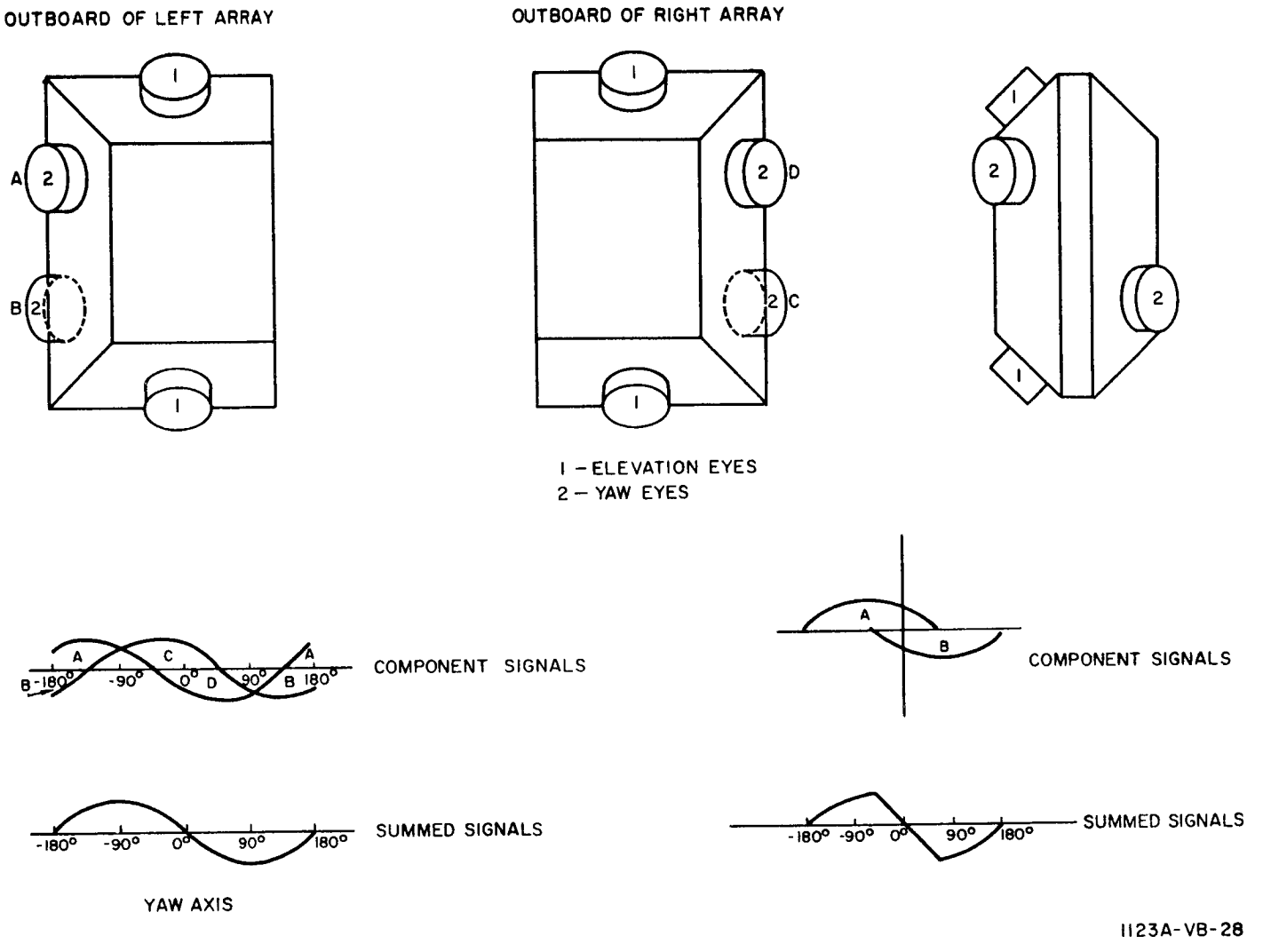

Figure 7-11: Solar Cell Configuration, Fully Oriented Array

None of the control functions need be extremely accurate. Slight variations in the 180° turn angle will be corrected by the control system. An error of 5° in the control of the vehicle would reduce the aspect ratio by only a small percentage. The pointing accuracy, using the sensors contemplated, will be within ± 3 degrees. The wheel will be dumped magnetically by the vehicle control system.

7.4 Yaw and Elevation Array Control System

In this system, the vehicle is controlled in pitch and roll axes to the local vertical, and in yaw such that the array axis (line X-X) is normal to the sun line. In addition, the array is controlled about its elevation axis such that the array plane is always normal to the sun line. Under these conditions, the angle between the array plane and satellite axes will vary as shown in Figures 7-3 and 7-4.

The solar sensor configuration is shown in Figure 7-11. The yaw sensors have a 360° field of view collectively, and only one stable point. Their summed signal drives a reaction wheel which is rate-feedback damped. The parameters are such that the satellite can be rotated through 180° in less than 4 minutes. The block diagram is shown in Figure 7-12.

The elevation sensors have a combined field of view of 270°. Duplicate sets are used on each side of the vehicle to prevent shadowing. Each sensor has an inboard reticle which prevents reflected light from producing errors. The sensors outputs are summed and the signal used to drive the elevation gimbal. In order to cancel the relatively high momentum of the array, a counter-rotating flywheel may be driven by this motor. Rate feedback is used for stabilization. The elevation gimbal is limited to ± 90° to avoid the necessity for slip rings, thereby increasing reliability. Occasionally the ± 90° limits will be exceeded.

When this occurs, a limit switch is operated, initiating a 180° yaw turn, in a direction such as to reduce the initial yaw wheel speed.

A zenith sun sensor pair defines the vehicle yaw axis, and is used to inhibit control when the yaw axis is within 5° of the sun line.

The azimuth drive mechanism is shown in Figure 7-13. It is completely sealed except for the output shaft bearing, which operates at low speed. This exposed bearing and the azimuth shaft bearings will be gold plated bearings in order to obtain long life characteristics. The flywheel will rotate at a maximum of about 1200 rpm. This speed is large enough to reduce the wheel size, but allow long bearing life.

The satellite configuration will be as shown in Figure 7-1. For the boost phase, the array can be locked parallel to the yaw axis, and its outer halves folded in toward the vehicle to reduce the overall dimensions.

7.5 Non-oriented Array

In this system, the vehicle is oriented in pitch and yaw to the local vertical, and in yaw to the velocity vector (arbitrary assumption). Under these conditions, the solar array must receive energy from any direction. Six separate plane areas of cells, normal to the positive and negative vehicle axes would be necessary to obtain consistent power. Care would have to be taken to prevent shadowing, since any vehicular protuberances would tend to shadow portions of the array and reduce power output. If shadowing were completely eliminated, very little vehicle area would be available for instrumentation and communication outlets.

As will be seen in Section 7.6, the area and weight of solar cells required exceed practical limits, for the vehicle size contemplated.

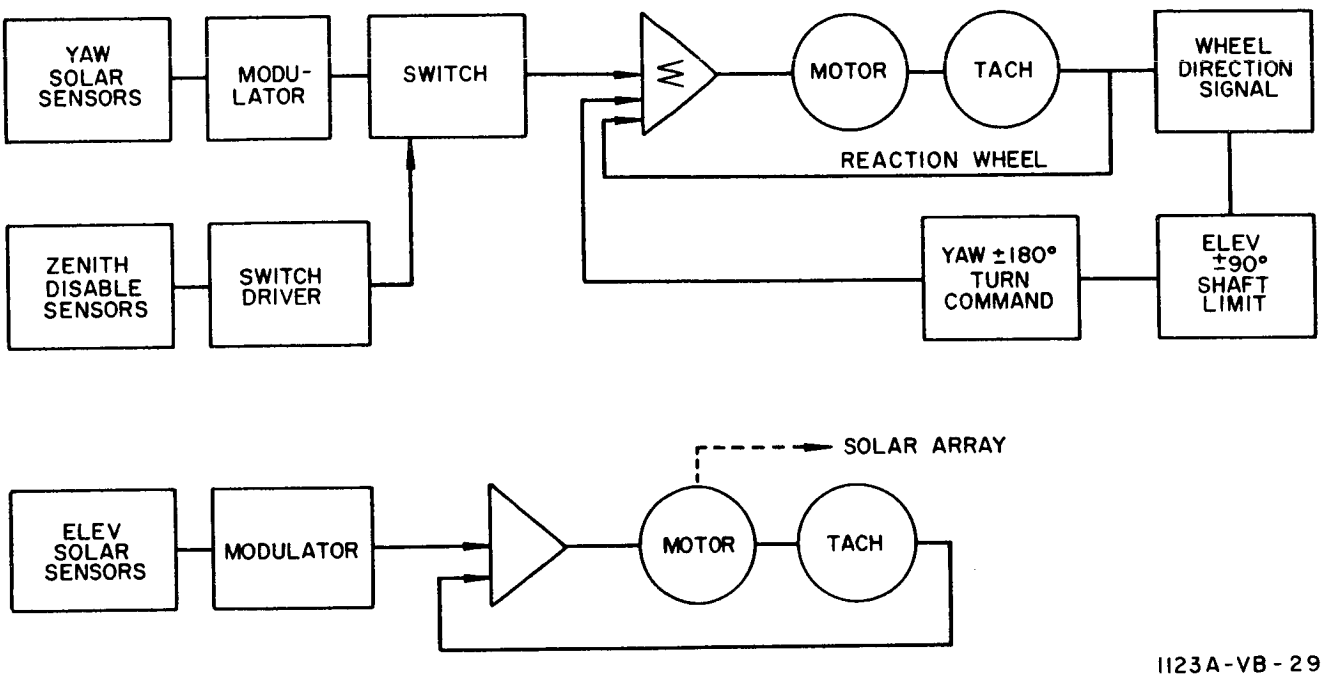

Figure 7-12: Block Diagram, Yaw and Elevation Oriented Array

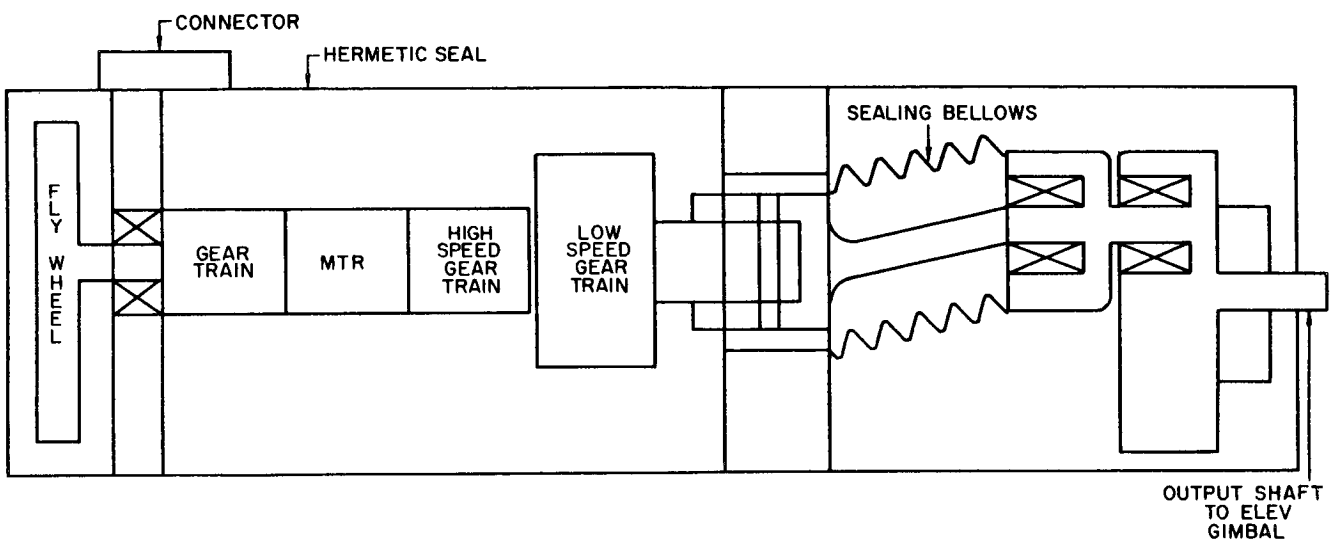

Figure 7-13: Array Drive

7.6 Power Supply Mechanization

Satellite power requirements of 500 watts or less to be supplied for a period not exceeding five years with good reliability can be most easily satisfied by a combination of solar cells and storage batteries. The solar cells convert solar energy into electrical power during the orbital day to operate equipment, and part of this power is stored in the battery for periods when solar power is not available. Examples for 6, 12, and 24 hour orbits have been worked out to obtain insight into power supply, weight, and size, and the effects of orientation thereon. The power to be obtained and the weights of the necessary voltage regulators and inverters, assuming an efficiency of 85% each, are listed in Table 7-B.

TABLE 7-B

Voltage	6 Hr. Orbit		12 Hr. Orbit		24 Hr. Orbit	
	Power, watts	Weight, lbs.	Power, watts	Weight, lbs.	Power, watts	Weight, lbs.
+28V±2%	210	3.5	230	3.6	296	5.0
-28V±2%	1	0.8	1	0.8	1	0.8
115V,400 cps						
ØA	18	1.8	18	1.8	12	1.6
ØB	8	1.4	8	1.4	8	1.4
ØC	8	1.4	8	1.4	8	1.4

The solar cell panels are required to provide power for load requirements during orbital daytime as well as power to be stored in the battery for operation during night-time periods. The night-time periods are approximately 44, 54.3, and 69.6 minutes for 6, 12, and 24 hour orbits respectively. An additional margin of power from the solar cells is necessary for battery charging efficiency, which is about 75%.

After correction for solar cell efficiency, transmissivity of glass covers, micrometeorite erosion, temperature, and packing factor, a conservative estimate of power available is 10 watts per square foot of solar panel normal to the sun line. For continuous perfect solar array orientation the panel area need be only 35 square feet for the 6 and 12 hour orbits and 41 square feet for the 24 hour orbit. (The 24 hour orbit requires 330 watts, as opposed to 250 and 270 watts for the 6 and 12 hour orbits). For the non-oriented array, these numbers must be multiplied by six to obtain adequate power. For the yaw-oriented array, a solar panel with cells on both sides is considered. In the worst case, half the cells will be oriented 45° from the sun line; in the best case, half the cells will be normal to the sun line. The average aspect ratio will be 0.4, 0.42, and 0.43, for the 6, 12 and 24 hour orbits, respectively.

During orbital night, operating power must be provided by the battery. Adequate cycle life of the battery can be assured only by limiting the depth of battery discharge to a percentage of its capacity. With the long orbital period, the capacity of the battery need be only the product of the maximum dark time and the required load current divided by discharge depth. However, for short orbital periods, the day-time period is short, while the night-time period is still nearly an hour. For the case where high charging currents are required, and the solar array output varies considerably during an orbit, the battery capacity will be controlled by the maximum allowable overcharge rate, which is usually specified as one-tenth the battery capacity. In the examples, battery capacity is obtained for both capacity drain and overcharge rates, and the limiting value used.

Design battery cycle life expectancy of 1095 cycles for the 24-hour orbits is satisfied by the use of silver cadmium batteries at a 30% depth of discharge and a ratio of 8 watt-hr. per pound. The 2190 cycle life requirement

for the lower altitude orbits requires the use of nickel-cadmium batteries at a 30% depth of discharge and a ratio of 4 watt-hours per pound. It is considered unnecessary to use redundant batteries since adequate reliability is obtained at 30% depth of discharge.

To protect the cells from micrometeorite erosion, glass covers of 0.060 inch thickness are used in the weights calculated for the 6 and 12 hour orbits, since these orbits lie in the Van Allen high-radiation regions. Glass with 0.04 inch thickness is used for the synchronous orbits, since the upper limit of the Van Allen regions extends well beyond this altitude.

The solar cells make up most of the power supply cost. They cost about $4,000 per square foot. Space batteries cost about $16 per watt-hour.

Sample calculations are shown below:

For a 6-hour orbit, using two-axis orientation, the raw power required by the regulators is calculated below.

For ±28 VDC: $\frac{211 \text{ watts}}{.85 \text{ efficiency}} = 248 \text{ watts}$

For 115V, 400 cps: $\frac{34 \text{ watts}}{.85 \text{ efficiency}} = 40 \text{ watts}$

The total is 248 + 40 = 288 watts, raw power.

Night operation will require, for a 44-minute night;

$$288 \text{ watts} \times \frac{44}{60} \text{ hour} = 211 \text{ watt hour}$$

The power required to recharge the battery after a night operation is

$$\frac{211 \text{ watt-hr.}}{.75 \text{ eff.} \times 5.2 \text{ hr. daylight}} = 54 \text{ watts}$$

The total solar cell power required is

288 watts (raw) + 54 watts = 342 watts.

This requires a solar cell area of 35 ft^2.

For a one-axis oriented system the following calculations indicate the requirements. The battery requirements here will be determined by allowable overcharge rather than by energy drain. The battery requirements due to night-time drain would be:

$$\frac{211 \text{ watt-hr}}{30\% \text{ depth} \times 32 \text{ V}} = 22 \text{ amp-hrs.}$$ However, at 10 watts/ft^2, the solar cell area is

$$\frac{342 \text{ watts}}{.4 \text{ aspect ratio} \times 10 \text{ watts/ft}^2} = 85.5 \text{ ft}^2, \text{ for both sides.}$$

For each side the area is 85.5 ft^2/2 = 42.7 ft^2.

The charge power received by the batteries is:

427 maximum watts - 288 watts (for best orientation) = 139 watts.

This power must be taken by the battery. The resultant battery charging current is then:

$$\frac{139 \text{ watts}}{32 \text{ V}} = 4.3 \text{ amp.}$$

Since the battery can tolerate only 10% overcharge, the battery capacity determined from the overcharge current must be:

4.3 amp (10 hr.) = 43 amp. hr.; this multiplying factor is an empirical one furnished by battery manufacturers. Note that this rating exceeds the drain requirement of 22 amp-hr.

All the data are tabulated below:

Two-Axis Orientation:	6 hr.	12 hr.	24 hr.
Raw power (watts)	288	312	383
Night operation power (watts)	211	282	444
Battery recharge power (watts)	54	35	26
Total power (watts)	342	347	408
Area, (ft.^{2})	35	35	41

One-Axis Orientation:	6 hr.	12 hr.	24 hr.
Battery drain capacity (amp-hrs.)	22.0	30.0	46.0
Solar Cell area, ($ft.^2$)	85.5	82.6	94.9
Solar cell area, each side, ($ft.^2$)	42.7	41.3	47.5
Battery charge power, (watts)	139.0	101.0	93.0
Battery overcharge capacity, (amp. hr.)	43.	32	30.
Battery charge current (amp.)	4.3	3.2	3.0

Using the above information the following data are obtained:

	6 hrs. Orbit		12 hr. Orbit		24 hr. Orbit	
1. Non-oriented array	Wt.-lb.	Cost ($\$10^3$)	Wt.-lb.	Cost ($\$10^3$)	Wt.-lb	Cost ($\$10^3$)
Battery	53	11	71	15	56	23.5
Solar Paddle	336	840	336	840	408	984
Total	394	851	407	855	464	1007.5
2. Yaw oriented array						
Battery	105	22	76	16	56	23.5
Solar cell	140	342	136	330	156	380
Total	245	364	212	346	212	403.5
3. Two axis oriented array						
Battery	53	11	71	15	56	23.5
Solar Paddle	58	140	58	140	68	164
Total	111	151	129	155	124	187.5

7.7 Comparisons of Systems

Since the non-oriented array must have equal equivalent areas projected in all directions, two problems exist. First, the number of required cells becomes so large that they make up a great portion of the total assumed vehicle weight, second, the required configuration makes mechanization difficult, and would badly compromise the ability to obtain a large ratio of moments of inertia for gravity gradient control. To obtain 250 watts of power, 336 lb. would be required. The required area would be 240 $ft.^2$. Neither of these values is practical for a 500 lb. vehicle. The comparisons of Tables 7-C and 7-D then consider only the yaw-oriented and yaw-and-elevation-oriented arrays.

TABLE 7-C

Weight, Lb.

Component	Yaw Orientation 6 hr.	12 hr.	24 hr.	Yaw -Elevation Orientation 6 hr.	12 hr.	24 hr.
Batteries	105	76	56	53	71	56
Solar Paddle	70	68	78	58	58	68
Reaction Wheel	8	8	10	8	8	10
Electronics	5	5	5	7	7	7
Gimbal Drive	-	-	-	10	10	12
Sensors	1	1	1	1	1	1
TOTAL	189	156	150	137	155	154

Power, Watts

Component	Yaw Orientation 6 hr.	12 hr.	24 hr.	Yaw-Elevation Orientation 6 hr.	12 hr.	24 hr.
Batteries	-	-	-	-	-	-
Solar Paddle	-	-	-	-	-	-
Reaction Wheel	6	6	6	5	5	5
Electronics	5	5	5	8	8	8
Gimbal Drive	-	-	-	5	5	5
Sensors	-	-	-	-	-	-
TOTAL	11	11	11	18	18	18

Component	Yaw Orientation 6 hr.	12 hr.	24 hr.	Yaw-Elevation Orientation 6 hr.	12 hr.	24 hr.
Batteries	3000	2250	1200	1570	2100	1200
Solar Paddle*	12300	11900	13700	10600	10600	11800
Reaction Wheel	200	200	250	200	200	250
Electronics	300	300	300	400	400	400
Gimbal Drive	-	-	-	125	125	150
Sensors	10	10	10	10	10	10
TOTAL	15810	14660	15460	12905	13435	13810

* Includes Support

TABLE 7-D

Reliability

Component	Yaw Orientation P_s, 1.5 yr. 6 hr. Orbit	P_s, 1.5 yr. 12 hr. Orbit	P_s, 3 yr. 24 hr. Orbit	Yaw & Elevation Orientation P_s, 1.5 yr. 6 hr. Orbit	P_s, 1.5 yr. 12 hr. Orbit
Batteries	.998	.998	.997	.998	.998
Solar Cells	.999	.999	.999	.999	.999
Reaction Wheel	.999	.999	.999	.999	.999
Electronics	.967	.967	.935	.946	.946
Gimbal & Drive	-	-	-	.963	.963
Sensors	.999	.999	.999	.999	.999
Connections	.954	.955	.901	.961	.961
TOTALS	.918	.919	.836	.871	.871

	P_s, 3 yr. 24 hr. Orbit
Batteries	.997
Solar Cells	.999
Reaction Wheel	.999
Electronics	.896
Gimbal & Drive	.927
Sensors	.999
Connections	.913
TOTALS	.752

The figures given for connection reliability are predicted upon the assumption that welded circuitry is used wherever possible, the latest

methods are used in making solder connections, and all infant failures are weeded out in prelaunch tests.

Battery life depends basically upon depth of discharge, number of charging cycles, and temperature, once infant failures are weeded out. According to NASA and commercial sources, the battery MTBF should be very high if good safety factors are applied to these parameters. According to published data, the P_S (1 yr.) is 0.999 for a battery.

Solar cells and solar sensors have an indefinite life if correctly used and adequately protected. A published figure for solar vells is P_S (1 yr.) = 0.9998. For the first failure, using 17000 solar cells, the Ps (1 yr.) would be 0.152. However, since the loss of 10 cells would be insignificant, the Ps (1 yr.), allowing 10 failed cells, would be 0.9999. Even the inclusion of several hundred diodes does not reduce the Ps (1 yr.) below 0.999, since the loss of several can be assumed without destroying solar panel operation.

The reaction wheel data were obtained from a wheel supplier.

The other reliabilities were obtained using currently published component reliability figures.

The values given do not include redundancy, except as noted for the solar cells.

Even without considering the wearout life of bearings, gears, and other mechanically moving components, it is obvious from the foregoing data that the one-axis control is more reliable than the two-axis control. And though redundant wheels could be easily included, it would be difficult to mechanize redundant bearings for a gimballed array. Further, although all reaction wheel bearings can be located in a sealed environment, it would be impossible to

obtain completely sealed array bearings; the environment of these bearings would be most stringent.

Consideration of the factors discussed above leads to the conclusion that to obtain a relatively large power output from a solar array, the non-gimballed, yaw-oriented array is the only system offering a reasonable reliability for periods longer than one year.

8.0 OPTIMIZATION OF THE WHEEL AND COIL SYSTEM

8.1 Errata to Previously Published Six-Hour Orbit Data

Figure 5-1, "System Parameters vs. Disturbance Torque Level" of the report "Electromagnetic Attitude Control System Study", dated 1 May, 1962, was found to be in error due to the insertion of a resistor of incorrect value in the analog computer simulation. Figure 8-1 shows the corrected curves.

8.2 Twelve-Hour Orbit

A three-axis simulation was made of an attitude control system actuated by reaction wheels with electromagnetic momentum removal for a 12-hour orbit in order to establish the optimum relation between the wheels and coils.

This work was similar to that for the 6-hour orbit described in the 1 May 1962 report; the general statements regarding method of test and results given in that report can also be applied to the new work. The purpose of the 12-hour orbit simulation was to note the changes in system performance brought about by the weaker earth's field at that altitude.

Four levels of disturbance torques (25, 50, 100, 200 dyne-cm) were used in the simulation. Figures 8-2 through 8-4 were drawn using data from the simulation and these were used to make the composite curves shown in Figure 8-5. For a disturbance torque of 200 dyne-cm, the wheel-plus-coil weight is 2.7 times larger in a 12-hour orbit than it is in a 6-hour orbit. The increase in wheel-plus-coil weight in a 12-hour orbit is due to the magnetic field magnitude being reduced by a factor of approximately 4. The coil torque and wheel momentum is approximately 3.4 times larger in a 12-hour orbit than it is in a 6-hour orbit for the same disturbance level of 200 dyne cm. The optimum gain in the 12-hour orbit is higher than the 6-hour orbit for any given disturbance torque. Higher gain is required in order to satisfy the required torque output since the available geomagnetic field is less in the 12-hour orbit.

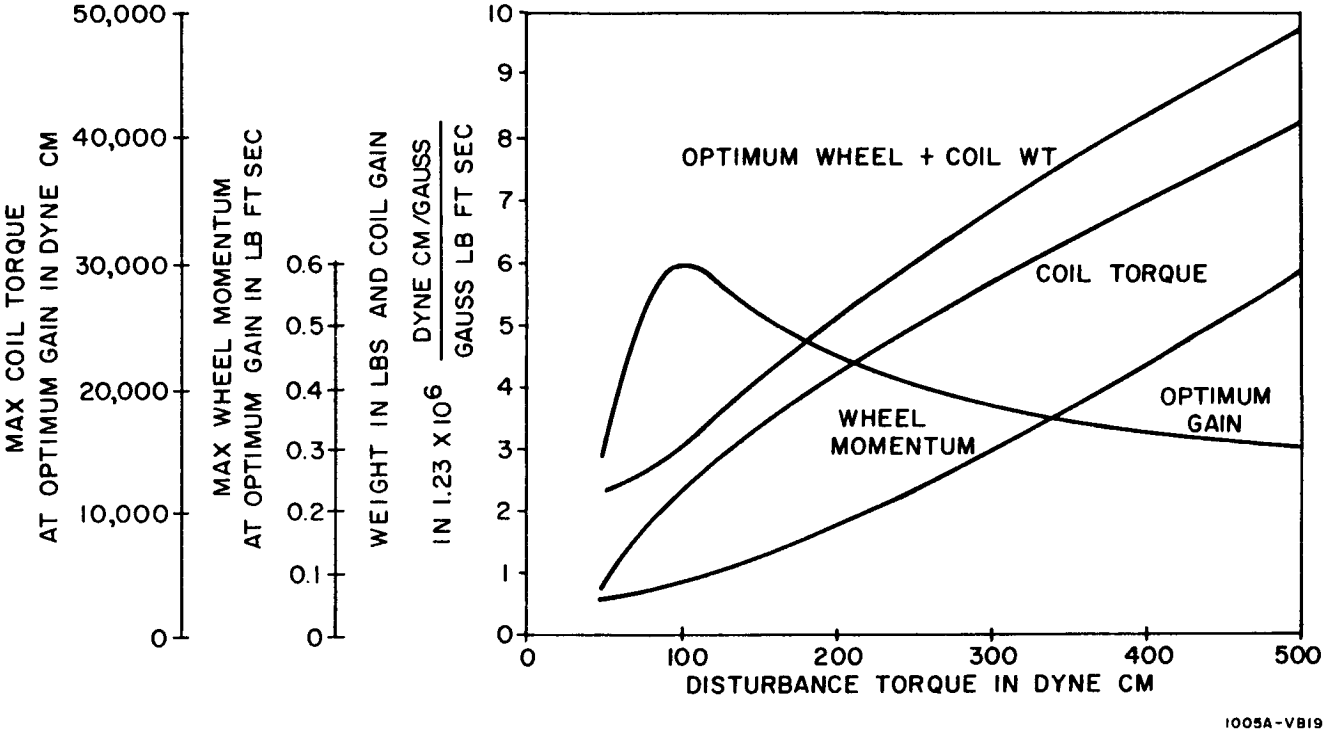

Figure 8-1: System Parameters vs Disturbance Torque Level
6-Hour Orbit

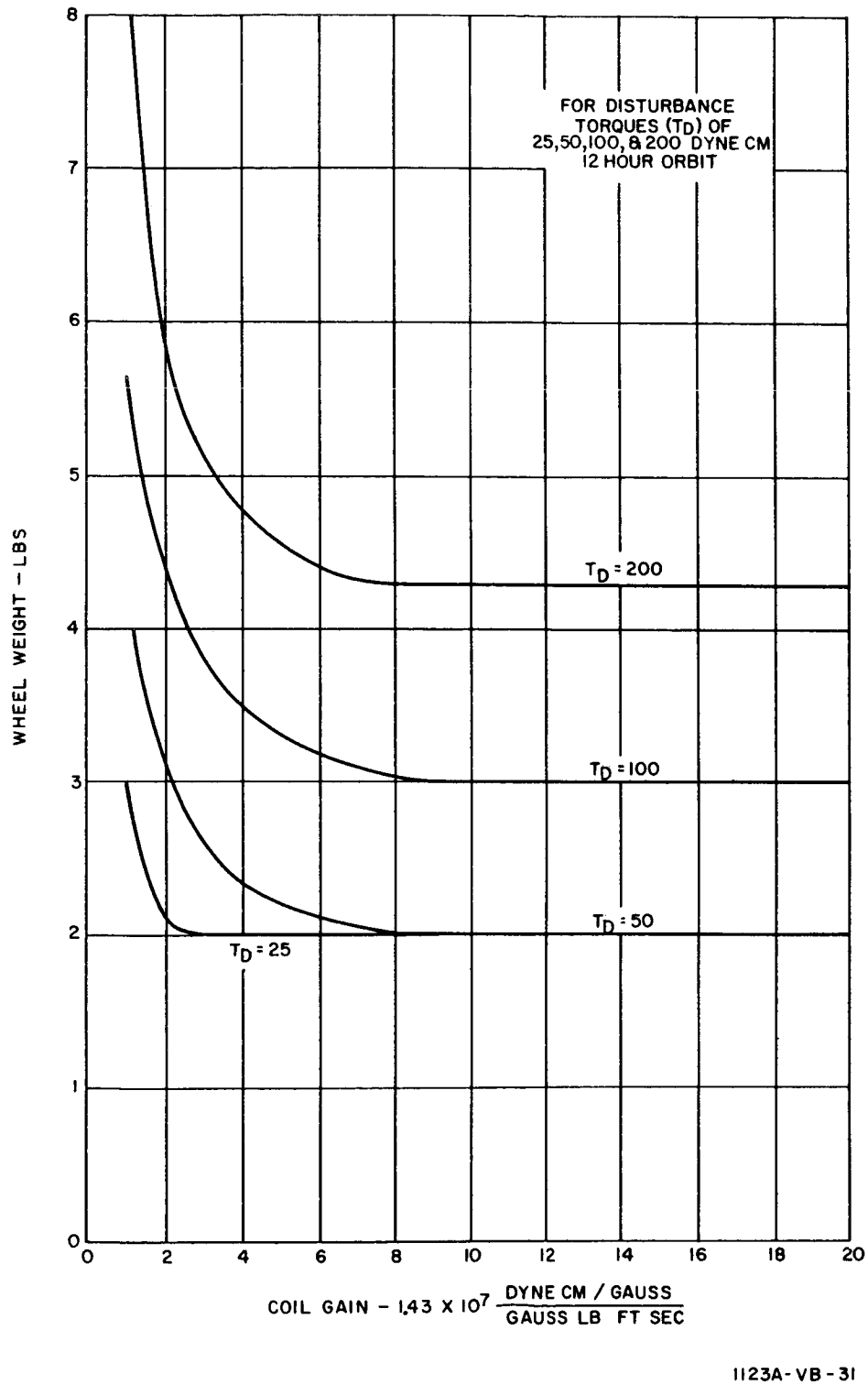

Figure 8-2: Wheel Weight vs. Coil Gain

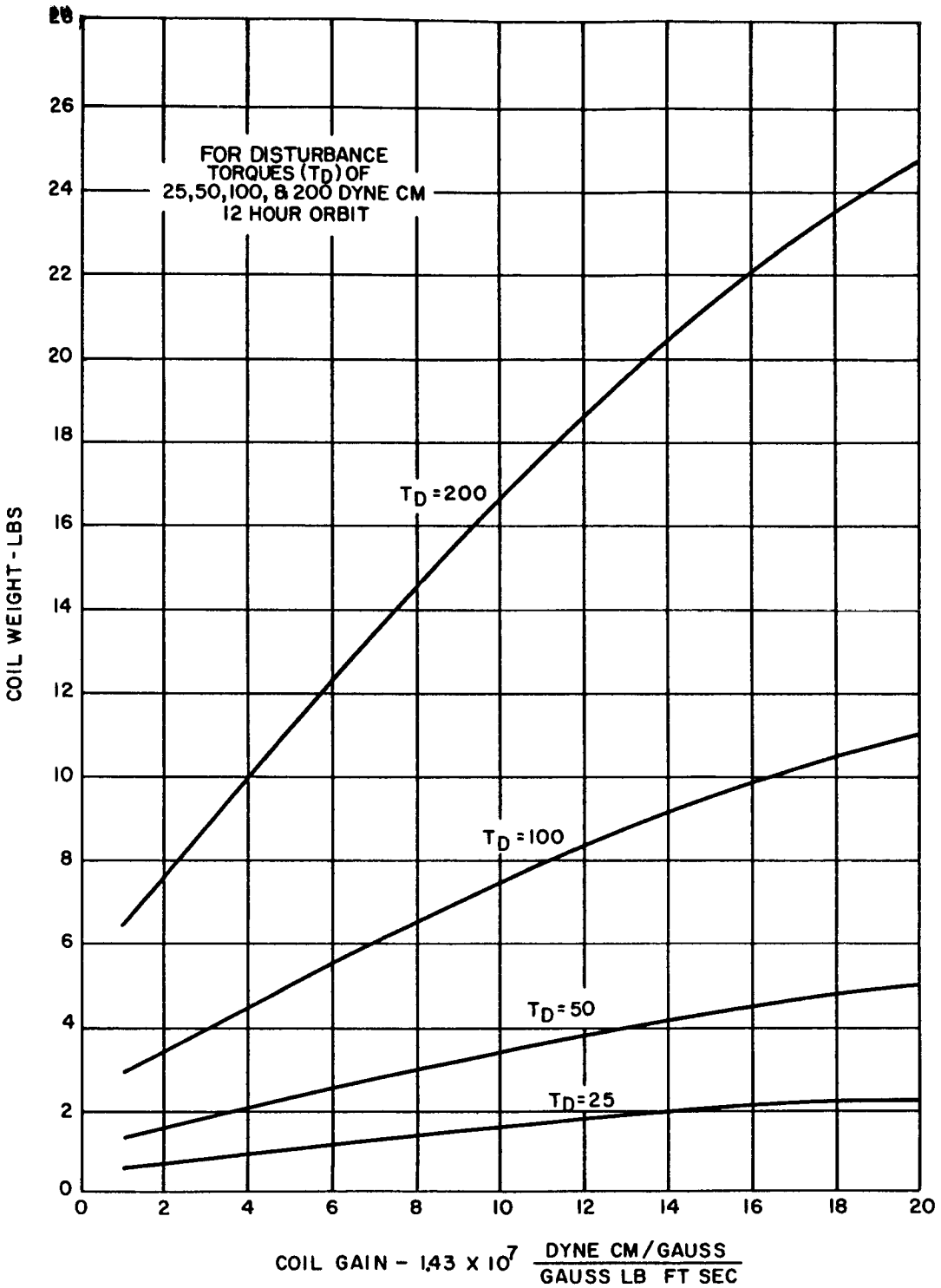

Figure 8-3: Coil Weight vs. Coil Gain

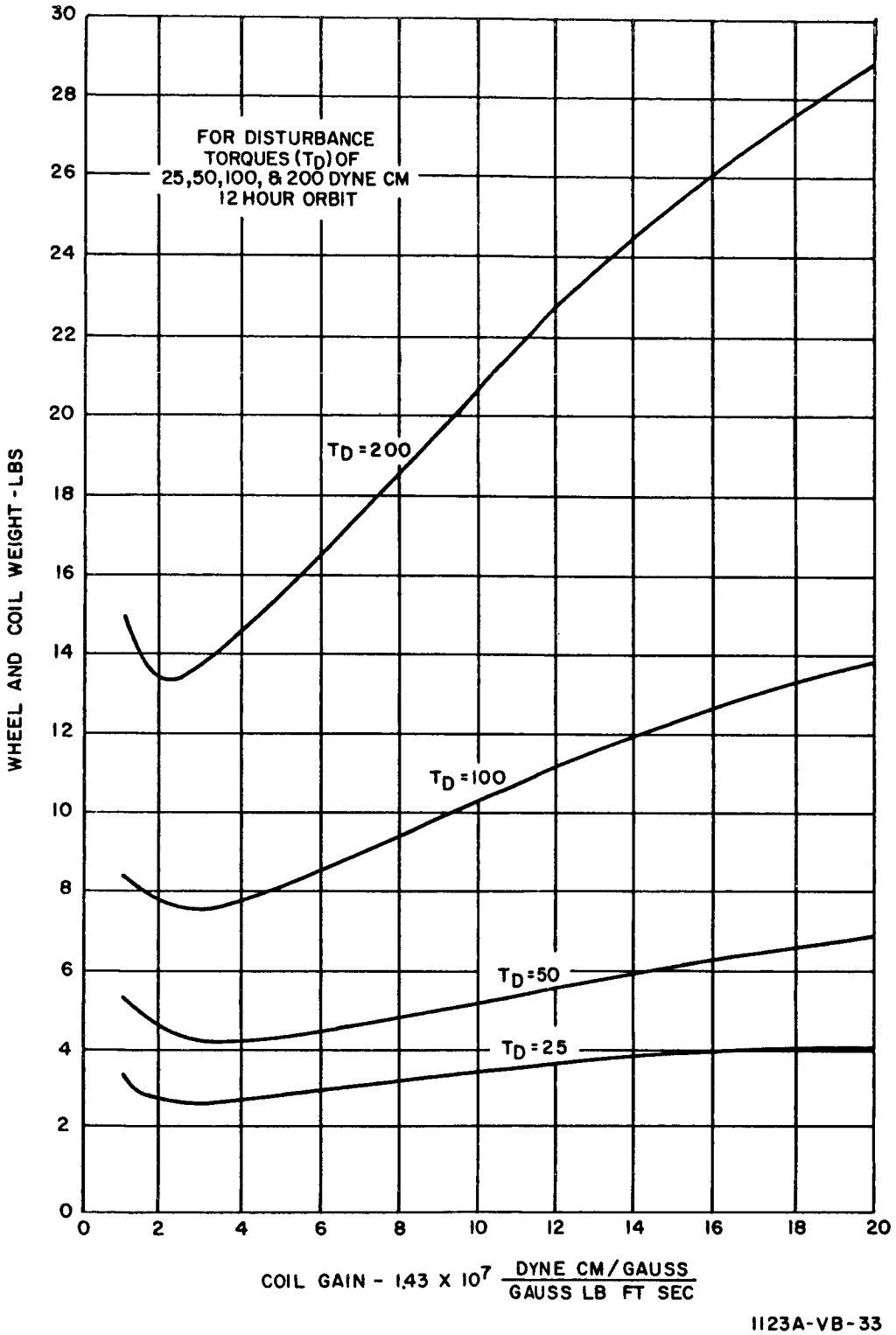

Figure 8-4: Wheel and Coil Weight vs. Coil Gain

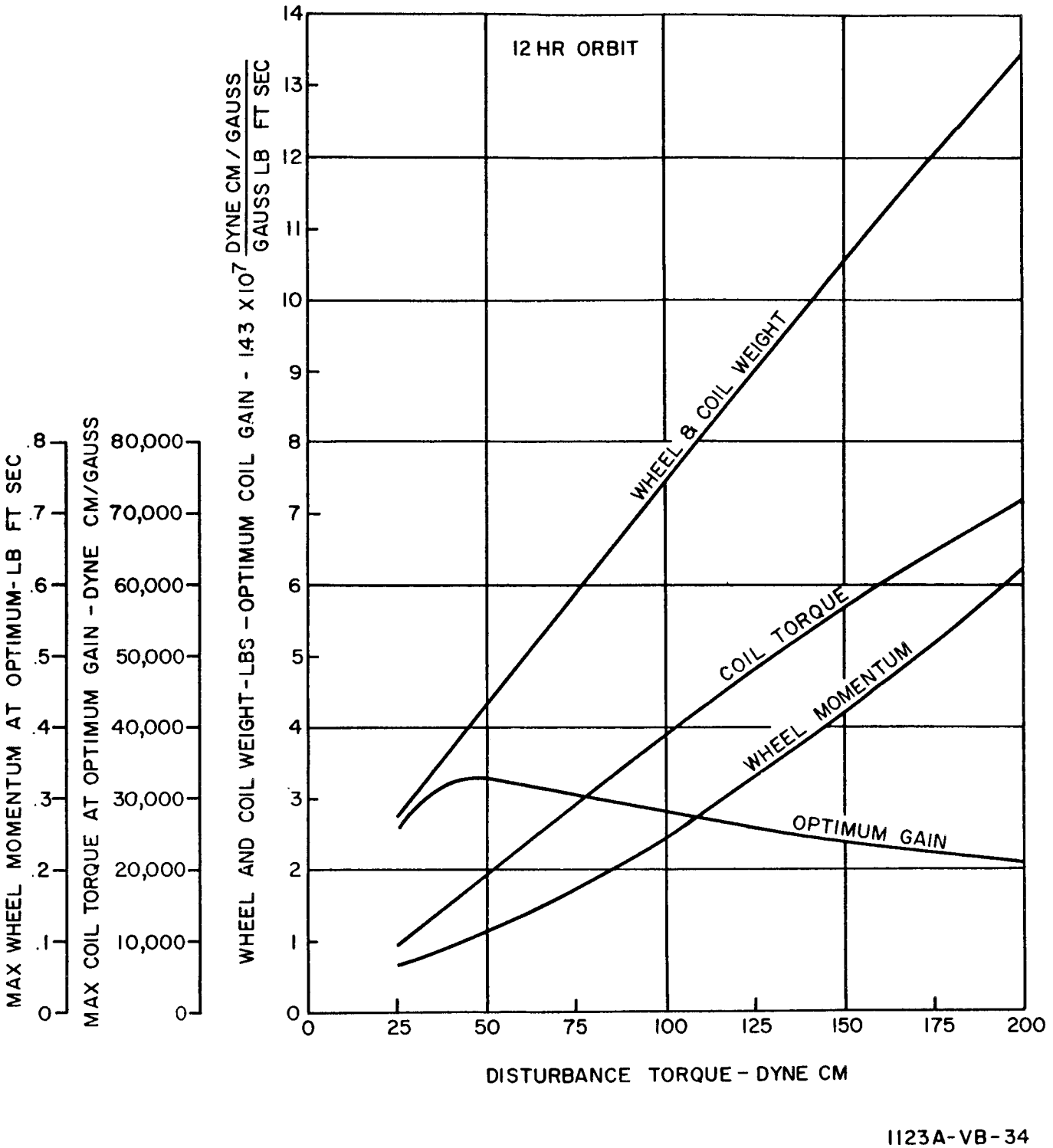

Figure 8-5: Optimum Actuation Data vs. Disturbance Torque

8.3 Synchronous Orbit

A satellite in a synchronous equatorial orbit does not move with respect to the earth. Thus, changes in the magnetic field direction in vehicle coordinates are independent of the orbital position of the vehicle. The variations are due to ring currents, solar activity and interplanetary effects, as discussed in section 9. The fact that the field will vary because of these effects cannot be relied upon. Thus, the magnetic field can be depended upon to dump momentum in only two axes in the synchronous orbit. Some other means must be used to dump momentum in the third axis (pitch axis). A system using solar paddles plus a yaw axis reaction wheel and three torque coils has been studied.

Figure 8-6 shows the vehicle orbiting the earth in a synchronous equatorial orbit where α is the angle between the vertical and a line lying in the orbital plane and perpendicular to the sunline, and ψ is the inclination of the solar paddle to the sunline.

The earth's magnetic field (B) is almost totally in the positive Y direction. By placing the paddles as shown with one side of each paddle reflecting and the other nonreflecting, positive and negative Y direction torques can be generated. The following study is to determine the magnitude of solar torques possible and therefore the momentum dumping capability of the solar torques.

Assume a box shaped satellite 10 feet long and 1 meter square. The solar paddles are 1 meter square. Letting the solar pressure be 1.0 dyne/meter^2 on the reflecting paddle and 0.5 on the non-reflecting paddle, the expression for solar pressure torque (T) is:

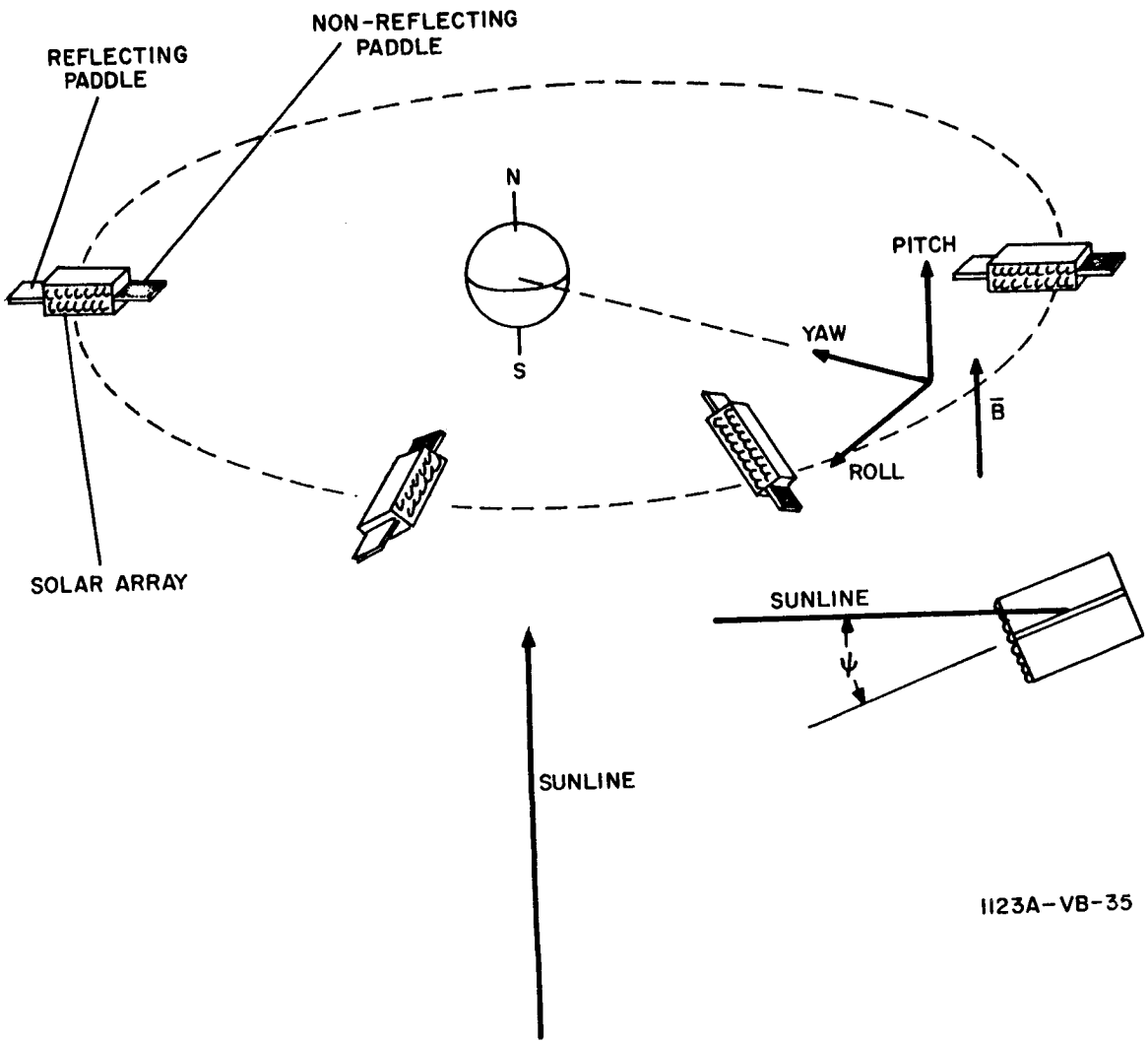

Figure 8-6: Solar Pressure Rate Damping and Momentum Dumping Concept

T = Moment Arm x Force

$= (1/2 \times 10 \times 30.48 + 50) \cos\alpha \times 0.5 \times 1 \times \cos\alpha \sin\psi$

$= 100 \cos^2\alpha \sin\psi$

Figure 8-7 is a plot of how ψ must vary with α to maintain the solar torque indicated. Since the solar cell output varies approximately as the $\cos\psi$, it is not desired to let ψ be much larger than 30°.

Using the solar torque expression,

$$T = 100 \cos^2\alpha \sin\psi$$

it can be seen that for constant ψ the torque varies as the $\cos^2\alpha$. This is shown in Figure 8-8 for three values of ψ. If ψ is held constant throughout the orbit, the momentum (M) dumping capability of the solar torque from $-\alpha$ to α is:

$$M = \int T \, dt$$

$$= 100 \sin\psi \int_{-\alpha}^{\alpha} \cos^2\alpha \, dt$$

$$= 100 \sin\psi \int_{-\alpha}^{\alpha} \cos^2\alpha \frac{1}{\omega} d\alpha$$

$$= \frac{100}{\omega} \sin\psi \left[\alpha + 1/2 \sin 2\alpha\right]$$

The momentum dumping capability of the solar torque from $-\alpha$ to α, for 90° is:

$$M = 0.0507 \sin\psi \left[2\alpha + \sin 2\alpha\right] \quad \text{lb.-ft.-sec.}$$

Figure 8-9 is a plot of this momentum dumping capability as a function of α for three constant values of ψ. From these curves it appears that little is gained by providing momentum dumping for values of $|\alpha|$ larger than 60 degrees. Therefore, assume zero solar pressure torque from α = 60° to α = 120° and from α = 240° to α = 300°.

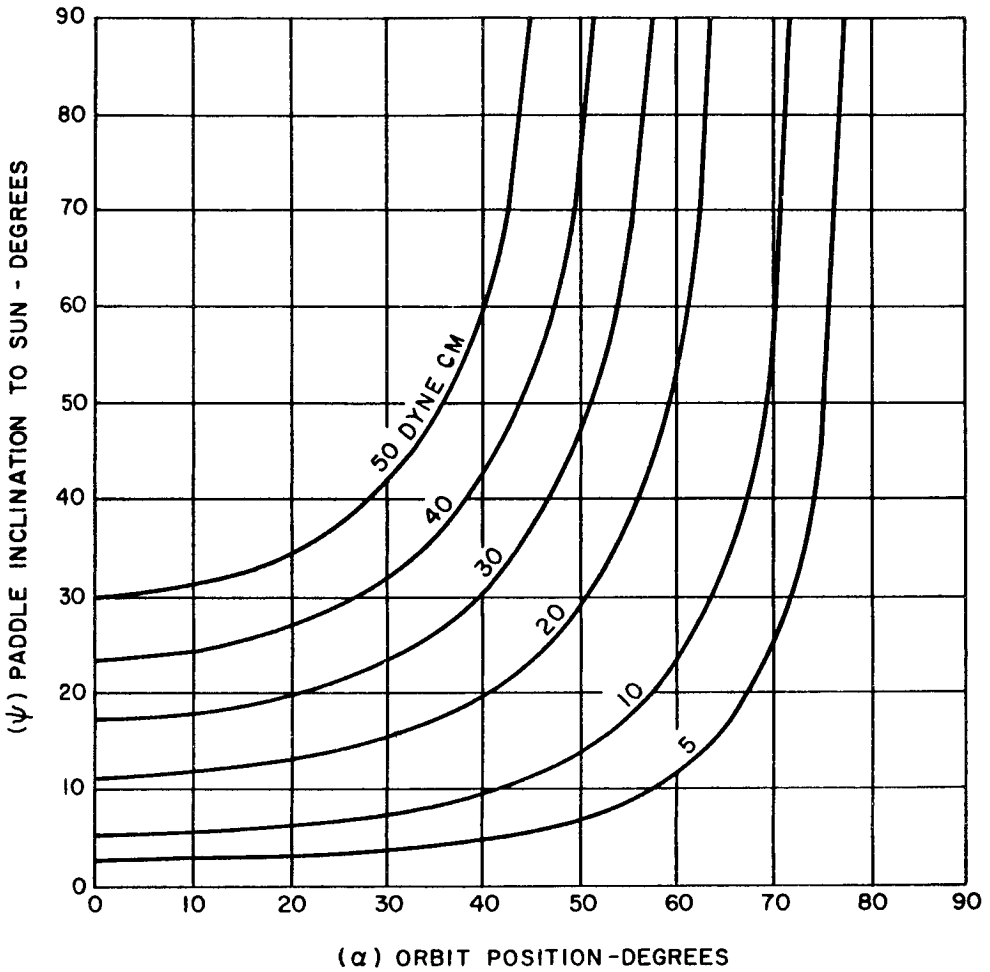

Figure 8-7: Solar Pressure Actuation, Ψ vs. α

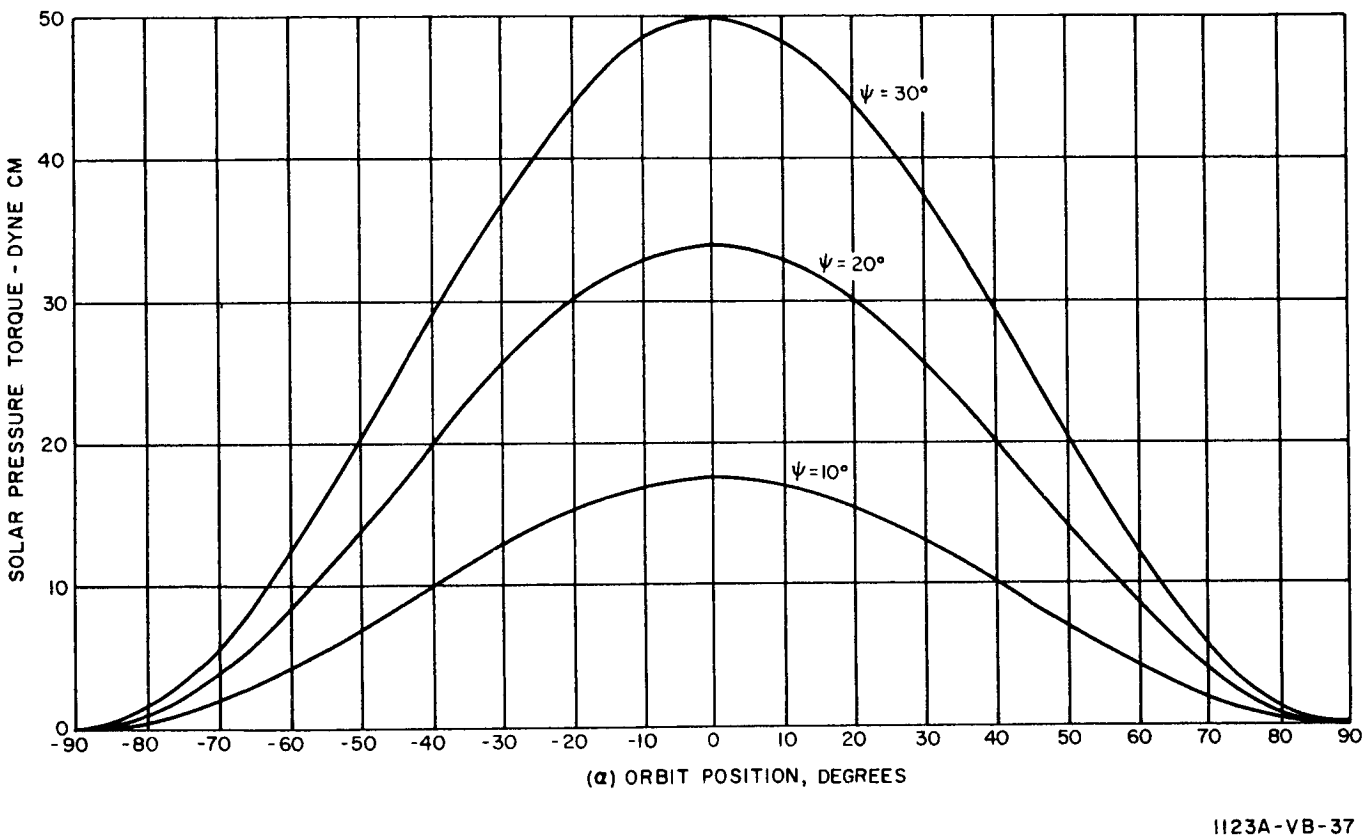

Figure 8-8: Solar Pressure Torque vs. Orbit Position

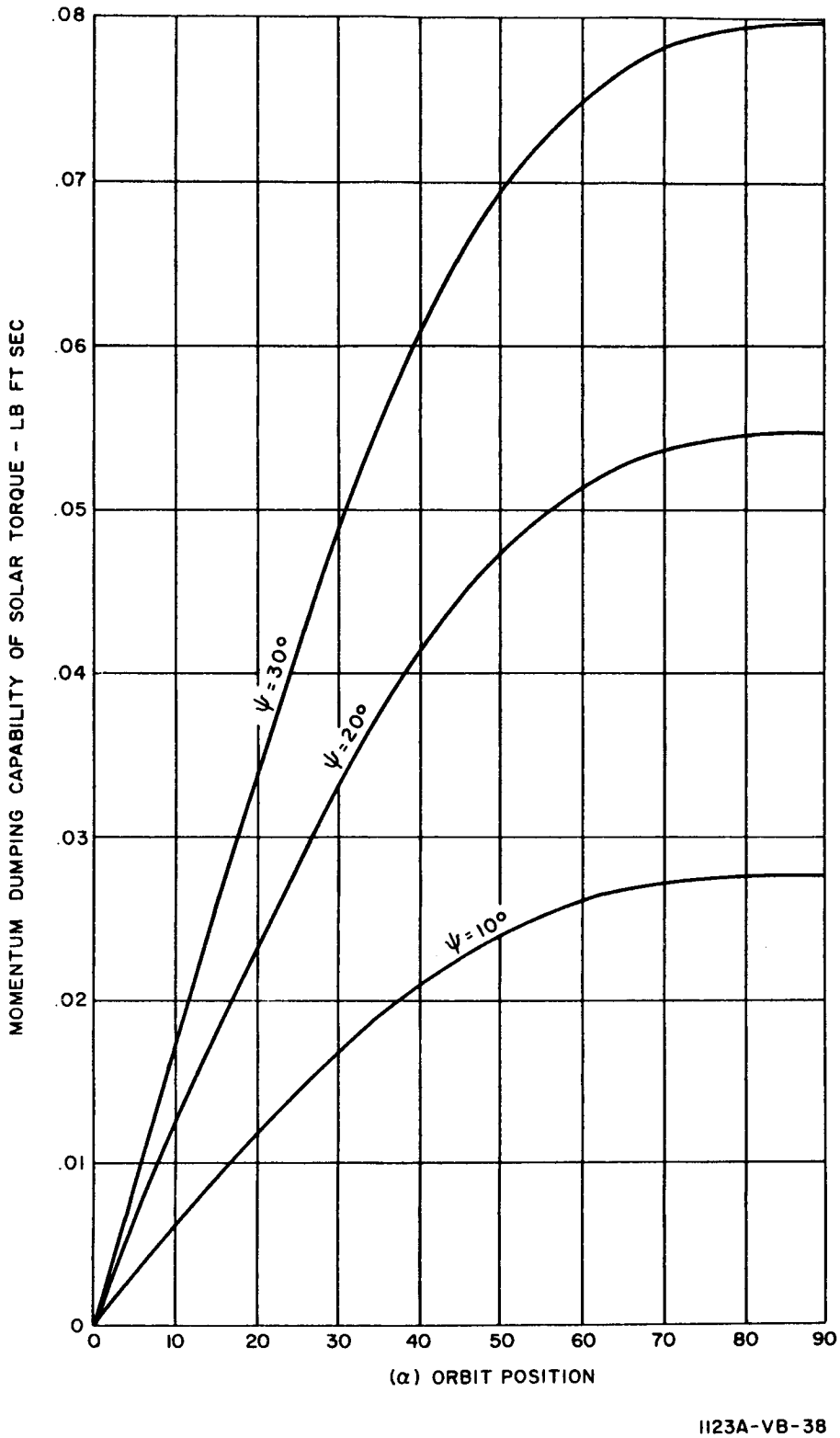

Figure 8-9: Solar Pressure Momentum Dumping Capability

Letting a constant disturbance torque act about the Y axis during these periods of zero solar torque produces certain pitch rates and angles. For a homogeneous satellite of the given dimensions and weighing 500 pounds the pitch moment of inertia is 143 slug ft^2. A constant 5 dyne-cm disturbance acting on this moment of inertia for 1/6 of the orbit produces a pitch rate ($\dot{\theta}$) and a pitch angle (θ) of:

$$\dot{\theta} = 0.00213 \text{ deg/sec.}$$

$$\theta = 15.3 \text{ deg.}$$

when $\alpha = 120^\circ$. The pitch momentum at this rate is:

$$M = .00533 \text{ lb.-ft.-sec.}$$

θ will continue to increase, because of $\dot{\theta}$, to approximately 18°.

For a given orbital position, the control torque varies as the sin ψ. A yaw axis reaction wheel will be used to control ψ. A pair of solar cells mounted on the solar array will be used to measure the angle ψ. This angle will be compared with the desired ψ to generate an error signal. The desired ψ will be computed from the pitch angle and pitch rate:

$$\psi = K_1\theta + K_2\dot{\theta}$$

During an orbit the vehicle will yaw to follow the sun - 360° per orbit. This will prevent undesirable solar torques caused by the sun's angle from the equatorial plane from occurring. In addition, this yaw movement will result in increased power because the solar array will point toward the sun for the major portion of each orbit.

The solar pressure torques are adequate to control small disturbance torques if a relatively large error can be tolerated. The solar cell array is located at right angles to the control paddles. Thus, the power to the solar

cells varies as cos ψ . For small pitch angles, the required satellite inclination, ψ , is not large enough to seriously impair solar cell operation.

9.0 THE CONSTANCY OF THE EARTH'S MAGNETIC FIELD

The surface geomagnetic field can be thought of as consisting of a steady unidirectional field with only a small regular systematic departure from its daily mean value. This systematic departure, sometimes called daily variation, may be no more than 20 gammas out of the total daily mean of 50,000 gammas.[1,2] The amount of departure depends in part upon the magnetic latitude and the time of day and season. The total daily mean depends upon the magnetic latitude and varies from approximately 31,500 gammas at the geomagnetic equator to 63,000 gammas at the geomagnetic poles. The total daily mean also has an irregular field superimposed on it which may be as high as 100 gammas or more. When the irregular change is large the change is said to be due to a magnetic storm. These magnetic storms are associated with sunspot activity and the emission of solar plasma along with other effects.

The diurnal regular geomagnetic field at the surface undergoes but small change compared to the field in geocentric altitudes of 27,000 Km and higher. The surface field varies only 1 part in 1500 or less whereas at 27,000 Km the field may vary 1 part in 20 or more. Knowledge of the constancy of the earth's magnetic field at various orbit altitudes is of paramount importance in magnetic field reference applications for satellite attitude control, although not too significant for magnetic torquing. If the field were found to be in a state of high regular change and/or high irregular change, then referencing applications utilizing the field would prove to be unfeasible. The following is an examination of the constancy of the earth's field, although it is necessarily approximate because little data are available for high altitudes.

9.1 Jensen-Whitaker Geomagnetic Data

The I.B.M. 7090 digital computer has been utilized to convert Jensen-Whitaker geomagnetic data into a vehicle coordinate system (vertically oriented) for use in electromagnetic actuation simulations. The Jensen-Whitaker data were used bacause of their availability on punched I.B.M. cards and slightly better accuracy at lower altitudes than Finch and Leaton data. The Jensen-Whitaker data were independently checked for accuracy of fit by Heppner, Stolarik, Shapiro, and Cain of NASA by comparing the computed field with magnetometer recordings obtained from the satellite 1959, Eta.[3] The recordings were made at altitudes from 500 to 3500 Km and latitudes between 33.5N to 33.5S. The fit was found to be within an accuracy of 1%, with the error terms being systematic and due to the first eight coefficients. The errors were probably due to the data being adjusted for good fit in the Antarctic region and thereby affecting agreement elsewhere.

The converted Jensen-Whitaker geomagnetic data, which have been used in the analog simulations for electromagnetic actuation systems, consisted of the magnetic daily mean values for altitudes of 250, 1000, 2500, 10,000, 22,380 miles, for inclination of 0, 30, 60, 90 degrees, for right ascensions of every 15°, and orbit angles every 5 degrees. It should be pointed out that the data do not take into account several effects on the magnetic field for any particular altitude and position. As pointed out above, the regular and the irregular field variations play an important role in the total field and in particular for altitudes in the 12 to 24 hour orbits. The following paragraphs will consider the constancy of these upper fields.

9.2 Upper Altitude Magnetic Fields

The geomagnetic field is sometimes considered as a dipole located at the earth's center and having a magnetic moment of approximately 8.06×10^{25} c.g.s. units.[4] In reality, there are probably several dipoles located at the earth's center that contribute to the surface field, as well as fields above. The geomagnetic field at the surface of the earth consists of a fairly steady unidirectional field with only slight regular and irregular departures from the daily mean value. It is thought that some of the departures are due to causes within the earth such as dipole changes and/or the flow of earth ground currents. However, the departure for the most part at upper altitudes, say above 17,000 Km geocentric distances, are due to causes outside the earth. These causes include interplanetary fields and sunspot activity and the emission of solar plasma. The solar plasma impinges on the earth's field causing ring currents and a secondary magnetic field that interacts with the earth's field.

There is only limited knowledge of fields present at upper altitudes, the number of probe or satellite magnetometer experiements being nine in number.[5] It is therefore difficult to speak of the actual field at upper altitudes with certainty. However, it can be said, based on several satellite experiements, that the magnetic fields present at altitudes corresponding to orbit periods of 12 and 24 hours are constantly in a state of change both in magnitude and direction.[6,7,5] The earth's field at high altitudes is of such small magnitude (see Figure 9-1) that variations in the order of 100 gammas can change the magnitude in a 24-hour orbit by 100% and its angle by as much as 180°. Even in a 12 hr. orbit, a 100 gamma variation can change the magnitude by as much as 23% and its angle by as much as 13°.

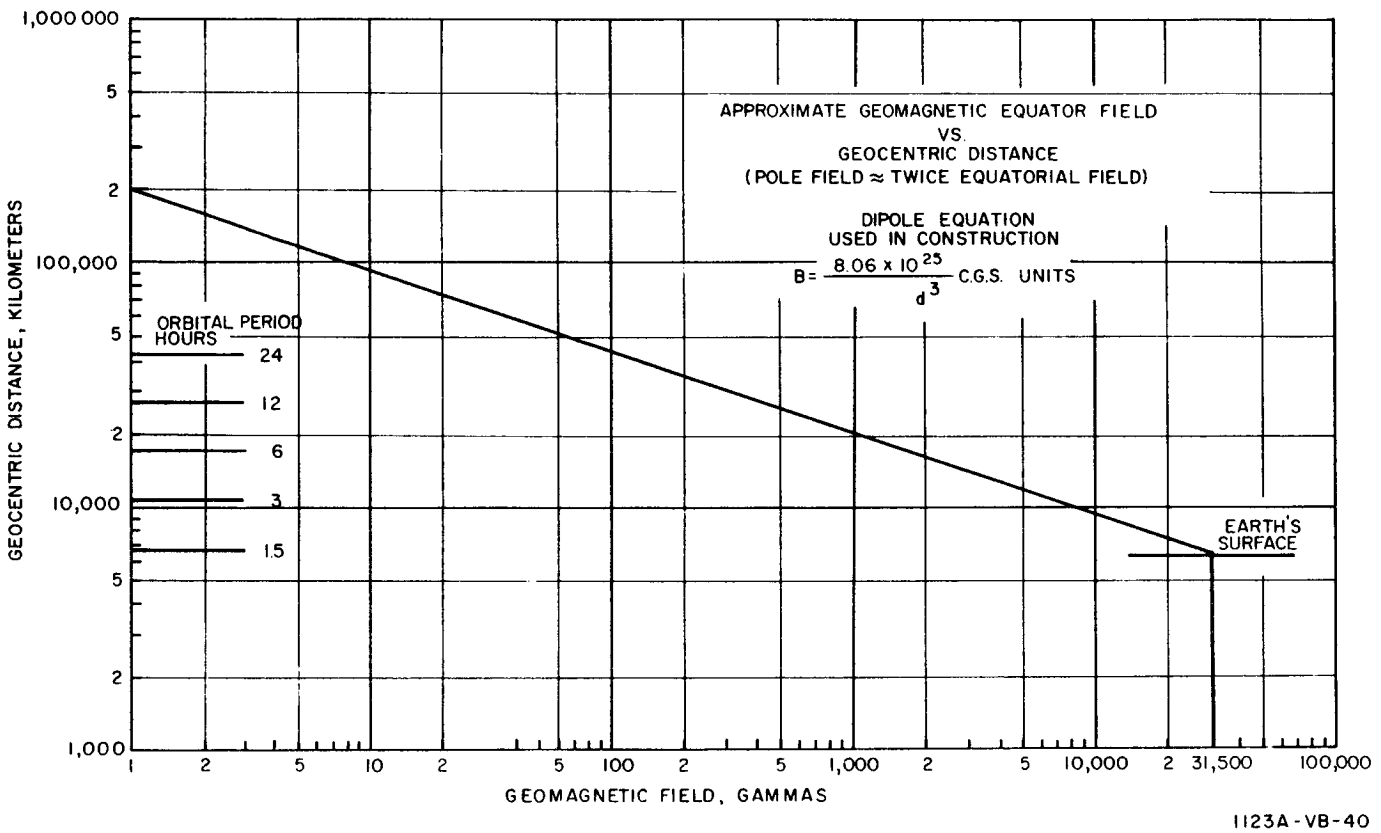

Figure 9-1: Approximate Geomagnetic Equator Field

Previously it has been assumed that the diurnal regular change of either angle or magnitude could be tabulated. However, it has been found that there can be as much as two hours difference between extreme values of magnitude or angle for the diurnal regular change occurring at the same time of day. It will therefore be assumed that the diurnal regular change cannot be predicted to the degree of accuracy required in a high altitude orbit. An estimate of the diurnal regular change of magnetic angle vs. geocentric distance is shown in Figure 9-2.

This curve was drawn on the assumption that there is a 20 gamma variation at any altitude and that a ring current of 10^6 amperes exists at 10 earth radii. The 20 gamma field was selected on the basis that it represents the approximate maximum diurnal regular field that is observed here on earth and that the same field that causes the 20 gamma field would have at least a 20 gamma field at any altitude. A ring current of 10^6 amperes was selected based on measurements made by Explorer VI and Pioneer V. The ring current was found at an altitude of 10 earth radii. Its cross-sectional diameter in this analysis was assumed to be between 1/4 and 1 earth diameter. Also, the 20 gamma field and the axial field of the ring current were calculated to act in a most diverse manner in changing the magnetic angle. The upper curve was drawn using the ring current with a cross-sectional diameter 1/4 that of the earth and the lower curve was drawn using the ring current with a cross-sectional diameter equal to the diameter of the earth. It is interesting to note that at the 6-hour orbit level the effects of the ring current are negligible and that the magnetic angle change is due to the 20 gamma fields.

Figure 9-2 indicates that the direction of the magnetic field could change by as much as 0.6 degrees in a 6-hour orbit, 4 degrees in a 12-hour orbit, and 22 degrees in a 24-hour orbit.

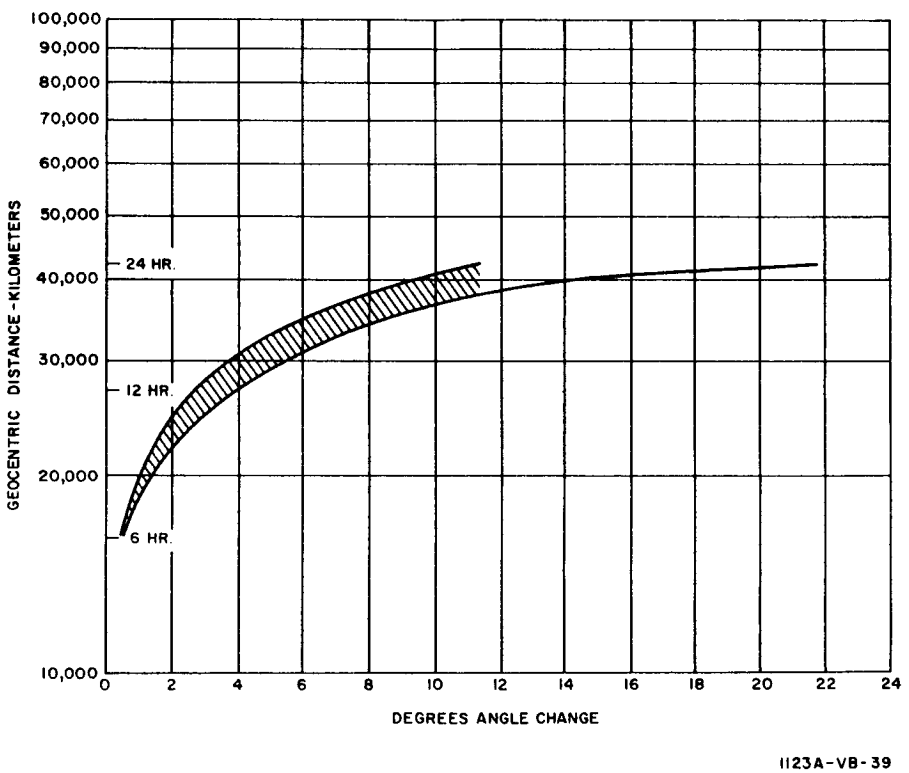

Figure 9-2: Estimate of Diurnal Regular Change of Magnetic Angle

References for Section 9

1. "Magnetism of the Earth", published by the U.S. Department of Commerce, Coast and Geodetic Survey

2. "Geomagnetic Field - Description and Analysis", by Vestine, Lange, Laporte and Scott

3. "Spheric Harmonic Analysis of the Geomagnetic Field", (paper given at the April 1960 meeting of the American Geophysical Union, Washington, D.C.) by Duane C. Jensen and W. A. Whitaker

4. "Magnetorquer - A Satellite Orientation Device", by L. J. Kamm, page 813 of the ARS Journal

5. "Magnetic Fields in Space", by Charles P. Sonett, published in Astronautics, page 38, August 1962

6. "Journal of Geophysical Research", 1958-1962 Works by David B. Beard, et.al., J. P. Heppner et.al., C. P. Sonett, et.al.

7. Transactions American Geophysical Union 1960-1962, J. P. Heppner, et.al., E. H. Vestine